LUND UNIVERSITY

The Development of a European Fire Classification System for Building Products - Test Methods and Mathematical Modelling

Sundström, Björn

2007

The Development of a European Fire Classification System for Building Products
Test Methods and Mathematical Modelling

Doctoral Thesis

Björn Sundström

Department of Fire Safety Engineering
Lund University, Sweden

Lund 2007

Department of Fire Safety Engineering
Lund Institute of Technology

Lund University
Box 118, SE-221 00 Lund
Sweden

Report 1035
ISSN 1402-3504
ISBN 978-91-628-7243-4
ISRN LUTVDG/TVBB-1035-SE

September 2007

Abstract

The fire technical properties of products are determining factors for the initiation and growth of fires. Measurement of fire technical properties and the understanding of how they relate to real hazards are therefore important for fire safety. This work deals with the fire technical properties of building products, their tendency to ignite and release heat in different fire scenarios.

Building products have traditionally been tested and classified according to national building codes in most countries of the world. In Europe, the different countries all used to have different fire tests and classification systems and it was not possible to translate data between them. Therefore, a common European system for reaction to fire testing and classification, known as the Euroclasses, was created. The SBI (Single Burning Item), used for testing and the FIGRA (FIre Growth RAte) parameter used for evaluation of a products reaction to fire properties were introduced. This work deals with this development and its significance for the European evaluation system for reaction to fire properties.

A fire growth that leads to full room involvement, flashover, can happen fast. Predicting flashover times using product data is therefore important for fire safety. Frequently used are the so-called thermal models that by calculations of the products surface temperature predict ignition time and flame spread rate. Alternatively, the ignition time for different heat fluxes are used directly. The products heat release rate, HRR, from a small-scale test is also needed. This work discusses some of the thermal models and presents a straightforward analytical formulation that works well for different room sizes and for the SBI test. In the model formulations heat release rate divided by ignition time appears. These parameters when taken from a small-scale test can be seen as a product property for example for linings in a room fire scenario. In addition, the FIGRA parameter, defined as the maximum of heat release rate divided by time, is shown to predict well the tendency to fire growth for a number of different products in different scenarios. FIGRA is also shown to predict HRR and time to flashover in the Room Corner Test for interior linings.

Key words: Reaction to fire, flashover, fire modelling, Room Corner Test, Cone Calorimeter, Single Burning Item, SBI, Euroclass, FIGRA, Fire Growth Rate, Duhamel's integral, CFD, FDS, Cone Tools, Conflame

Acknowledgements

I sincerely wish to express my gratitude to my supervisor Professor Göran Holmstedt at the Department of Fire Technology, Lund University. Göran, I owe you many thanks for your support and leadership.

I sincerely wish to express my gratitude to my assistant supervisor Professor Ulf Wickström at the Department of Fire Technology, SP. Ulf, your sharp eye and the in depth discussions have been of great value to me.

I also would like to thank my former supervisor for my licentiate work Professor Sven Erik Magnusson who started it all.

Experimental fire research and putting results into practical use are performed in teams and I have had the privilege to work with many competent colleagues at SP and from other organisations in various countries. Of special importance for me was the co-operation with my colleagues and former colleagues in projects mentioned in this work; Johan Söderbom, Ulf Göransson, Ingrid Wetterlund, Jesper Axelsson, Per Thureson and Patrick Van Hees. I am most grateful to you. I am indebted to the technical staff performing complicated experiments of excellent quality at SP.

I would like to acknowledge Brandforsk (The Swedish Fire Research Board), NORDTEST, Nordisk Industrifond (The Nordic Fund for Technology and Industrial Development), the European Commission, individual industries, the European industrial group representing pipe insulation and European industrial groups representing cable and cable raw materials industry who were sponsors in the various projects from which data is used in this work.

I would like to acknowledge SP Technical Research Institute of Sweden for giving me time and support of this work

I am most grateful to the managing director of SP Claes Bankvall who personally spent time to support my work.

Finally, it was the unlimited support and patience from my wife Birgitta and my children Dan and Lina that helped me through the endeavours in writing this thesis.

List of publications

This thesis also includes the following papers:

I. Sundström, B., ”European classification of building products”, Keynote paper, Proceedings of the 8th International Fire Science & Engineering Conference (Interflam ‘99), Edinburgh, Scotland, 1999.

II. Sundström, B., ”The relationship of the SBI test to the reference scenario”, Fire Safe Products in Construction: A Benefit of the Construction Products Directive, European Commission, EGOLF (European Group of Organisations for Fire Testing, Inspection and Certification) and EAFP (the European Association for Passive Fire Protection), conference proceedings, Luxembourg, 24 June, 1999.

The first paper was given at Interflam, which has a broad attendance of fire scientists. The second paper was given at the first major conference organised for European industry and regulators on the fire issues of the Construction Product Directive, CPD. The two papers are included because they are two of the earliest presentations of the common European testing and classification system for reaction to fire to large groups being directly affected by it or having an interest to know how it works.

In addition, the author has contributed to publications listed below, which contain material that is directly used in this thesis or serve as background. Chapter 1 describes the outline and objective of this work and contains references to some of these publications in order to explain their relevance for the thesis.

III. Sundström, B., “ISO TC 92 Fire Safety” Forum Workshop on Establishing the Scientific Foundation for Performance-Based Fire Codes: Proceedings, NSTIR (to be published), NIST, Washington, USA, 2006.

IV. Sundström, B., “Flammability Tests for Cables”, Chapter 8, pp187-199, Flammability testing of materials used in construction, transport and mining, Handbook edited by Vivek B. Apte, Woodhead Publishing, ISBN-13: 978-1-85573-935-2, Cambridge, England, 2006.

V. Sundström, B., “Test Methods and their use for Fires Safety Engineering”, proceedings of the 5th international conference of fire safety, pp 141-150, ISBN 83-7913-810-6, Institut Techniki Budowlanej, Warsaw, Poland, 2005.

VI. Sundström, B., "European Union", chapter 10.4, pp 266-277; "Nordic countries", chapter 10.13, pp 345-360 and "International Organization for Standardization (ISO)", chapter 10.23 pp 418-432, Plastics Flammability Handbook-Principles, Regulations, Testing and Approval, 3rd edition, Edited by Jürgen Troitzsch, Carl Hanser Verlag, Munich, Germany, 2004.

VII. Sundström, B., Axelsson, J., Van Hees, P., "A proposal for fire testing and classification of cables for use in Europe." Report to the European commission and the fire regulators group. SP, 2003-06-19, Brussels, Belgium, 2003.

VIII. Hertzberg, T., Sundström, B., Van Hees, P., "Design fires for enclosures - A first attempt to create design fires based on Euroclasses for linings, SP report 2003, nr 02, ISBN 91-7848-930-X, Borås, Sweden, 2003.

IX. Sundström, B., and Axelsson, J., "Development of a common European system for fire testing of pipe insulation based on EN 13823 (SBI) and ISO 9705 (Room/Corner Test)", SP-report 2002:21. ISBN 91-7848-871-0, Borås, Sweden, 2002.

X. Axelsson, J., Sundström, B., Rohr, U., "Development of a common European system for fire testing and classification of pipe insulation", Proceedings of the 9th International Fire Science & Engineering Conference (Interflam 2001), Volume 1, pp 485-494, Edinburgh, Scotland, 2001.

XI. Sundström, B., Christian, D., "What are the New Regulations Euroclasses and Test Methods Shortly to be Used Throughout Europe?", Fire and Materials 2001, 7th International Conference, San Francisco, USA, 2001.

XII. Sundström, B., "Euroclass i svensk byggnorm – Jämförelse mellan svenska och europeiska brandklasser för byggprodukter", 2001, SP-report 2001, nr 29, ISBN 91-7848-873-7, Borås, Sweden, 2001

XIII. Sundström, B., "The Euroclasses: System and Background of European Classification of Building Materials", Fire Risk and Hazard Research Application Symposium, Atlantic City, New Jersey, USA 28-30 June, 2000.

XIV. Sundström, B., "European classification of building products. EUROCLASSes and the background of the classification limits for reaction to fire, Bezpieczenstowo Pozarowe Budowli Czestochowa, 6-8 Pazdziernika, Roku, Poland, 1999.

XV. Van Hees, P., Sundström, B., Thureson, P., "Testing and classification of wall and ceiling linings in a harmonised European system", Fire and Material Conference proceedings, San Antonio, USA, February, 1999.

XVI. Sundström, B., ”Nya brandklasser i Europa”, Artikel i ByggForskning nr 5/98.

XVII. Sundström, B., Van Hees, P., Thureson, P., ”Results and Analysis from Fire Tests of Building Products in ISO 9705, the Room/Corner Test”, The SBI Research Programme, SP report 1998, nr 11. ISBN 91-7848-716-1, Borås, Sweden, 1998.

XVIII. Sundström, B., ”High Speed Passenger Ships - Fire Calorimetry is used to identify high performance products”, proceedings of ASIAFLAM, 15-16, Hong Kong, March, 1995.

XIX. Sundström, B., "IMO, the International Maritime Organisation, uses modern fire testing technology for selection of materials for high speed passenger ships", Fire and Materials 3rd international conference and exhibition, Washington, USA, October 27-28, 1994.

XX. Sundström, B., "EUREFIC; Results from a major research programme on surface linings", 1st Japan Symposium on Heat Release and Fire Hazard, Tsukuba, Japan, 1993-05-10—11.

XXI. Sundström, B., "Classification of Wall and Ceiling Linings", EUREFIC Seminar Proceedings, Interscience Communications Ltd, ISBN 0 9516320 19, London, England, September 1991.

XXII. Sundström, B., ” A New Generation of Large Scale Fire Test Methods”, Thesis for Technical Licentiate, Lund University, Department of Fire Safety Engineering, SE-LUTVDG/TVBB-3054, Lund 1990, also Technical Report SP - RAPP 1990:12, Borås, Sweden 1990.

XXIII. Sundström, B., Göransson, U., ”Possible Classification Criteria and their Implications for Surface Materials Tested in Full Scale According to NT FIRE 025, ISO DP 9705, Technical Report SP - RAPP 1988:19, Borås, Sweden 1988.

XXIV. Sundström, B., Kaiser, I., Wickström, U., ”Corner Test - Zur Einsschätzung des Brandrisikos von Innenbekleidungen in Räumen”, Supplement 4 - 87 Materialprüfung, Git Verlag, Technical Report SP - RAPP 1988:15, Borås, Sweden 1988.

XXV. Sundström, B., ”The New ISO Full-Scale Fire Test Procedure for Surface Linings Nova ISO Procedura za Pozarno Ispitivanje Povrsinskih Obloga u Realnoj Velicini)” The First Yugoslav Scientific Meeting with International Participation - On Behaviour of Materials and Constructions in Fire, Sarajevo, Bosnia and Herzegovina, 1987.

XXVI. Sundström, B., ”Full-Scale Fire Testing of Surface Materials. Measurements of Heat Release and Productions of Smoke and Gas Species”, Technical Report SP - RAPP 1986:45, Borås, Sweden, 1986.

XXVII. Magnusson, S.E., Sundström, B., Combustible Linings and Room Fire Growth - A First Analysis”, ASTM Special Technical Testing Publication 882 Philadelphia 1985, pp 45 - 69. Department of Fire Safety Engineering, Institute of Science and Technology, Lund University, Report LUTVDG/ (TVBB - 3030), Lund, Sweden, 1985.

XXVIII. Sundström, B., ”Room Fire Tests in Full Scale for Surface Products: Nordtest project 143 - 78”, Technical Report SP - RAPP 1984:16, Borås, Sweden, 1984.

XXIX. Wickström, U., Sundström, B., Holmstedt, G., ”The Development of a Full Scale Room Fire Test”, Fire Safety Journal 5 1983, pp 191 - 197

XXX. Sundström, B., Wickström, U., ”Fire: Full Scale Tests Calibration of Test Room - Part 1”, Technical Report SP - RAPP 1981:48, Borås, Sweden, 1981.

XXXI. Sundström, B., Wickström., U, ”Fire: Full Scale Tests, Background and Test Arrangements. Nordtest projec t 143 - 78”, Technical Report SP - RAPP 1980:14, Borås, Sweden, 1980.

XXXII. Sundström, B., ”Brand: Storskaleförsök, bakgrund och försöksuppställning. Nordtest - projekt 143 - 78”, Technical Report SP - RAPP 1980:1, Borås, Sweden, 1980.

Nomenclature

Other parameters or acronyms used in this work and not given below are explained directly as they appear in the text.

A_0	Area first ignited by the ignition source flame
A	Burning area
α	Absorption coefficient
C	Scenario dependent coefficient
c	Specific heat capacity at constant pressure
d	Thickness
E_A	Activation energy
ε	Emission coefficient
FIGRA	FIre Growth RAte parameter
FIGRA_{RC}	FIGRA for the Room Corner Test
h_c	Convective heat transfer coefficient
h_{eff}	Effective heat transfer coefficient
K	Flame area coefficient
k	Thermal conductivity
l	Characteristic length of flames
$\dot{m}''$	Rate of pyrolysis
$\dot{Q}$	Heat release rate, HRR
$\dot{Q}'$	Heat release rate per unit length
$\dot{Q}''$	Heat release rate per unit area
$\dot{Q}''_p$	Peak heat release rate per unit area in the Cone Calorimeter
$\dot{Q}''_{ave180s}$	Average heat release rate per unit area from ignition to 180s as measured in the Cone Calorimeter
$\dot{q}''_e$	External radiant heat flux to the sample in the Cone Calorimeter
$\dot{q}''_s$	Heat flux at the sample surface
$\dot{q}''_{cr}$	Critical radiant heat flux for ignition

$\dot{q}''_{0,ig}$	Minimum radiant heat flux for ignition, Quintiere's method
$\dot{q}''_{\min}$	Minimum radiant heat flux for ignition
$\dot{q}''_f$	Heat flux at the fuel surface due to radiant and convective heat exposure to the surface from the flames of the advancing flame front
R	Universal gas constant
ρ	Density
ρ_s	Density of solid
σ	Stefan-Boltzmann constant
T_{ign}	Ignition temperature
t	Time
t_{ign}	Time to ignition due to heat exposure from ignition source
t_c	Characteristic time used to mathematically describe a Cone Calorimeter HRR curve
τ	Time to ignition due to heat exposure from advancing flame front on the fuel
V	Flame spread rate
x_p	Length of pyrolysis zone
x_f	Flame length

Subscripts

i	Initial
s	Surface

Contents

1 Objective and outline

During almost 30 years, I have been active in international research projects regarding the area of fire dynamics. Fire initiation and growth phenomena as well as the development of test methods and systems for classification of products have been my major objectives. Much of my research work described in this thesis has been put in practical use in many countries in Europe and elsewhere in the world. Thus, important parts of the harmonised classification system for the reaction to fire of building products now used in national building codes throughout Europe are based on my work for the European Commission, CEC, and the European Standardisation organisation, CEN.

In the international fire community, research on fire dynamics has taken place quite separately from the development of test procedures and systems for classification of products. Models on flame spread therefore often require test data that are rarely available and difficult and sometimes even impossible to measure with any adequate accuracy. On the other hand, test methods are rarely developed with a view of producing data for mathematical modelling for predicting fire development. Exchange of competences between mathematical fire modellers and test developers are therefore needed. An objective of this thesis is to show how test data according to the European system relates to product fire hazard and how it can be applied to predict fire growth.

The European system for reaction to fire testing and classification under the construction products directive, CPD, is described. The hazard assessment included in the so-called Euroclasses is analysed, chapter 2.1 in this thesis. Some models for fire growth in rooms and compartments based on thermal theories for ignition and flame spread are explored, and computed results are compared with test data, see chapter 3. Theoretical considerations on how to use the parameter FIGRA for predictions of flashover is given in chapter 4. Simulations with the CFD (Computational Fluid Dynamics) code Fire Dynamics Simulator (FDS) are discussed in chapter 5.

1.1 The European system

My most important contribution to the pan-European system is the parameter FIre Growth RAte, FIGRA. FIGRA is a way to interpret test data for product fire classification and hazard assessment. FIGRA is used for building products as a part of the verification for CE-marking. So far, rules have been developed for surface linings (excluding floorings), pipe insulation and cables. FIGRA values are calculated using data from the SBI test (EN 13823) for linings [1] and the intermediate scale tests prEN 50399-2-1---2-2 for cables.

The FIGRA parameter was developed in the so-called SBI project which was first presented to the European Commission in 1998 [2], [3]. It was subsequently published in the references [I], [II], [VI], [XI], [XIII], [XIV] and [XVII]. FIGRA has at present been introduced in the regulations in about 30 countries; the EU member states plus the countries having agreements with the EU e.g. Norway and Switzerland. The translation from the old national Swedish fire classes to the new fire classes in the Swedish building code is found in ref. [XII].

The European Commission published the assessment system for pipe insulation in 2003. A typical installation of pipe insulation in the Room Corner Test is identified as the reference scenario. The classification limits for FIGRA was identified from a large number of reference tests in that scenario, see ref. [IX] and [X].

The development of the proposal to classify the reaction to fire properties for cables was done at the request of the European Commission. The basic work that made this possible was the so-called FIPEC project [4]. Experts at SP in co-operation with the European cable industry (Europacable) developed the final proposal, see [VII]. Again, FIGRA came in practical use by a European Commission decision in October 2006.

1.2 Room fire growth

Most of the test data analysed in chapter 3 comes from work that I performed or contributed to. For reasons of space all data is not reproduced in the thesis, instead references are given were the data can be found in detail.

Room Corner Test data related to the energy balance in a room, e.g. temperature, heat exposures and flame spread mainly comes from work reported in SP-report 1986:45, [XXVI].

Much product data comes from the EUREFIC project [5] where tests on similar products were performed in national classification tests of Germany, UK, France, Italy and in the ASTM surface spread of flame test, the Cone Calorimeter, the Room Corner Test and very large room scale. There were many researchers involved in producing the data and the references are given at the places where the data is used in this work. EUREFIC was a quite large project financed and led by the Nordic countries. Twelve institutes were involved from seven European countries and Japan. EUREFIC had a large influence on the introduction of fire calorimetry for ordinary testing especially in Europe. I was a member of the project steering group and a specific contribution was to develop a proposal for product classification [XXI].

The SBI project [6] is the other prime data source. The project was financed by the European Commission and led by a European group of laboratories in co-operation with a group of European regulators, one from each member state, representing the national regulators. The project included the development of the SBI test, a first round robin, tests in the Room Corner Test and the development of a classification system. I was responsible for the large-scale tests in the reference scenario, the Room Corner Test, [XVII]. I also worked with the development of the FIGRA parameter and proposed it for classification, see below.

Because it has been standardised the Room Corner Test has become the most common source of large-scale test data. It is an ISO standard, ISO 9705, an ASTM standard, ASTM E 2257, a Nordic test, NT FIRE 025, and a European standard, EN 14390. Pioneering work on developing the Room Corner Test was done in USA, [7], [8]. During the early 80s, I contributed to the development of the test procedure, [XXVII], [XXVIII], [XXIX], [XXXII] and my thesis for technical licentiate [XXII] is on the subject of development of a new generation of large-scale fire test methods. I chaired the ISO group (ISO TC 92 SC1 WG 7) and later the CEN group (CEN TC 127/ad hoc 36) which worked out the ISO and the EN standard respectively. Much of the original text for the ISO and EN standards was taken from ref. [XXVIII], which was published as a common Nordic method NT FIRE 025 in 1986. The Room Corner Test is now used worldwide as a research tool but also in international regulations of linings fire properties. It is a reference scenario test for the European classification system for reaction to fire of linings. International Maritime Organisation, IMO, requires that so called “fire-restricting materials” used on high speed ships are tested and classified according to the Room Corner Test [9], [10], [XVIII] and [XIX].

2 The European system and the parameter FIGRA

2.1 The European construction products directive, CPD

The European construction products directive, CPD, is aiming at removing barriers of trade for construction products between member states of the European Union and those countries outside of EU having an agreement with EU to use the CPD, for example Norway [11]. To ensure a free flow of products between countries their fire properties must be tested, classified and declared in a harmonised way. Further, the building codes in each country must be adapted to the CPD. Harmonising the European system for reaction to fire was not straightforward as the national systems were very different throughout the union. For that reason, a completely new system was created and introduced through a number of decisions by the European Commission.

Tests and classes are unique and the national systems in the EU member states do not automatically fit which can lead to costly changes. The construction sector in the EU has a value added of about 414 000 million EUR (2003) [12]. So called "building completion" involves painting and glazing, floor and wall covering and plastering, i.e. use of building products. This part alone has a value added of about 62 000 million EUR for 2003. Introducing a new system for reaction to fire testing and classification of construction products as a mandatory requirement on this market therefore involves very large economical values. Market distortions are not wanted and national regulators want to maintain their perceived safety level.

European EN-standards are tools for harmonisation. An EN-standard must be implemented in all member states and conflicting national standards must be withdrawn. A product may be CE-marked when there is a so-called product standard available. The product standard contains specifications for all required data on a product, for example strength, thermal properties as well as fire properties. When CE-marking is possible, this is the official way to declare product properties in the EU. National systems are not allowed. Therefore, the test methods and the classes appearing in Commission decisions are mandatory and they are the only option for reaction to fire classification under the CPD.

2.1.1 FIGRA

The classification parameter FIGRA, FIre Growth RAte, was first introduced in 1998 as a way to classify the fire properties of building products for the purpose of the CPD [13], [14]. The parameter FIGRA is specific for two reasons:

1. It predicts burning behaviour of a large variety of building products in reference scenarios. These reference scenarios are in their turn related to real life fire scenarios.
2. It is a part of the European harmonised directions under the construction products directive, CPD. Therefore, FIGRA is relevant for products on a very large market.

FIGRA is defined as the growth rate of the burning intensity, HRR, during a test, for example the SBI, see Figure 1. FIGRA is calculated as the maximum value of the function (heat release rate)/ (elapsed test time). The unit is W/s. In addition, certain threshold values of HRR and the total heat release rate must first be reached before FIGRA is calculated. Threshold values are needed to avoid that very small and early values of HRR are included as this leads to unrealistic FIGRA values. The detailed definition of FIGRA can be found in EN 13823 (SBI).

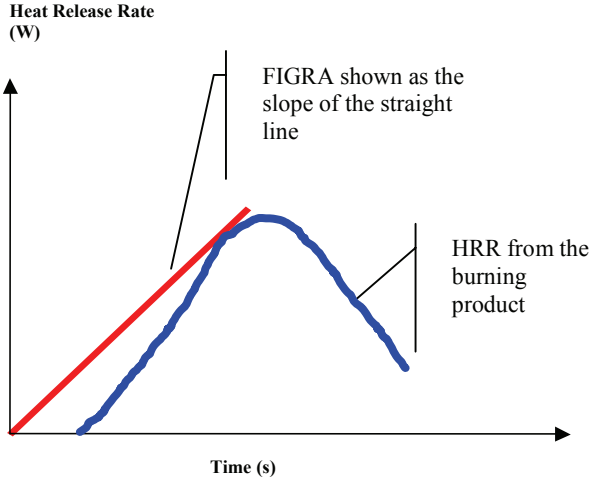

Figure 1. The parameter FIGRA is the maximum value of the function (heat release rate)/ (elapsed test time); shown as the slope of the straight line in the figure.

2.2 FIGRA and classification of interior linings

FIGRA is the main parameter for classification of building products based on the SBI (Single Burning Item) [1] test in the so-called Euroclass-system. SBI evaluates the potential contribution of a surface lining to the development of a fire. It simulates a single burning item in a corner of a room. The test is used for the European classes A1, A2, B, C and D, see Table 1. The classification table is included in a decision taken by the European Commission [14]. It covers construction products under the CPD excluding a few product groups like floorings and so-called linear products, for example cables and pipe insulation. The test methods listed in column 2 are harmonised European standards.

Table 1: Classes of reaction to fire performance for construction products excluding floorings [14].

Class	Test method(s)	Classification criteria	Additional classification
A1	EN ISO 1182 ([1]); *And*	$T \leq 30°C$; *and* $m \leq 50\%$; *and* $t_f = 0$ (i.e. no sustained flaming)	-
	EN ISO 1716	$PCS \leq 2.0$ MJ.kg^{-1} ([1]); *and* $PCS \leq 2.0$ MJ.kg^{-1} ([2]) ([2a]); *and* $PCS \leq 1.4$ MJ.m^{-2} ([3]); *and* $PCS \leq 2.0$ MJ.kg^{-1} ([4])	-
A2	EN ISO 1182 ([1]); *Or*	$T \leq 50°C$; *and* $m \leq 50\%$; *and* t_f 20s	-
	EN ISO 1716; *And*	$PCS \leq 3.0$ MJ.kg^{-1} ([1]); *and* $PCS \leq 4.0$ MJ.m^{-2} ([2]); *and* $PCS \leq 4.0$ MJ.m^{-2} ([3]); *and* $PCS \leq 3.0$ MJ.kg^{-1} ([4])	-
	EN 13823 (SBI)	$FIGRA \leq 120$ W.s^{-1}; *and* LFS < edge of specimen; *and* THR_{600s} 7.5 MJ	Smoke production([5]); *and* Flaming droplets/ particles ([6])
B	EN 13823 (SBI); *And*	$FIGRA \leq 120$ W.s^{-1}; *and* LFS < edge of specimen; *and* $THR_{600s} \leq 7.5$ MJ	Smoke production([5]); *and* Flaming droplets/ particles ([6])
	EN ISO 11925-2([8]): *Exposure = 30s*	$Fs \leq 150$mm within 60s	

Class	Test method(s)	Classification criteria	Additional classification
C	EN 13823 (SBI); *And*	FIGRA $\leq$ 250 W.s^{-1}; *and* LFS < edge of specimen; *and* $THR_{600s} \leq 15$ MJ	Smoke production([5]); *and* Flaming droplets/ particles ([6])
	EN ISO 11925-2([8]): *Exposure = 30s*	Fs $\leq$ 150mm within 60s	
D	EN 13823 (SBI); *And*	FIGRA $\leq$ 750 W.s^{-1}	Smoke production([5]); *and* Flaming droplets/ particles ([6])
	EN ISO 11925-2([8]): *Exposure = 30s*	Fs $\leq$ 150mm within 60s	
E	EN ISO 11925-2([8]): *Exposure = 15s*	Fs $\leq$ 150mm within 20s	Flaming droplets/ particles ([7])
F	No performance determined		

(*) The treatment of some families of products, e.g. linear products (pipes, ducts, cables etc.), is still under review and may necessitate an amendment to this decision.

([1]) For homogeneous products and substantial components of non-homogeneous products.

([2]) For any external non-substantial component of non-homogeneous products.

([2a]) Alternatively, any external non-substantial component having a PCS $\leq$ 2.0 MJ.m^{-2}, provided that the product satisfies the following criteria of EN 13823(SBI) : FIGRA $\leq$ 20 W.s^{-1}; *and* LFS < edge of specimen; *and* $THR_{600s} \leq 4.0$ MJ; *and* s1; *and* d0.

([3]) For any internal non-substantial component of non-homogeneous products.

([4]) For the product as a whole.

([5]) **s1** = SMOGRA $\leq$ 30m^2.s^{-2} *and* $TSP_{600s} \leq$50m^2 ; **s2** = SMOGRA $\leq$ 180m^2.s^{-2} *and* $TSP_{600s} \leq$ 200m^2; **s3** = not s1 or s2.

([6]) **d0** = No flaming droplets/ particles in EN13823 (SBI) within 600s; **d1** = No flaming droplets/ particles persisting longer than 10s in EN13823 (SBI) within 600s; **d2** = not d0 or d1; Ignition of the paper in EN ISO 11925-2 results in a d2 classification.

([7]) Pass = no ignition of the paper (no classification); Fail = ignition of the paper (**d2** classification).

([8]) Under conditions of surface flame attack and, if appropriate to end–use application of product, edge flame attack.

The classification system is rather complicated including several test methods with corresponding classification parameters [15]. In most cases, FIGRA is the determining parameter for a certain class, except for non-combustible products of class A1 and low performance products of class E where the SBI is normally not used [16].

The SBI test apparatus is of intermediate scale size, see Figure 2. Two test samples, 0,5 m x 1,5 m and 1,0 m x 1,5 m are mounted in a corner configuration where they are exposed to a gas flame ignition source giving a heat output of 30 kW. The test time is 20 minutes. As for the Room Corner Test, a direct measure of fire size (Heat Release Rate, HRR) and light obscuring smoke (Smoke Production Rate, SPR) are the most important measurements in the test. To minimise noise the HRR data is calculated as a 30s running average. Other properties such as the occurrence of burning droplets/particles and maximum lateral flame spread, LFS, are observed and used for classification. The LFS is intended for products of very low HRR but still able to spread flame to the edge of the sample. The classification limit for the total heat release, THR, covers products giving low HRR under a long time.

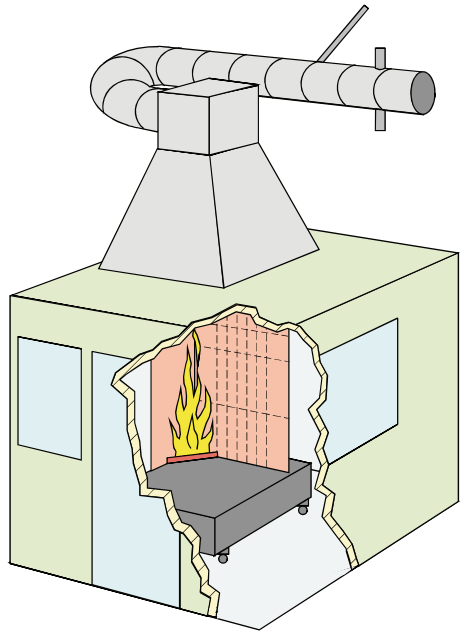

Figure 2. EN 13823, SBI, the Single Burning Item. The test enclosure has the size of small room.

Data has been compared between the SBI and the Room Corner Test for linings [13]. Using similar products, a round robin between a number of European laboratories was performed. One result was a valuable database that was used for further development of the SBI test and refinement of the classification system. In addition to the data from the SBI project (26 large-scale tests), also data from earlier work was included [5], [17]. Totally 62 large-scale tests according to the Room Corner Test was available.

It is not possible to use FIGRA directly to compare test data from the SBI with the Room Corner Test as most of the products went to flashover during an experiment. The HRR at flashover is the same for all products as the process is controlled by ventilation and not the fuel. Therefore, data on a continuous basis was compared by means of a parameter for the Room Corner Test calculated as the maximum HRR during the test divided by the time that this occurred. In case of flashover, the HRR from the product was taken to be 900 kW or 700 kW for an ignition source HRR of 100 kW or 300 kW respectively. The definition of this parameter is very similar to FIGRA and is referred to as $FIGRA_{RC}$. $FIGRA_{RC}$ is defined in the European standard of the Room Corner Test, EN 14390 [18]. It was possible to identify limit values for $FIGRA_{RC}$ that with almost no exception correlated with the occurrence of flashover [13], [16], see Figure 3.

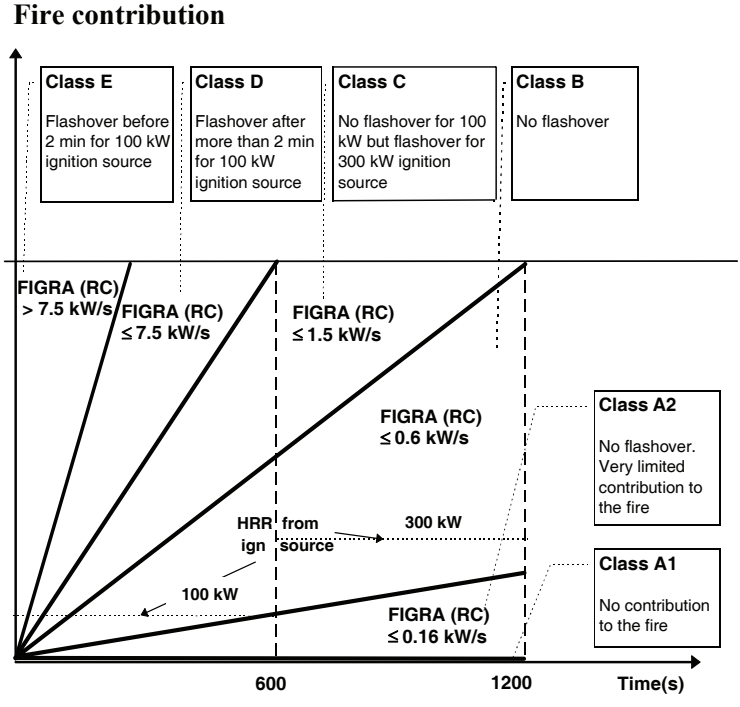

Figure 3. The value of $FIGRA_{RC}$, and the occurrence of flashover for large scale experiments according to the Room Corner Test. The classes refer to the Euroclass-system. Ref [16], (rev. Class B FIGRA is 0,58 as drawn in the diagram which is 0,6 rounded off).

Figure 3 shows what the European classes for linings means in terms of their tendency to create flashover or contribute to the fire in a small room. The upper horizontal line in the diagram can be seen as the point of flashover. It also shows the corresponding limit values of $FIGRA_{RC}$. The figure is published in an informative annex, (Figure A.1, without limit values of $FIGRA_{RC}$) in the classification standard EN 13501-1 [15]. The tendency for a lining to cause flashover in the Room Corner Test is not a legal way for reaction to fire classification in Europe. However, in cases when the SBI is found to give incorrect results for a product category then there is a possibility to appeal to the European Commission. Pan-European industry groups or individual countries can appeal. It is encouraged that the technical background for an appeal is based on data from the Room Corner Test. Obviously the Room Corner Test status as reference scenario and the relation shown in Figure 3 is quite helpful when appeal is discussed.

$FIGRA_{RC}$ was also directly compared with the FIGRA in the SBI test. The correlation is shown in Figure 4. The large-scale data is taken from ref [13]. The SBI test data is from the first international Round Robin and as later analysed in [19]. The later analysis in 2005 included improvements in the calculations of FIGRA that also improves the correlation to the Room Corner Test.

There were 4 products included in the first SBI round robin that have been omitted from Figure 4. These are cables, water pipes, steel covered EPS sandwich panel and FR polycarbonate panel. The cables and the water pipes are not linings and were later included in the so-called “linear products” for which there are specific testing and classification solutions. The burning behaviour of the sandwich panel is depending on the mechanical properties of the steel sheet that protects the combustible core. This effect is not properly modelled in the SBI test, which is discussed in section 3.5. The FR polycarbonate panel was a three layer self-supporting transparent product used in roofs. It was not mounted in a realistic way in the large-scale test and was melting and softening and thus moving away from the ignition source in an arbitrary way.

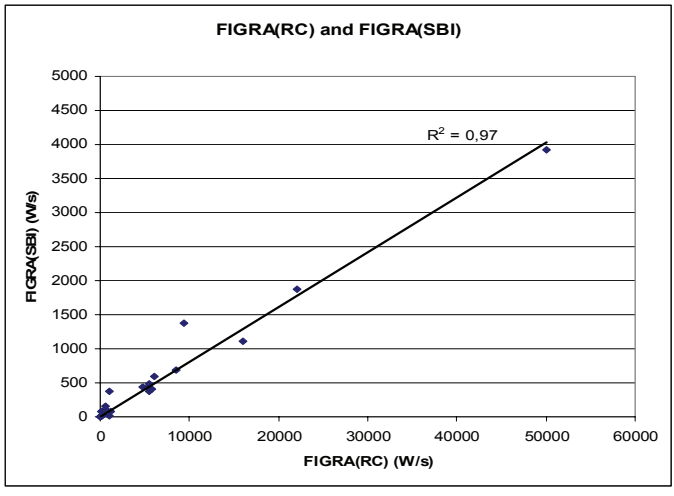

Figure 4. Correlation between $FIGRA_{RC}$ and FIGRA(SBI) for 26 different lining products. Each product was tested in both tests.

The correlation is quite good although the last point with a high FIGRA value has a heavy weight on the least square fit. In Figure 5 below the data for a lower fraction of the full range is shown. The correlation is still good; R^2 is now 0,87.

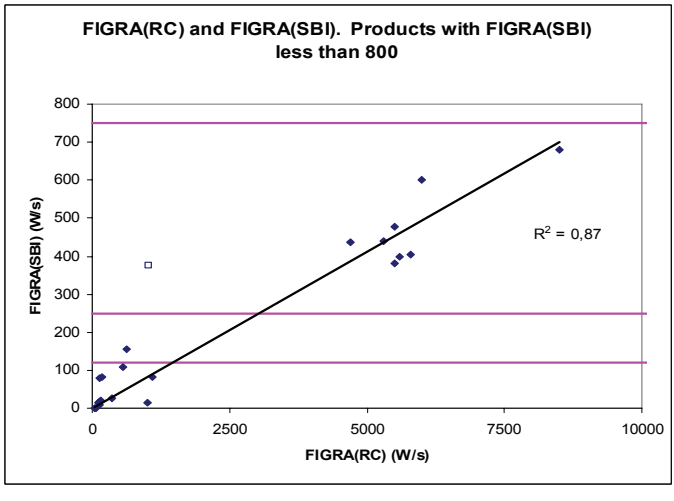

Figure 5. Correlation between $FIGRA_{RC}$ and FIGRA(SBI) for products having FIGRA(SBI) less than 800. The horizontal lines show the borders for Euroclass B (125), C (250) and D (750).

The outlier that has a FIGRA (SBI) of about 370 W/s and a $FIGRA_{RC}$ of about 1000 W/s is the PVC wall carpet SBI M10. As discussed in section 3.4.1 PVC products tend to be "over predicted" by the tests in smaller scale.

Products appear in clusters. Between $FIGRA_{RC}$ 1500 W/s and 5000 W/s there is hardly any data. The reason is that most products go to flashover during the first 3-4 minutes during a test, directly after the 10 minutes when the burner HRR is raised to 300 kW or give no flashover at all. The same trend is seen in the SBI, there are few intermediate products. The final selection of limit values of FIGRA for the Euroclasses were based on the correlation with flashover. However, consideration was also taken to place a limit well between clearly separated groups of products and to respect national systems in Europe. The result is seen in Table 1 and Figure 5.

So-called linear products, pipe insulation and cables, were excluded from the original Commission decision, and specific technical solutions for testing and classification were developed later as shown below.

2.3 FIGRA and classification of pipe insulation

The classification system using FIGRA for pipe insulation was developed during 2002-2003 [20], [21], [22]. The principles are similar to the system for linings and the SBI test is used to measure FIGRA, see Table 2.

Table 2. Classes of reaction to fire performance for pipe insulation.

Class	Test method(s)	Classification criteria	Additional classification
$A1_L$	EN ISO 1182 ([1]); And	$T \leq 30°C$; and $m \leq 50\%$; and $t_f = 0$ (i.e. no sustained flaming)	-
	EN ISO 1716	$PCS \leq 2.0$ MJ.kg^{-1} ([1]); and $PCS \leq 2.0$ MJ.kg^{-1} ([2]); and $PCS \leq 1.4$ MJ.m^{-2} ([3]); and $PCS \leq 2.0$ MJ.kg^{-1} ([4])	-

$A2_L$	EN ISO 1182 ([1]); Or	$T \leq 50°C$; and $m \leq 50\%$; and t_f 20s	-
	EN ISO 1716; And	PCS ≤ 3.0 MJ.kg^{-1} ([1]); and PCS ≤ 4.0 MJ.m^{-2} ([2]); and PCS ≤ 4.0 MJ.m^{-2} ([3]); and PCS ≤ 3.0 MJ.kg^{-1} ([4])	-
	EN 13823 (SBI)	FIGRA ≤ 270 W.s^{-1}; and LFS < edge of specimen; and THR_{600s} 7.5 MJ	Smoke production([5]); and Flaming droplets/ particles ([6])
B_L	EN 13823 (SBI); And	FIGRA ≤ 270 W.s^{-1}; and LFS < edge of specimen; and $THR_{600s} \leq 7.5$ MJ	Smoke production([5]); and Flaming droplets/ particles ([6])
	EN ISO 11925-2([8]): Exposure = 30s	Fs $\leq$ 150mm within 60s	
C_L	EN 13823 (SBI); And	FIGRA ≤ 460 W.s^{-1}; and LFS < edge of specimen; and $THR_{600s} \leq 15$ MJ	Smoke production([5]); and Flaming droplets/ particles ([6])
	EN ISO 11925-2([8]): Exposure = 30s	Fs $\leq$ 150mm within 60s	
D_L	EN 13823 (SBI); And	FIGRA ≤ 2100 W.s^{-1}	Smoke production([5]); and Flaming droplets/ particles ([6])
	EN ISO 11925-2([8]): Exposure = 30s	Fs $\leq$ 150mm within 60s	
E_L	EN ISO 11925-2([8]): Exposure = 15s	Fs $\leq$ 150mm within 20s	Flaming droplets/ particles ([7])
F_L	No performance determined		

([1]) For homogeneous products and substantial components of non-homogeneous products.

([2]) For any external non-substantial component of non-homogeneous products.

([3]) For any internal non-substantial component of non-homogeneous products.

([4]) For the product as a whole.

([5]) s1 = SMOGRA ≤ 105 m^2.s^{-2} and $TSP_{600s} \leq 250$ m^2 ; s2 = SMOGRA ≤ 580 m^2.s^{-2} and $TSP_{600s} \leq 1600$ m^2; s3 = not s1 or s2.

([6]) d0 = No flaming droplets/ particles in EN13823 (SBI) within 600s; d1 = No flaming droplets/ particles persisting longer than 10s in EN13823 (SBI) within 600s; d2 = not d0 or d1; Ignition of the paper in EN ISO 11925-2 results in a d2 classification.

([7]) Pass = no ignition of the paper (no classification); Fail = ignition of the paper (d2 classification).

([8]) Under conditions of surface flame attack and, if appropriate to end–use application of product, edge flame attack.

Pipe insulation is circular and therefore the mounting of the samples in the SBI test had to be carefully defined, see Figure 6.

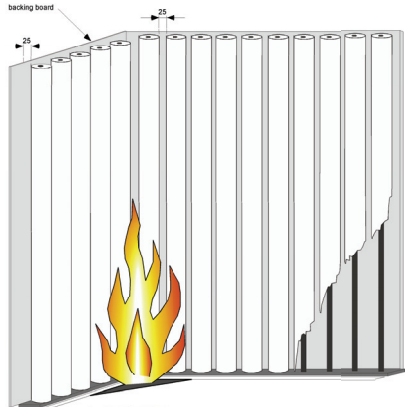

Figure 6. Schematic drawings of the mounting of the test specimen in the SBI. From ref [21].

The Room Corner Test procedure is again reference scenario. A large number of large-scale tests were performed using different mounting configurations representing end use conditions for pipe insulation installations. The reference configuration is shown in Figure 7.

Figure 7. Schematic drawing of the pipe insulation installation in the Room Corner Test . The roof and left wall have been removed for better view. From ref [21].

The ignition source and other requirements in the test procedure were taken over from the Room Corner Test standard, ISO 9705. This large-scale test for pipe insulation is also becoming international standard ISO/DIS 20632 [23].

Results from the large-scale test were compared with the results from the SBI test in a similar way as for the lining products. Data from 24 pipe insulation products was available [20], [21]. The products varied from non-combustible mineral wool to different types of plastic foam like polyethylene and polyurethane. The result from the tests is shown in Figure 8.

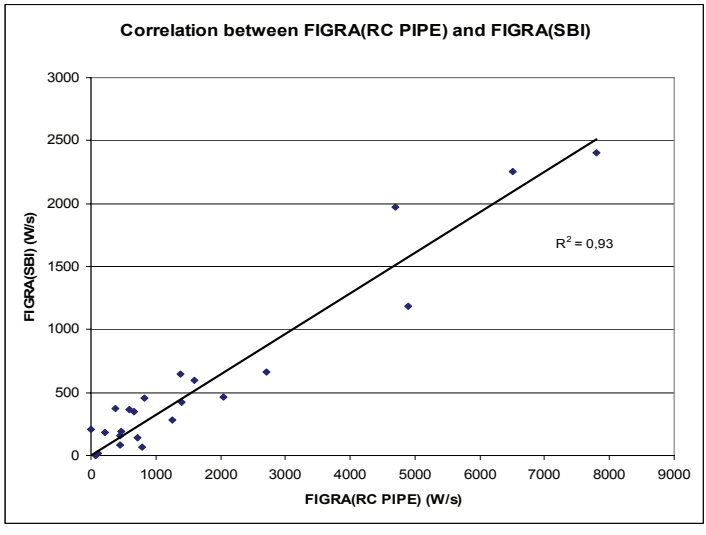

Figure 8. Correlation between FIGRA(RC PIPE) and FIGRA(SBI) for 24 different pipe insulation products. Each product was tested in both tests.

The correlation between the Room Corner Test for pipe insulation and the SBI is good and similar to the linings. The definition of FIGRA(RC PIPE) is the same as the definition used for the SBI except that the filtering values are adjusted to fit the large scale test. If flashover occurs, the HRR from the product is taken to be 900 kW or 700 kW as before. However, flashover is very rare as the amount of pipe insulation mounted in the Room Corner Test is small compared to linings.

2.4 FIGRA and classification of cables

The proposal was developed in co-operation with European regulators and the cable industry in Europe and presented in 2003 [24], [25]. The European Commission decided on a testing and classification system on cables during 2006 [26], see Table 3. Again, the system is built in the same way as for linings and pipe insulation. The exception is the voluntary possibility to declare acidity of the smoke gases, the sub-classes a1, a2 and a3. By request of the European cable industry and some member states, it was introduced as a possibility to select halogen free alternatives. This possibility delayed the decision and caused a worldwide discussion due to its market implications. Certain plastics containing halogens may face an unfavourable situation. Finally, after wide consultation including circulation for comments to the world trade organisation, WTO, acidity was included. Classifying the acidity of smoke gases is unique for cables in the CPD and is not found in any other international regulation. Future will show if acidity of smoke gases and the closely related issue of toxicity of smoke gases will become a common part of international regulations. Research initiatives are required as the knowledge is rather scarce.

Table 3. Classes of reaction to fire performance for cables

Class	Test method(s)	Classification criteria	Additional classification
A_{ca}	EN ISO 1716	PCS ≤ 2,0 MJ/kg (1)	
$B1_{ca}$	FIPEC$_{20}$ Scen 2 ([5]) *And* EN 60332-1-2	FS ≤ 1.75 m *and* THR$_{1200s}$ ≤ 10 MJ *and* Peak HRR ≤ 20 kW *and* FIGRA ≤ 120 Ws^{-1} H ≤ 425 mm	Smoke production ([2, 6]) and Flaming droplets/particles ([3]) and Acidity ([4, 8])
$B2_{ca}$	FIPEC$_{20}$ Scen 1 ([5]) *and*	FS ≤ 1.5 m; *and* THR$_{1200s}$ ≤ 15 MJ; *and* Peak HRR ≤ 30 kW; *and* FIGRA ≤ 150 Ws^{-1}	Smoke production ([2, 7]) and Flaming droplets/particles ([3]) and Acidity ([4, 8])
	EN 60332-1-2	H ≤ 425 mm	
C_{ca}	FIPEC$_{20}$ Scen 1 ([5]) *And*	FS ≤ 2.0 m; *and* THR$_{1200s}$ ≤ 30 MJ; *and* Peak HRR ≤ 60 kW; *and* FIGRA ≤ 300 Ws^{-1}	Smoke production ([2, 7]) and Flaming droplets/particles ([3]) and Acidity ([4, 8])
	EN 60332-1-2	H ≤ 425 mm	
D_{ca}	FIPEC$_{20}$ Scen 1 ([5]) *And*	THR$_{1200s}$ ≤ 70 MJ; *and* Peak HRR ≤ 400 kW; *and* FIGRA ≤ 1300 Ws^{-1}	Smoke production ([2, 7]) and Flaming droplets/particles ([3]) and Acidity ([4, 8])

Class	Test method(s)	Classification criteria	Additional classification
	EN 60332-1-2	H ≤ 425 mm	
E_{ca}	EN 60332-1-2	H ≤ 425 mm	
F_{ca}	No performance determined		

([1]) For the product as a whole, excluding metallic materials, and for any external component (i.e. sheath) of the product.
([2]) **s1** = $TSP_{1200} \leq 50$ m^2 *and* Peak SPR ≤ 0.25 m^2/s
s1a = **s1** and transmittance in accordance with EN 61034-2 ≥ 80%
s1b = **s1** and transmittance in accordance with EN 61034-2 ≥ 60% < 80%
s2 = $TSP_{1200} \leq 400$ m^2 *and* Peak SPR ≤ 1.5 m^2/s
s3 = not s1 or s2
([3]) For $FIPEC_{20}$ Scenarios 1 and 2: **d0** = No flaming droplets/particles within 1200 s; **d1** = No flaming droplets/ particles persisting longer than 10 s within 1200 s; **d2** = not d0 or d1.
([4]) EN 50267-2-3: **a1** = conductivity < 2.5 µS/mm *and* pH > 4,3; **a2** = conductivity < 10 µS/mm *and* pH > 4.3;
a3 = not a1 or a2. No declaration = No Performance Determined.
([5]) Air flow into chamber shall be set to 8000 ± 800 l/min.
$FIPEC_{20}$ Scenario 1 = prEN 50399-2-1 with mounting and fixing as below
$FIPEC_{20}$ Scenario 2 = prEN 50399-2-2 with mounting and fixing as below
([6]) The smoke class declared for class $B1_{ca}$ cables must originate from the $FIPEC_{20}$ Scen 2 test.
([7]) The smoke class declared for class $B2_{ca}$, C_{ca}, D_{ca} cables must originate from the $FIPEC_{20}$ Scen 1 test.
([8]) Measuring the hazardous properties of gases developed in the event of fire, which compromise the ability of the persons exposed to them to take effective action to accomplish escape, and not describing the toxicity of these gases.

SBI is not used for testing cables. Instead prEN 50399-2-1 and prEN 50399-2-2 is used, see Figure 9. These test specifications come from work done in a large project funded by the EU called FIPEC, Fire Performance of Electric Cables [4]. The FIPEC project includes also a study of cable installations and relevant reference scenarios as well as a comprehensive test program of different kinds of cables. All of that was used together with some additional test data in the development of the proposal for European testing and classification system.

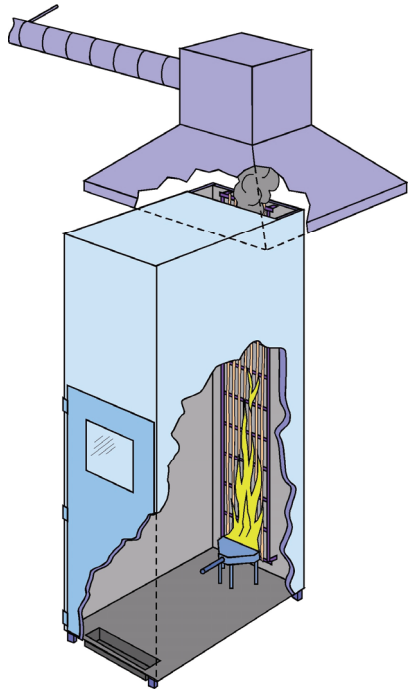

Figure 9. The large-scale test prEN 50399-2-1/2 used for classification of cables. The test chamber is 4 m high.

The cables are mounted on a ladder and the ignition source is a gas burner. Test specifications are shown in Table 4.

Table 4. Test conditions for classification of cables

Class $B1_{CA}$	• prEN 50399-2-2 with mounting according to FIPEC Scenario 2 • 30 kW ignition source • 20 minutes testing time
Class $B2_{CA}$- Class D_{CA}	• prEN 50399-2-1 with mounting according to FIPEC Scenario 1 • 20 kW ignition source • 20 minutes testing time

The reason for the differences in test procedure between class $B1_{CA}$ and the other classes mainly has to do with the need for a class of very high performance and therefore the more severe test. The top class A_{CA} is for products that practically cannot burn, i.e. made of ceramic materials.

In the same way as for the other product groups, reference scenarios were used to identify the class limits. In this case, there were two reference scenarios, a horizontal and a vertical.

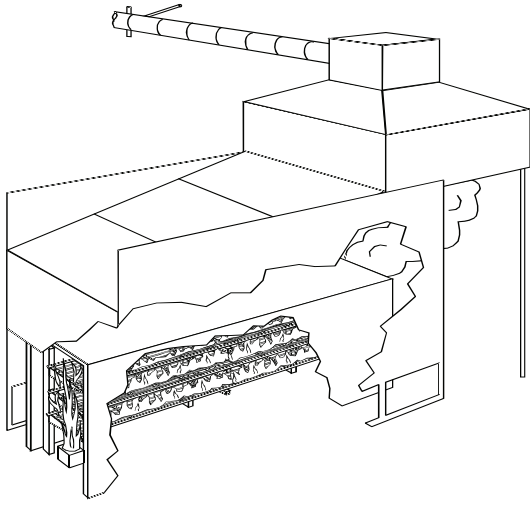

Figure 10. Horizontal reference scenario for cables, from the FIPEC project [4].

The horizontal reference scenario comprises three cable ladders mounted horizontally on top of each other. They are ignited in one end with a burner giving 40 kW for 5 minutes, then 100 kW for another 10 minutes and finally 300 kW for 10 minutes. The supply of air is by natural ventilation.

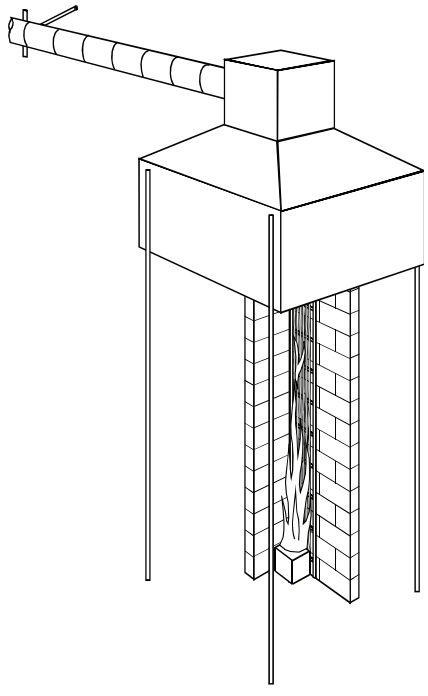

Figure 11. Vertical reference scenario for cables, from the FIPEC project [4].

In the vertical scenario, a cable ladder is mounted in a corner. The heat output from the burner is the same as for the horizontal scenario.

The performances of the different classes are approximately as follows.

Class A_{ca}
Level of highest performance corresponding to products that practically cannot burn, i.e. ceramic products.

Class $B1_{ca}$
Products that are combustible but show no or very little burning when exposed to both the reference scenario tests and the classification test procedures prEN 50399-2-1 and prEN 50399-2-2.

Class $B2_{ca}$ and Class C_{ca}
Products that do not give a continuous flame spread when exposed to the 40-100 kW ignition source in the horizontal reference scenario; and that do not give a continuous flame spread, show a limited fire growth rate and show a limited heat release rate when tested according to prEN 50399-2-1 with mounting according to FIPEC Scenario 1.

Class D_{ca}
Products that show a fire performance better than ordinary not flame retardant treated polyethylene and a performance approximately like wood when tested in the reference scenarios. When tested according to the prEN 50399-2-1 with mounting according to FIPEC Scenario 1 the products show a continuous flame spread, a moderate fire growth rate, and a moderate heat release rate.

Class E_{ca}
Products where a small flame attack is not causing rapid flame spread.

A large number of tests is available [24], [25] were FIGRA in the reference scenarios can be compared with the actual classification tests, see Figure 12, Figure 13 and Figure 14.

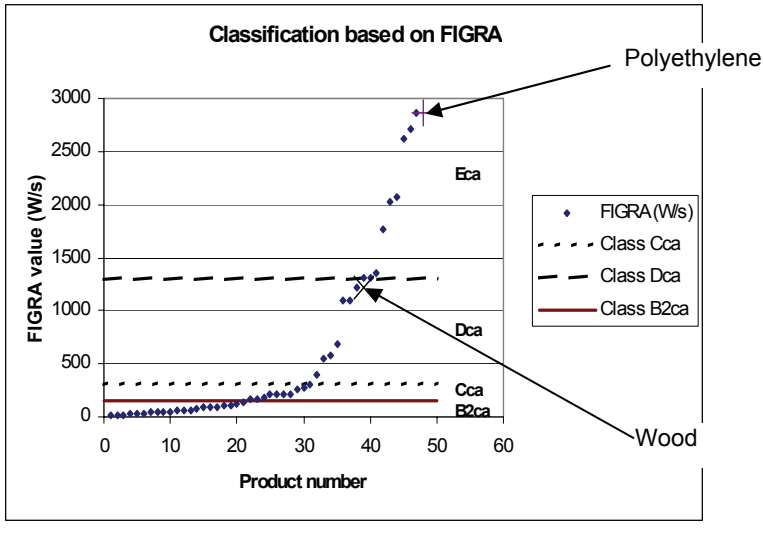

Figure 12. The class limits for FIGRA for the classes $B2_{ca}$, C_{ca} and D_{ca} compared to data from 50 products. Cables with FIGRA > 3000 W/s not shown. Ref [25].

We see from Figure 12 that the limit value for class D_{ca} was chosen very similar to that of wood (tested in bars of 10 mm diameter). We also see that untreated polyethylene cables falls into class E_{ca}.

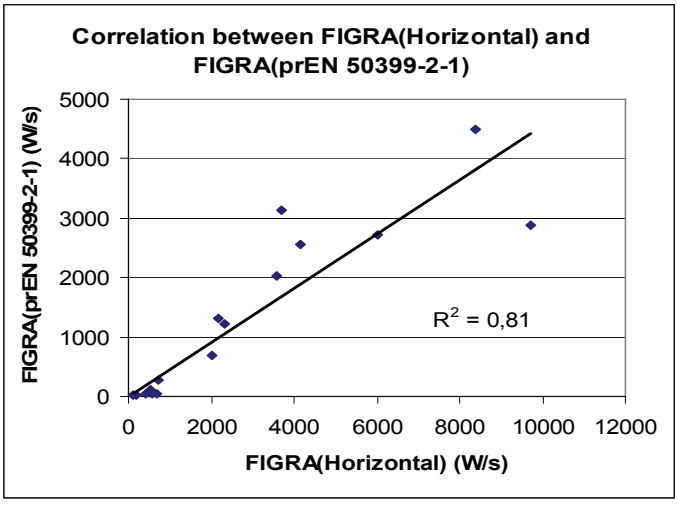

Figure 13. Correlation between FIGRA for the horizontal reference scenario and FIGRA(prEN 50399-2-1). From ref [24] but with the regression line taken through the origin. 17 tests in each method.

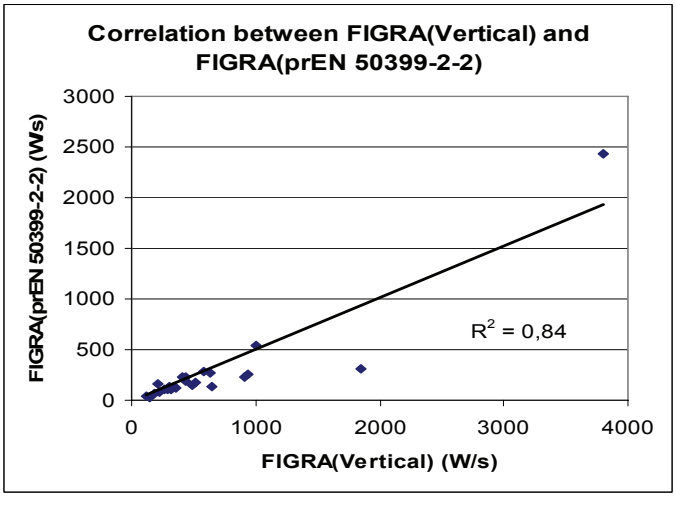

Figure 14. Correlation between FIGRA for the vertical reference scenario and FIGRA(prEN 50399-2-2). From ref [24] but with the regression line taken through the origin. 25 tests in each method.

FIGRA for the reference scenarios and the classification tests are calculated using the SBI principle with a threshold value of 50 kW and HRR averaged over 30 s. The correlations between the classification tests and the reference scenarios are good.

2.5 FIGRA and quality assurance testing in small scale

ISO 21367 [27] was developed by an ISO technical committee, TC 61 plastics. It is a small-scale screening test for quality assurance purposes. The test sample is a vertical flat sheet 0,5 m x 0,7 m. The lower part of the sample is exposed to heat from an electrical heater, 10 kW/m^2 – 60 kW/m^2. A pilot flame ignites flammable gases from the specimen. HRR is measured and FIGRA is obtained. Work has been done by LNE, Laboratoire national de métrologie et d'essais, on comparing the SBI test with ISO 21367 [28], see Figure 15.

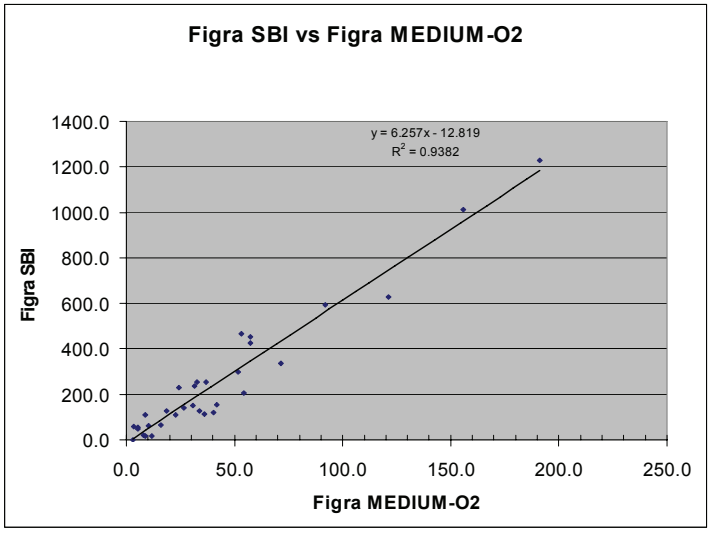

Figure 15. Correlation between FIGRA for ISO 21367, called MEDIUM-O2, and FIGRA(SBI). From ref [28].

The intention with this test is to use it as a cheap and simple way to do quality assurance testing or product development on plastics. The correlation with SBI is therefore established through FIGRA. The result is quite good and it demonstrates that FIGRA also works in “the other direction” from the intermediate scale, the SBI, to the small scale ISO 21367.

2.6 FIGRA and hazard assessment under the CPD

Section 2.1.1 - 2.5 show how FIGRA can be used to compare product performance for a variety of fire scenarios. Table 5 gives a summary.

Table 5. Versatility of the parameter FIGRA.

TYPE OF PRODUCT	TEST PROCEDURE	REFERENCE SCENARIO	CORRELATION COEFFICIENT	COMMENTS
Surface linings used in buildings	SBI, Single Burning Item , EN 13823	Room Corner Test, ISO 9705/EN 14390	$R^2 = 0,97$ ($R^2 = 0,87$ in the classification region)	Correlates with flashover in the Room Corner Test
Pipe insulation	SBI, Single Burning Item , EN 13823	Room Corner Test adapted for pipe insulation, ISO/DIS 20632	$R^2 = 0,93$	Simulates typical pipe insulation installations
Cables	Vertical cable ladder test, prEN 50399-2-1	Horizontal installation of three cable ladders on top of each other burning from one end	$R^2 = 0,81$	Simulates typical cable installations
Cables	Vertical cable ladder test, prEN 50399-2-2	Vertical cable installation in corner	$R^2 = 0,84$	Simulates typical cable installations
Plastic materials	SBI, Single Burning Item , EN 13823	Small-scale test for plastics, ISO 21367. Not reference scenario	$R^2 = 0,94$	ISO 21367 is a small scale quality assurance test

It is clear that the FIGRA index ranks products similarly for different tests or going from a test to a reference scenario for a variety of situations. However, product ranking is of limited value for the regulator if the ranking cannot be explained in terms of perceived hazard.

The process of linking real fires to a small-scale test to a hazard is shown in Figure 16.

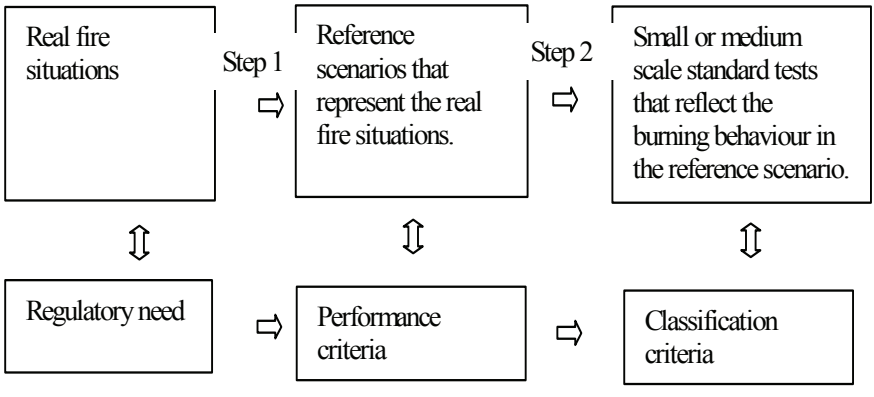

Figure 16. A process of how to create a system for product classification based on hazard.

The European system for reaction to fire corresponds well to Figure 16 but not always perfectly. The CPD was created to take away trade barriers for construction products and therefore the European system also considers market needs for industry and legal situations in member states which sometimes influences the strict system of Figure 16.

Starting point is a real fire situation where there is a regulatory need, for example interior surface linings. Almost all building codes worldwide consider that there is a need to regulate linings fire performance.

The reference scenario for a lining is the Room Corner Test. The fire growth during a test can be seen to represent ordinary rooms in buildings. The HRR from the ignition source (at 300 kW) reaches about 1/3 of the HRR needed for flashover, which is a severe heat attack for the tested lining. A similar ignition situation in a larger room was found to give a slower fire growth and a longer time to flashover [29].

Thus, the Room Corner Test can be seen to represent ordinary room fires for linings under severe conditions. The performance criteria is the occurrence of and time to flashover. In Europe, the national systems were quite different before harmonisation. However, many countries had a class corresponding to plaster board, no flashover, and wood, flashover. Thus, the flashover performance criterion for the Room Corner Test is applicable in many countries.

The SBI test and the FIGRA parameter can predict the flashover in the Room Corner Test. The classes can be defined with a link to the hazard and all the steps in Figure 16 are then taken.

Similar principles as for linings were applied for pipe insulation and cables although flashover is not the performance criteria in these cases.

All systems described above contain six classes and a class for no performance determined. The classes largely have common properties regarding fire growth even if the products are quite different. Classes A1, $A1_L$ and A_{ca} represent the top class and comprise non-combustible products for example mineral wool with limited binder content, ceramics and metals. Classes B, B_L and $B1_{CA}$ represent behaviour of products that would not show any fire growth even when exposed to quite large ignition sources like the 300 kW burner. A typical example is the plasterboard or a fluorinated plastic cable. Classes D, D_L and D_{ca} reflect the typical behaviour of untreated wood products excluding insulating low-density board. The intermediate classes show intermediate behaviour. For example, a class C lining will not give flashover for the 100 kW burner but will for the 300 kW burner.

Step 2, the correlation between the reference scenario and the classification test must ideally work for every type of product on the market. This is however not the case. There will be exemptions, for example steel sandwich panels with insulation. These products must be tested in large scale, perhaps even larger than the reference scenario. Mechanical properties of the steel that protects the underlying combustible insulation determine most often the hazard of the product. The SBI test or any small-scale test is not useful to measure that.

The correlation of data between the smaller scale tests and the reference scenarios can be normalised by setting the highest value in a set of data equal to 100. Then all the data appears on the same scale, 0-100, and can be plotted into one diagram see Figure 17.

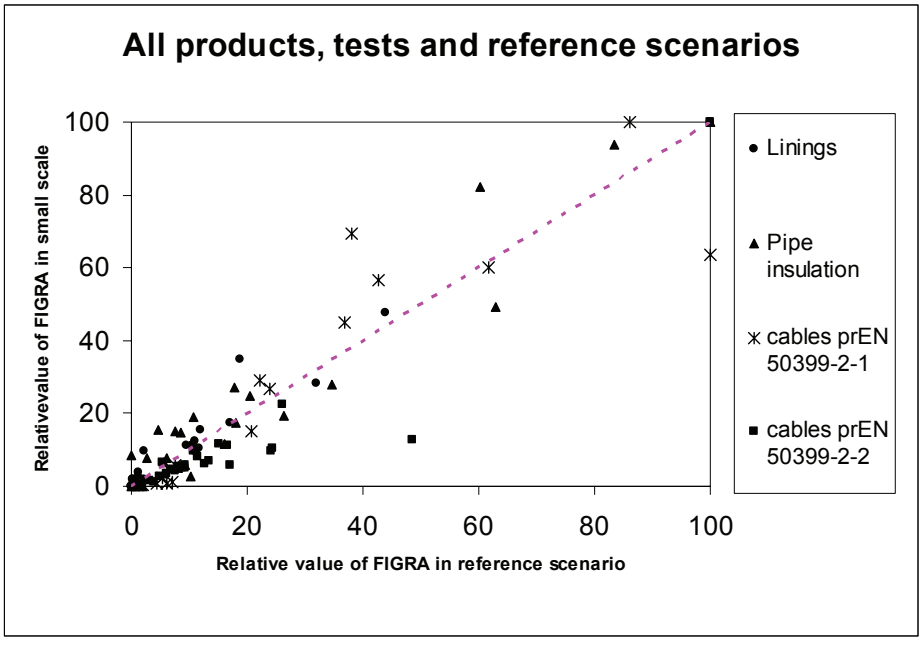

Figure 17. Correlation between small-scale and reference scenario for all data. Normalised data. The dotted middle line is the one-to-one relation. The least square correlation R^2 for all data points is 0,89.

Most data points appear below the value 40. This is because only few products in each series show extreme fast burning. The two clear outliers are cables. The reference scenarios are the Room Corner Test, large-scale pipe insulation installation, horizontal cable installation and vertical cable installation respectively. The small-scale test data comes from the SBI, prEN 50399-2-1 and prEN 50399-2-2 respectively. The data from the small-scale ISO standard 21367, see Figure 15, was omitted, as this test is not a part of the legal system of CPD. The products represented are surface linings for example boards, wall coverings, laminates, insulation. Others are pipe insulation, high and low voltage power cables and communication cables. The materials involved are wood, plaster, PVC, melamine, PUR, PIR, PE, EPS, XPS, vinyl rubber, wool, cotton, calcium silicate, stone wool, glass wool, varnish, paint and so on. The number of large-scale scenario tests shown in Figure 17 is about 100 and the number of small-scale tests is about 1000 including replicates. The data comes from 17 laboratories around Europe [6], [13], [16], [19], [20], [21], [24], [25]. The mentioned products represent well the European market and they are all covered by the CPD.

Therefore, Figure 17 gives a good picture on the accuracy of the European system for reaction to fire testing under the CPD to predict hazard of fire growth defined by reference scenarios. The least square correlation R^2 for all data points is 0,89. If we accept that the reference scenarios in their turn represent real hazards then Figure 17 is seen to represent the ability of the legal system to predict product hazard in terms of their tendency to contribute to fire growth.

The use of FIGRA as a classification tool makes it versatile due to its relation to hazard in realistic scenarios and by its robustness. It works for different products, tests and scenarios. FIGRA has been in operation now for some years on a large market with surprisingly small problems.

3 Room fire growth on linings in wall and ceiling configuration - Analysis based on heat transfer

Consider flame spread on the walls and the ceiling in a room scenario that may lead to flashover. The room scenarios considered in this work all have the linings mounted on both the walls and the ceiling. This is the Room Corner Test standard configuration.

We now wish to predict the heat release rate as a function of time for an experiment, especially the period close to flashover. The materials property data needed in this work will be mainly from the Cone Calorimeter, ISO 5660.

3.1 Thermal theories for prediction of ignition time and flame spread

3.1.1 Ignition

In the standard ISO 13943, "Fire Safety Vocabulary" [30] ignition is defined as "initiation of combustion". The ignition phenomena involve heat transfer, physical processes and chemical reactions in a complex interaction. Attempts to model ignition therefore require simplifications. The very comprehensive Ignition Handbook by Babrauskas [31] provides an excellent source of information on various aspects of ignition.

The energy balance for a control volume can be expressed as:

$$\begin{bmatrix} Net\ rate\ of\ energy \\ flow \end{bmatrix} = \begin{bmatrix} Rate\ of\ energy \\ stored \end{bmatrix} + \begin{bmatrix} Rate\ of\ energy \\ used\ for\ pyrolysis \end{bmatrix} + \begin{bmatrix} Rate\ of\ energy \\ used\ for\ melting \end{bmatrix}$$
$$+ \begin{bmatrix} Rate\ of\ energy \\ used\ for\ evaporation\ of\ water \end{bmatrix} + \cdots + \cdots +$$

However, often all the energy terms except the storage term are ignored in ignition models. One reason is that materials data is not available. Such data maybe very difficult or even impossible to measure.

Some ignition models only consider energy conservation and assume that the solid is inert up to the point of ignition. For the purpose of this work, they are called "thermal models". Pyrolysis, melting, evaporation of water and any other energy production or consumption inside the solid are ignored. Instead, the temperature development is assumed to be controlled by the Fourier heat transfer equation as found in many textbooks. In one dimension assuming constant thermal properties, it becomes.

$$k\frac{\partial^2 T}{\partial x^2} = \rho c\ \frac{\partial T}{\partial t} \qquad 1$$

Below the thermal model is used to analyse ignition processes.

In the Cone Calorimeter, ISO 5660, a horizontal sample is heated from above at constant heat exposure. As the sample surface temperature rises, it will loose heat by radiation and convection. Then at a certain surface temperature, the sample ignites. The net heat flow at the surface may be written as

$$\dot{q}_s'' = \alpha_s \dot{q}_e'' + \alpha_s \sigma T_\infty^4 - \varepsilon_s \sigma T_s^4 + h_c (T_\infty - T_s) \qquad 2$$

Then the heat balance at the surface gives in one dimension the boundary condition $\dot{q}_s'' = -k\left.\frac{\partial T_s}{\partial x}\right|_{x=0}$

The initial temperature of the solid is assumed to be equal to the ambient temperature, $T_i = T_\infty$, and then by taking $\alpha_s = \varepsilon_s$ (Kirchhoff's identity) and by rearranging the boundary condition becomes

$$-k\left.\frac{\partial T_s}{\partial x}\right|_{x=0} = \varepsilon_s \dot{q}_e'' - \varepsilon_s \sigma (T_s^4 - T_i^4) - h_c (T_s - T_i) \qquad 3$$

Solving the Fourier equation for time to ignition with the boundary conditions of eq 3 has to be done numerically. Different ways to simplify it has been proposed. Lawson and Simms [32] used

$$\dot{q}_s'' = \dot{q}_e'' - h_{eff} (T_s - T_i\ ) \qquad 4$$

where h_{eff} is taken as an effective heat transfer coefficient including the radiation and the convective heat losses at the surface. The solid is also assumed to absorb all of the incident radiant heat flux, i.e. ε = 1. Ignition will occur when T_s reaches T_{ign}. The quantity $h_{eff}(T_{ign} - T_i)$ is called critical flux for ignition, $\dot{q}''_{cr}$, and at ignition temperature we can write

$$\dot{q}''_s = \dot{q}''_e - \dot{q}''_{cr} \qquad 5$$

If the heat flux at the surface as well as the material properties are assumed constant and the exposed body may be assumed semi-infinite, than the Fourier equation can be solved by Laplace transforms and the surface temperature rise may be calculated as

$$T_s - T_i = \frac{2\dot{q}''_s}{\sqrt{\pi k\rho c}}\sqrt{t} \qquad 6$$

which is found in textbooks on heat transfer [33].

Thus the time to reach the ignition temperature for a semi-infinite solid is

$$t_{ign} = \frac{\pi\, k\rho c\,(T_{ign} - T_i)^2}{4\dot{q}''^2_s} \qquad 7$$

and by inserting eq 5

$$t_{ign} = \frac{\pi\, k\rho c\,(T_{ign} - T_i)^2}{4(\dot{q}''_e - \dot{q}''_{cr})^2} \qquad 8$$

The quantity $k\rho c$ is often referred to as the "thermal inertia". It is an important material parameter in fire safety engineering as it determines the rate at which material surfaces can be heated and ignited. The assumption that $\dot{q}''_s = \dot{q}''_e - \dot{q}''_{cr}$ is the lowest value that $\dot{q}''_s$ gets during the ignition process. The ignition time according to eq 8 is therefore overestimated.

Tewarson [34] introduced the so called the thermal response parameter, TRP, defined as

$$TRP = (T_{ign} - T_i)\sqrt{k\rho c}\sqrt{\frac{\pi}{4}} \quad 9$$

When inserted into eq 8 it gives the time to ignition as

$$t_{ign} = \left(\frac{TRP}{\dot{q}''_e - \dot{q}''_{cr}} \right)^2 \quad 10$$

or

$$\dot{q}''_e - \dot{q}''_{cr} = TRP \cdot \frac{1}{\sqrt{t_{ign}}} \quad 11$$

TRP is found by plotting $1/\sqrt{t_{ign}}$ versus the external heat flux, $\dot{q}''_e$ and determining the slope.

Janssens [35], [36] uses the assumptions according to equation 4 and applies statistical analysis for an approximate solution. He proposes the expression

$$\dot{q}''_e - \dot{q}''_{cr} = 0{,}73\dot{q}''_{cr}\left(\frac{k\rho c}{h_{eff}^2} \right)^{0{,}55} \frac{1}{t_{ign}^{0{,}55}} \quad 12$$

For thermally thin solids, a simple heat balance gives the solution for the case of constant heat flux at the surface we have

$$t_{ign} = \frac{c\rho d\,(T_{ign} - T_i)}{\dot{q}''_s} \quad 13$$

However, this expression suffers from the same approximation as for thermally thick products. The heat flux at the surface of the sample is not constant in reality.

Janssens [35] used numerical methods and proposes the correlation for the thermally thin case when the back face is insulated, which in most cases corresponds to the situation in the Cone Calorimeter up to ignition

$$\dot{q}''_e - \dot{q}''_{cr} = 1{,}9\dot{q}''_{cr}\left(\frac{c\rho d}{h_{eff}}\right)\frac{1}{t_{ign}} \qquad 14$$

For equations 11, 12 and 14 described above a plot of $1/t_{ign}^{n}$ versus $\dot{q}''_e$ gives a straight line (n=1 for the thermally thin case and n= 0,5 or 0,55) for the thermally thick case. The straight line will intercept the x-axis at $\dot{q}''_{cr}$ and the slope will be the group of parameters represented in the different equations above. Janssens [37] uses the equation

$$\varepsilon\dot{q}''_{cr} = h_c(T_{ign} - T_i) + \varepsilon\sigma(T_{ig}^4 - T_i^4) = h_{eff}(T_{ig} - T_i) \qquad 15$$

which is found by combining eq 3,4 and 5 at ignition temperature.

Janssens has also measured the convective heat transfer coefficient, h_c, at different heat fluxes in the Cone Calorimeter [37]. When h_c and $\dot{q}''_{cr}$ is known it is possible to calculate the effective thermal inertia and the ignition temperature using eq 12 and 15.

Janssens correlations above were applied to Cone Calorimeter data from the EUREFIC project [38] and SP database [39], see Figure 18.

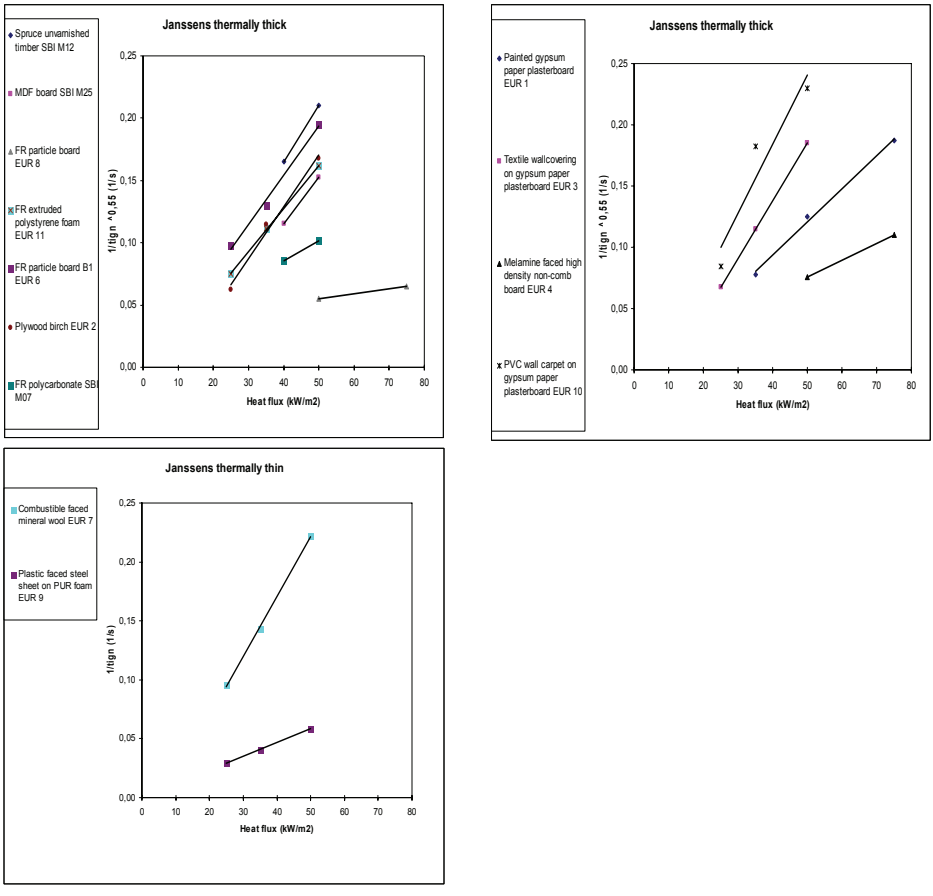

Figure 18. Plots of ignition data versus external heat flux for building products tested in the Cone Calorimeter.

Each data point is an average from three replicate tests. The critical heat flux for ignition should according to the theory be found at the intercept of the x-axis. The uncertainty is however large as extrapolating a straight line from high heat fluxes to a critical value at thermal equilibrium ignores processes that are not linear over that range. Babrauskas [31] chapter 7 discusses this in depth. He recommends that an experimental value of the minimum flux for ignition is used, $\dot{q}''_{\min}$, as alternative to $\dot{q}''_{cr}$ and that it is determined in tests where the heat exposure is changed in steps of 1 kW/m^2. When $\dot{q}''_{\min}$ is much larger than $\dot{q}''_{cr}$ more realistic values of the ignition temperature are calculated according to ref [31]. Tewarson also uses an experimental value.

He defines "Critical Heat Flux", CHF, as the minimum heat exposure for ignition for a test in the Fire Propagation Apparatus [40] of a sample that is blackened to achieve the emissivity equal to unity [34].

A procedure derived by Quintiere [41] uses the so-called LIFT apparatus [42]. The critical flux, $\dot{q}''_{0,ig}$, using the Quintiere procedure is found experimentally as the lowest level were an ignition is observed. The sample in the LIFT test is vertical. Therefore, the flow pattern of fuel and air around the sample will be different from the Cone Calorimeter where the sample is horizontal.

It is clear that the different procedures to determine thermal parameters will give different results. The critical flux for ignition is defined in two ways. It may be the theoretical intercept with the x-axis or a minimum value found experimentally. Depending on definition, the calculated ignition temperature will differ. Plotting $1/t_{ign}^{0,5}$ (Tewarson) or $1/t_{ign}^{0,55}$ (Janssens) versus $\dot{q}''_e$ will give slightly different results for the slope and the critical flux for ignition. Finally, there are different test procedures used to determine the thermal parameters, which will give different results as discussed above.

Janssens discusses a problem with a glass fibre reinforced polyester composite [37]. When the ignition data at heat exposures of 50 kW/m^2 and less was plotted versus $\dot{q}''_e$ the result was a very low value of $\dot{q}''_{cr}$ and when the data above 50 kW/m^2 the result was even negative. Janssens concludes that the data points taken above 50 kW/m^2 are uncertain due to the short ignition times at high heat fluxes. However, a similar tendency is seen in Figure 18 were some regression lines result in low or even negative values of $\dot{q}''_{cr}$. Each data point is the result of a triplicate test but data on more heat exposure levels is needed for a detailed analysis. For the purpose of this work, thermal properties of the products are not deduced. The reasons are the uncertainties of methods, calculation procedures and the need for a lot of test data.

However, the experimentally determined slopes of the lines in Figure 18 appears to be reliable for calculating the ignition time for a certain flux based on experimental data from another heat flux. When there is data from three heat exposures, they appear on a straight line only with few exceptions. However, the thermal theory says that the heat flux at the surface should be constant. Therefore, it is interesting to estimate the deviation from that assumption for different heat fluxes.

Janssens [37] has measured the convective heat transfer coefficient in the Cone Calorimeter and gives for heat fluxes less than 50 kW/m^2 the relation $h_c = 0{,}0118 + 3{,}4 \cdot 10^{-4} \dot{q}''_e$ which is 0,0237 kW/m^{2}K at 35 kW/m^2. Selecting ε to 0,9 we get from eq 3 the surface heat flux versus surface temperature, Figure 19.

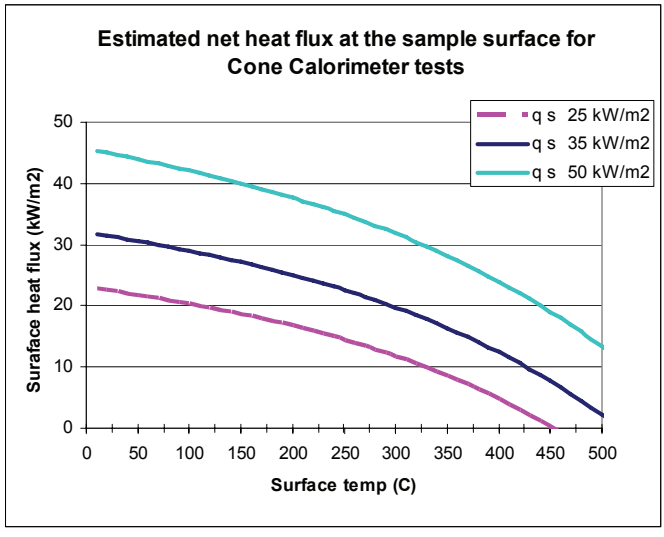

Figure 19. Estimated net heat flux at the sample surface as a function of surface temperature in a Cone Calorimeter test using data of the convective heat transfer coefficient, h_c, from Janssen [37] and eq 3.

The net heat flux at the surface starts at 90% of the external radiation as ε = 0,9. Then there is a drop following the temperature rise on the sample surface to become minimum at the ignition temperature. Typical ignition temperatures are between 250 and 350 degrees C. At an external flux of 50 kW/m^2, the surface heat flux has dropped about 30% when the surface temperature is 300 C (excluding the initial drop of 10 % due to the value of ε). However, at 25 kW/m^2 the surface heat flux has dropped about 50% at 300 C. Equation 7 assumes constant heat flux at the surface and is therefore less accurate at the lower heat fluxes as earlier discussed even if there is ignition data down to 10 kW/m^2 found to correlate well for various products under well-controlled experiments [43]. Ignition data from very high heat fluxes works well with the theory but there is a new uncertainty added in the accuracy of the time measurement. Time to ignition is recorded manually as flaming of a certain duration.

The uncertainty becomes easily one or two seconds for these measurements. When ignition times are at the same order of magnitude, which frequently happens at a heat exposure of 75 kW/m^2, then the errors can be large.

For the purpose of this work, it is concluded that data to characterise a products ignition properties should be ignition time for different heat fluxes, in favour of deduced data on thermal inertia and ignition temperature. Ignition data from the Cone Calorimeter in the region of >25 kW/m^2 and $\leq$ 50 kW/m^2 should be used where the ignition times are relatively long and the heat fluxes are relatively high.

3.1.2 Flame spread

Data from Room Corner Test experiments [17] show a typical fire history. After a period of time the wall area under direct flame exposure starts to burn. The ceiling above the burner ignites and then there is fast flame spread along the ceiling and the upper parts of the walls. The ignition of the ceiling is critical for the major HRR growth in the room and is of the most importance for the occurrence of flashover.

The flame spread can be considered as a series of ignitions. The flame spread rate can be expressed as $V = l/\tau$ where l is a characteristic length related to the heated zone in advance of the flame and τ is the corresponding time to ignition, i.e. the time when the flame front arrives [44]. In the Room Corner Test the flame spread that is important for the rapid fire growth is wind aided. The flame spread along the ceiling and the upper walls quite rapidly can result in flashover. Gas flow and flame spread follows the same direction, i.e. concurrent or wind aided. Only the flame spread down along the wall towards the floor moves opposite the direction of the flow. However, for the case when the combustible linings cover the walls and the ceiling this flame spread happens at a later stage, is of less importance, and is not considered in this work. A frequently used model for flame spread was published by Saito, Quintiere and Williams [45], see Figure 20.

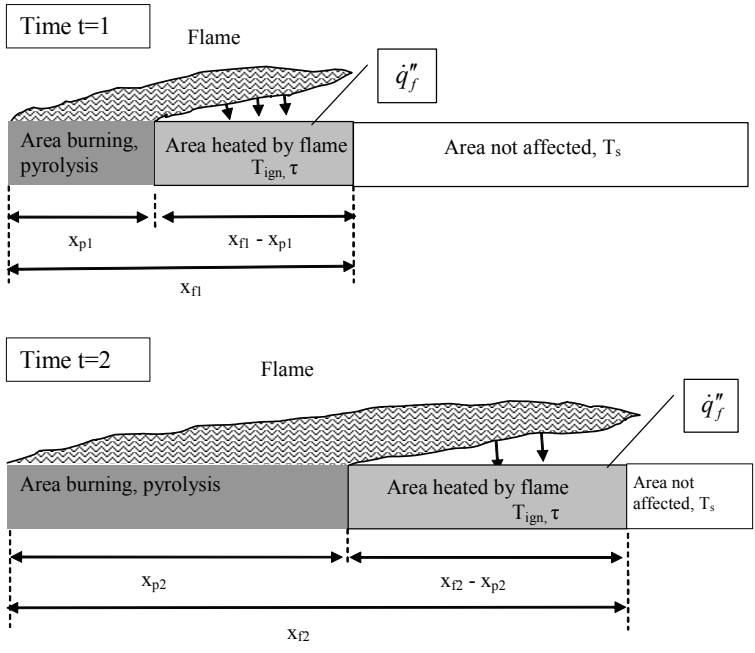

Figure 20. Principle of wind-aided flame spread model ignoring burnout.

The flame leans over the not yet ignited material and heats it to ignition temperature, T_{ign}, assuming that the heat flux, $\dot{q}''_f$, at the surface is constant. Outside of the flame area the heat exposure from the flames is neglected, the surface heat flux is assumed zero and the temperature equals the surface temperature. The characteristic length becomes the length heated by the flame, i.e. $l = x_{f1} - x_{p1}$ at time t = 1. Generally, the flame spread rate can be approximated by

$$V = \frac{x_f - x_p}{\tau} \qquad 16$$

The flame length is often correlated with the heat release rate according to

$$x_f = K(\dot{Q}')^n \qquad 17$$

where $\dot{Q}'$ is the HRR per unit width producing flames in the room.

The factor K is a correlation factor that is dependant of the scenario. It has one value for a corner scenario, another for an open wall and so on. The exponent n varies between 0,5 and 1,0. n = 1 is used for the models studied in this work, i.e. the flame length is linearly dependent on the HRR. K is called flame area constant (with the unit m^2/kW for n=1) when used in expressions for area growth rate.

The HRR along the length of the pyrolysis zone can be obtained from

$$\dot{Q}' = \int_0^{x_p} \dot{Q}''(x)dx \qquad 18$$

where $\dot{Q}''$ maybe derived from Cone Calorimeter test data.

Combining this information leads to expressions for flame spread rate and HRR described for example in [46] and shown in section 3.3.2.

The ignition time τ can be taken from the heating of a thermally thick solid, cf. eq 7

$$\tau = \frac{\pi k\rho c (T_{ign} - T_s)^2}{4(\dot{q}''_f)^2} \qquad 19$$

where $\dot{q}''_f$ is the heat flux at the surface assumed constant over the characteristic length and zero outside of this length.

All of the assumptions and simplifications made in arriving at eq 7 apply also to eq 19. The additional assumption of constant heat flux absorbed by the fuel is a simplification. The surface heat flux will vary with position due to convection and the flame characteristics will give different radiant heat flux due to the soot content of the flame. So-called computational fluid dynamics models, CFD, can do better approximations of the flame. In a CFD model, chemical reactions of the combustion process and the soot fraction of the flame are included and the calculations are done for a large number of control volumes over the volume of the flame.

The models by Karlsson [46] and Wade [47] (the BRANZFIRE model), basically use the above approach for flame spread. Both models assume a constant value of surface heat flux; 35 kW/m^2 and 30 kW/m^2 respectively.

Quintiere mentions 25 kW/m^2 for upward turbulent flame spread on a vertical surface for relatively small fires $x_f < 1{,}4$ m [48], [49].

When fuel is completely consumed the flame base will no longer begin at x = 0 but some where further along the fuel surface, burnout. BRANZFIRE also includes burnout to determine the flame spread. For the models discussed below burnout is included when superposition is used, see eq 23. However, in a Room Corner Test experiment, burnout will only happen for the products not showing flame spread. When there is a flame spread this is faster than the time for an area to burn out before flashover occurs except in extraordinary cases.

During a Room Corner Test experiment, the flame spread rate will vary with time and location. Equation 19 implies a constant or shorter ignition time, τ, depending on the importance of the preheating. For a product that has a constant or growing HRR per unit area we expect longer flames as the pyrolysis area becomes larger and the HRR in the room grows. For wooden products, showing a high and steady HRR per unit area during the first few minutes of burning the flame spread is predicted to grow exponentially with time, [46], [50]. It is easily seen if $\dot{Q}''$ is constant, eq 18, then $\dot{Q}' = \dot{Q}'' x_p$ and $x_f = K\dot{Q}'' x_p$ which inserted into eq 16 and solved gives

$$x_p = a e^{\frac{K\dot{Q}''-1}{\tau} \cdot t} \qquad 20$$

where $x_{p0} = a$ at time t=0.

If x_p is assumed proportional to the HRR than the HRR will grow exponentially.

3.2 Conflame, an analytical formulation for prediction of the HRR history assuming an average constant flame spread rate.

In Figure 21 the measured flame spread rates along the ceiling during Room Corner Test experiments are shown [17].

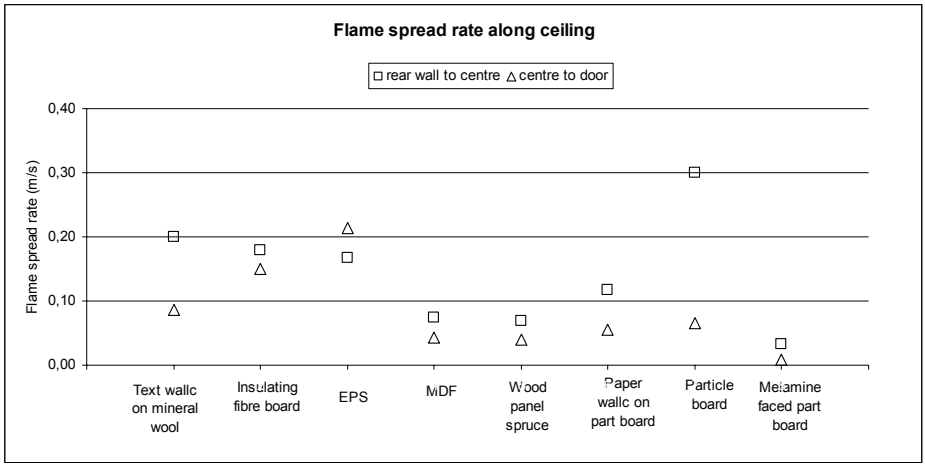

Figure 21. Measured flame spread along the ceiling during Room/Corner Test experiments. 100 kW ignition source.

Flame spread rate is calculated for two locations on the ceiling. The closest to the burner is from 0,9 m to 1,8 m from the rear wall, called rear wall to centre, and the other is from 1,8 m to 2,7 m, called centre to door. A surface temperature of 300 deg C was used as criterion for arrival of the flame front as it corresponded to the point where there was a sharp temperature rise. The span of the flame spread rate can be more than a factor three but it is often around ± 25% of the average value. In most cases, the flame spread rate is slower further away from the rear wall. For example the flame spread rate of spruce is 0,07 m/s close to the rear wall and 0,04 m/s at the second location further away from the rear wall. For particle board the values are 0,3 m/s and 0,066 m/s respectively. A possible explanation is that the heat attack is higher close to the rear wall were the plume and flames from the ignition source are located. The rate of gas movement along the ceiling, the ceiling jet, must also have an influence and if this is slower away from the corner plume then the flame spread is affected.

In any case, this data is not showing increase of flame spread rate over the ceiling with growing HRR as the flame spread theory discussed above predicts; but rather a decrease or constant rate. For the purpose of this work, we therefore consider the flame spread rate in the ceiling as a constant average value.

Then consider again $V = l/\tau$ similar to eq 16 but now assume that the flame spread rate is constant in two dimensions over the interior surface of the room, i.e. an area growth proportional to the square of time. In reality, the flame spread rate in different directions will differ as the fire grows but it is not one-dimensional in any case. During the development of Cone Tools [51], [52] the burning area as a function of time was taken from video recordings of Room Corner Test experiments and it was also found to be proportional to the square of time.

At the time, t_{ign}, the ignition burner ignites the product on an initial area, A_0. During the subsequent flame spread the size of the pyrolysis area at a certain time, $A(\xi)$, in the room is assumed proportional to the square of the flame spread rate and

$$A(\xi) = A_0 + C\xi^2 / \tau^2 \qquad 21$$

where ξ is the time elapsed after ignition, i.e. $\xi = t - t_{ign}$

The coefficient C may be seen as a scenario dependant correlation factor (m^2) and assumed product independent, i.e. be of the same character as the flame area constant mentioned above.

The value of A_0 can be considered as the area directly impinged by the flames from the ignition burner. This area is at the order of 0,5-1,5 m^2. However, ignition will probably first happen on a much smaller area where there is a local high heat exposure quickly followed by ignition of other areas exposed both to the flames from the ignitions source and the burning small area, i.e. rapid flame spread. Therefore, we ignore the initial phase in the expression for growth and use

$$A(\xi) = C\xi^2 / \tau^2 \qquad 22$$

If we know the size of the pyrolysis area with time according to eq 22 then the heat release rate, HRR, as a function of time in a Room Corner Test experiment can be calculated as the summation over the HRR from each pyrolysis area element.

It is assumed that the HRR per unit area as measured in the Cone Calorimeter is the same as the HRR per unit area that will be evolved by the surface elements in the room during the course of the fire. That is not necessarily true as the burning environment differ in the cone compared to the room, for example in supply of air and sample orientation. However, many mathematical models uses cone HRR data quite successfully and any deviations from the room situations are probably absorbed in correlation coefficients. As the burning area grows with the flame spread, the different area elements will show different HRR per unit area as they started to burn at different times. They will have reached different positions on the HRR curve. A convenient way of integrating the total HRR over the area elements is by superposition and the so-called Duhamel integral. The following integral applies in this case.

$$\dot{Q}(\xi) = \int_0^{\xi} \dot{Q}''_{cone}(\xi - s)\frac{d}{ds}(A(s))ds \qquad 23$$

$\dot{Q}(\xi)$ is the predicted HRR in the large-scale test and s is a dummy variable used for the integration.

This form of superposition for the Room Corner Test was first introduced by Wickström and Göransson [51] and was later coded into Cone Tools [52], a model used for predicting Room Corner Test experiments, see section 3.3.

The ignition burner in the Room Corner Test gives 100 kW during 10 minutes and then 300 kW for another 10 minutes. The heat exposure from the burner to the corner walls varies from 40 kW/m^2 at about 1,5 m height to 30 kW/m^2 at about room height, Kokkala et al [53]. For the purpose of this work 35 kW/m^2 is used as relatively large areas are exposed to that flux and therefore deemed representative for the ignition in the corner. For similar reasons 55 kW/m^2 for the 300 kW burner HRR is selected [53], [54]. Thus, t_{ign}, is taken from a Cone Calorimeter experiment at an external heat flux of 35 kW/m^2 and 55 kW/m^2 to represent the heat attack from the Room Corner Test ignition source.

The flame heat exposure caused by the wind aided flame spread along the ceiling and the upper walls is taken to be represented by a Cone Calorimeter test at 35 kW/m^2 which gives the value of τ. Note that both t_{ign} and τ can be calculated if reliable data on thermal inertia and ignition temperature is available. However, as discussed in 3.1.1 such data is difficult to find.

The HRR per unit area required for eq 23 can be the full cone curve, which implies that the equation must be solved numerically.

However, we wish to use an analytical form of the Cone Calorimeter HRR curve based on scalar data that allows eq 23 to be solved analytically. The reason is to explore single analytical expressions for room fire growth.

If occurring, the typical time period to flashover in a Room Corner Test experiment is within 3 minutes either from ignition of the burner or from the increase of the heat output to 300 kW after 10 minutes. Data reported from a Cone Calorimeter test includes $\dot{Q}''_{ave180s}$, which is the scalar value of the average HRR calculated from the time of ignition of the sample during 3 minutes. Accordingly, we select $\dot{Q}''_{ave180s}$ from the Cone Calorimeter as the characteristic HRR per unit area given off by the fuel. The heat exposure to the fuel in the Room Corner Test when burning was measured in the EUREFIC programme [55]. A heat flux meter was placed in the ceiling during an experiment. When the flame front just had passed approximately 50 kW/m^2 was measured. The level rose rapidly when flashover occurred. Therefore, $\dot{Q}''_{ave180s}$ for 50 kW/m^2 exposure in the Cone Calorimeter is chosen. Note that this is not the flame heat exposure ahead of the flame. The heat flux used for the $\dot{Q}''_{ave180s}$ is when the fuel is already heavily burning and must therefore be higher.

It now remains to give $\dot{Q}''_{cone}(t)$ a suitable analytical form to allow for an analytical solution of the integral equation above. The HRR curve from a Cone Calorimeter test is roughly bell shaped but with the early part after ignition rising rapidly compared to the decay part. Functions having this form are exponential expressions often used as probability density functions. Therefore, the cone curve is approximated by

$$\dot{Q}''_{cone}(t) = 2{,}72 \cdot \dot{Q}''_p \frac{t}{t_c} e^{-\frac{t}{t_c}} \qquad 24$$

where t is time after ignition in the test.

Kokkala et al used this form [56] taking a value of t_c when $\dot{Q}''_p$ occurs, the peak HRR measured in the Cone Calorimeter test. The value 2,72 = e is selected so that the peak of the HRR curve is about the same as the peak of the measured data. The equation is bell-shaped and the characteristic time, t_c, controls the width of the curve.

In order to conserve energy it is additionally required that the average HRR, $\dot{Q}''_{ave180s}$, shall be the same for the analytical expression. By keeping the same average value as for the experiment, the energy becomes the same when the 3 min period is finished

Then t_c can be obtained from the equation below.

$$\dot{Q}''_{ave180s} = \frac{1}{180} \frac{2{,}72 \cdot \dot{Q}''_p}{t_c} \int_0^{180} t \cdot e^{-\frac{t}{t_c}} dt \qquad 25$$

This means that t_c will not exactly be the value at $\dot{Q}''_p$ and there are two solutions for t_c, eq 25, one large and one small. The smaller value gives the good fit and is therefore used in this work. In Figure 30, chapter 3.5, two examples of analytical HRR curves are given.

Note that average values from replicate cone tests are used, typically three tests. The calculated HRR curve is an "average" curve and therefore less sensitive to variation compared to a single test.

The approximation does not represent the second peak HRR for products that after a long time of testing in the Cone Calorimeter burns through and involves the backside of the sample. This behaviour results in two HRR peaks. For wood of thickness 10-12 mm this happens after about 10 minutes. However, that period of the fire is post flashover in a Room Corner Test experiment and not included in this analysis.

Insertion of eq 21 and 24 into eq 23 gives

$$\dot{Q}(\xi) = \int_0^{\xi} \frac{d}{ds}(A(s))\dot{Q}''_{cone}(\xi - s)ds = 5{,}44\frac{C\dot{Q}''_p}{\tau^2 t_c}\int_0^{\xi}(s(\xi - s)e^{-\frac{(\xi - s)}{t_c}})ds = \qquad 26$$

$$5{,}44 \cdot C\dot{Q}''_p t_c \frac{1}{\tau^2}\left[e^{-\frac{\xi}{t_c}}\left(\xi + 2t_c\right) + \xi - 2t_c\right]$$

Inserting $\xi = t - t_{ign}$ gives

$$\dot{Q}(t) = 5{,}44 \cdot C\dot{Q}''_p t_c \frac{1}{\tau^2}\left[e^{-\frac{(t - t_{ign})}{t_c}}\left(t - t_{ign} + 2t_c\right) + t - t_{ign} - 2t_c\right] \qquad 27$$

for $t \geq t_{ign}$, t is time elapsed after the start of the test.

As earlier discussed t_{ign} as measured in the Cone Calorimeter for an external heat flux of 35 kW/m^2 is used. If the time to ignition in the cone is available at other heat fluxes, than it can be calculated for 35 kW/m^2 using Janssens procedure as shown in Figure 18. If data from only one heat flux level is available then the time to ignition at 35 kW/m^2 is calculated as $t_{ign35} = t_{igntested}\left(\frac{\dot{q}''_{tested}}{35}\right)^{1{,}82}$ or $t_{ign35} = t_{igntested}\left(\frac{\dot{q}''_{tested}}{35}\right)$ when thermally thin

Finally, the coefficient C in eq 27 must be determined. It is assumed that C will include the scenario dependant factors that are included in the area growth during a Room Corner Test experiment and that these factors are product independent. C is a function of the experimental design and must therefore be taken from experimental data. The experimental data from wood products was used because of the availability of good data from a selection of different products. In this way a value of C = 1,2 m^2 was selected.

$$\dot{Q}(t) = 1{,}2 \cdot 5{,}44 \cdot \dot{Q}''_p t_c \frac{1}{\tau^2}\left[e^{-\frac{(t - t_{ign})}{t_c}}\left(t - t_{ign} + 2t_c\right) + t - t_{ign} - 2t_c\right] \qquad 28$$

for $t \geq t_{ign}$, t is time elapsed after the start of the test.

In the Room Corner Test, the maximum area that can burn is 32 m^2 as this is the area covered by the product. Eq 28 therefore overestimates the HRR if used for areas more than 32 m^2.

However, this did not happen as the predicted area never exceeded 32 m^2 before flashover. Experimental data also show that the area involved is about 20 m^2 at flashover [17].

There is no flame spread for high performance products and then eq 28 does not apply. However, they may ignite only where the flames from the ignition source attack. Then there is no flame spread but burning from a constant area. This area is taken to 1,5 m^2 corresponding roughly to the area of flames from the burner when giving 100 kW. For this case eq 28 is replaced by.

$$\dot{Q}(t) = 1{,}5 \cdot 2{,}72 \dot{Q}''_p \frac{t - t_{ign}}{t_c} e^{-\frac{t - t_{ign}}{t_c}} \qquad 29$$

for $t \geq t_{ign}$, t is time elapsed after the start of the test.

After 600 s when the burner heat output is raised to 300 kW another 3 m^2 of area is assumed to ignite. The value 1,5 in eq 29 then becomes 3,0 when there is no flame spread and t_{ign} is taken from a Cone Calorimeter experiment at 55 kW/m^2.

A criterion for flame spread to occur is that the heat exposure from the flames of the product itself must exceed a certain critical value, which can be expressed as a critical heat release rate, CHRR. Below CHRR there is no flame spread. Tewarson [57] reports an average CHRR value of 96 kW/m^2 ranging from 65-108 kW/m^2 for a number of polymers like polyethene, polyurethane and polystyrene. Quintiere [58] discusses a CHRR of 50-100 kW/m^2. He mentions 50 kW/m^2 as the condition for sustained burning and 100 kW/m^2 as the condition for upward flame spread.

A critical value of $\dot{Q}''_{ave180s}$ from the Cone Calorimeter can be used as criterion for continuous flame spread [31]. $\dot{Q}''_{ave180s}$ is an average value over 180s while the definition of CHRR for flame spread uses the characteristic HRR value prior to ignition. This HRR must be maintained for sometime before the products ignite but an average over 180s is a little bit to long. Therefore, Quintieres value of 100 kW/m^2 used directly for $\dot{Q}''_{ave180s}$ will be too high. In the European Union project called CBUF [59] (Combustion Behaviour of Upholstered Furniture) $\dot{Q}''_{ave180s}$ was estimated to be at least 65 kW/m^2 for a propagating fire to occur in upholstered chairs. Upholstery is generally easier to ignite than building products so they should have a lower critical value of $\dot{Q}''_{ave180s}$.

Thus we select somewhat arbitrary a value of $\dot{Q}''_{ave180s}$ = 75 kW/m^2 in the middle of the interval suggested by Quintiere and use that as the CHRR for flame spread.

During the 100 kW burner period in the Room Corner Test the heat exposure of the sample is about 35 kW/m^2. When the burner HRR is increased to 300 kW after 10 min the heat exposure increases to about 55 kW/m^2 and acts over a larger area. In addition to the higher heat flux, there has been 10 min preheating. Therefore, CHRR of 75 kW/m^2 for $\dot{Q}''_{ave180s}$ from the product is higher than needed to start flame spread and instead $\dot{Q}''_{ave180s}$ = 55 kW/m^2 is used. The reduction, 20 kW/m^2, is the same as the increase in heat exposure from the ignition burner.

Equations 28 and 29 with the conditions given above can then be compared with experiments. The analytical formulation is called “Conflame”.

3.3 Room fire growth models

3.3.1 Cone Tools

Wickström and Göransson developed already in the late 80’s a superposition technique including the Duhamel integral for predicting the Room Corner Test based on Cone Calorimeter data. The theory was later coded into Cone Tools [52], [51]. It was then further developed to include predictions of other scenarios like the SBI test and to predict smoke data, [60]. In the following only the principle for predictions of Room Corner Test data is presented. However, the SBI model follows similar principles.

The size of the pyrolysis area in the Room Corner Test with time is given as

$$A(t) = A_0\left[1 + a\,(t - t_x)^2 \big/ t_{ign}\right] \qquad 30$$

Where “a” is a correlation coefficient (= 0,025 s^{-1} and 0,1 s^{-1} for the 100 kW and 300 kW ignition source respectively) obtained from observations of the pyrolysis area growth in several experiments. The time t_x is chosen so that the burning area growth rate matches the critical condition for flame spread given below. A_0 is the area which is first to ignite behind the burner. Ignition time, t_{ign}, is taken from the Cone Calorimeter for a heat flux of 25 kW/m^2.

Cone Tools uses the full HRR curve history as measured in the Cone Calorimeter and assume that finite surface elements of the walls ignite and follow this HRR curve one after another along with the growth of the pyrolysing area. The total HRR is calculated using the summation formula, cf. Equation 23.

$$\dot{Q}(t) = \sum_{i=1}^{N} \Delta A_i \dot{Q}''^{N-i}_{cone} \qquad 31$$

where $t = N\Delta t$ and Δt is the time increment

The critical condition for flame spread to start is taken as a critical fictitious surface temperature. This surface temperature is calculated from a fictitious gas temperature which in turn is assumed proportional to $\dot{Q}^{2/5}$. To estimate the surface temperature development the tested linings are supposed to be homogenous and semi-infinite and the thermal inertia of the product is assumed proportional to the inverse of the time to ignition measured in the Cone Calorimeter. Then the response function for the surface temperature change due to a step change of the surface temperature is employed and the surface temperature is obtained by superposition. The critical surface temperature is then used as criterion for flame spread both for the 100 kW and for the 300 kW ignition burner heat output.

Cone Tools is widely used in practical applications especially for product development for prediction of SBI results.

3.3.2 Karlssons model

Karlsson [46] developed a sophisticated model for the fire growth in the Room Corner Test in 1992 using experimental data from the same base as used in this work. He modelled upward flame spread in the corner where the ignition source is located and then the flame spread along the ceiling. His basic equation is

$$\dot{Q}_{tot}(t) = \dot{Q}_b + A_w \dot{Q}''_c(t - \tau_w) + A_0 \dot{Q}''_c(t_1) + \int_0^{t_1} \dot{Q}''_c(t_1 - t_p) V_A(t_p) dt_p \qquad 32$$

where $t > \tau_w$ and $t_1 > t_p$

With Karlssons nomenclature $\dot{Q}_{tot}(t)$ is the predicted HRR for the Room Corner Test, $\dot{Q}_b$ is the HRR from the ignition burner, $\dot{Q}_c''$ is the HRR from the Cone Calorimeter, A_w is the area of the wall behind the burner assumed to ignite after a time τ_w calculated from an assumed heat exposure (45 kW/m^2 for the Room Corner Test) assuming a thermally thick solid, A_0 is a pyrolysing area in the ceiling above the burner igniting at $\tau_w + \tau$, i.e. a sequence later than the wall ignition, $t_1 = t - (\tau_w + \tau)$, V_A is the growth rate of the burning area under the ceiling $\frac{d}{dt}(A(t)$ (m^2/s) and finally t_p is a dummy parameter for the integration.

The first three terms of eq 32 deal with the HRR from the burner and HRR from relatively small constant areas burning under direct exposure from or close to the flames from the ignition source. The input HRR is from the Cone Calorimeter and the curves are shifted in time with τ_w and $\tau_w + \tau$ respectively. The fourth term $\int_0^{t_1} \dot{Q}_c''(t_1 - t_p) V_A(t_p) dt_p$ describes the HRR given off when the area burning is growing due to the flame spread in the ceiling. This term will dominate for the cases when fires approach flashover as the process of flame spread in the ceiling precedes flashover. Using the symbols in this work, we get $\int_0^t \dot{Q}_{cone}''(t-s) \frac{d}{ds}(A(s)) ds$ for Karlssons forth term, cf. eq 23.

For the area growth rate, Karlsson uses the expression

$$V_A(t) = \frac{1}{\tau}\left[A_0 + K\left(A_0 \dot{Q}_c''(t) + \int_0^t \dot{Q}_c''(t - t_p) V_A(t_p) dt_p \right) - \left(A_0 + \int_0^t V_A(t_p) dt_p \right) \right] \quad 33$$

The first two terms in the brackets represent the flame area derived from the HRR data from the Cone Calorimeter. The last term in the brackets represents the pyrolysis area. The flame area minus the pyrolysis area divided by the ignition time gives the area growth rate, compare Figure 20. K , the flame area coefficient is taken to be 0,01 m^2/kW by Karlsson.

The ignition time is taken from (cf. eq 19)

$$\tau = \frac{\pi k \rho c (T_{ig} - T_s)^2}{4(\dot{q}''_f)^2} \qquad 34$$

For the Room Corner Test Karlsson selected the value 35 kW/m^2 corresponding to $\dot{q}''_f$. The thermal inertia and the ignition temperature are deduced from data of the products tested in the LIFT apparatus or the Cone Calorimeter using the procedures earlier discussed.

Karlsson uses the HRR curve from the Cone Calorimeter as measured or an analytical expression $\dot{Q}''_{\max} e^{-\lambda t}$ where $\dot{Q}''_{\max}$ is the maximum HRR from the Cone Calorimeter test and λ is a decay coefficient.

Karlsson tests his model on 22 products mostly from the same selection as is analysed in this work. The results are quite good and the model is also developed to handle the stepwise increase of the ignitions source to 300 kW after 10 minutes of testing in the Room Corner Test.

3.3.3 BRANZFIRE

BRANZFIRE is a computer model developed for predicting fire growth in buildings with combustible linings including the hazard from the building contents [47], [61], [62], [63], [64]. It is a multi-room model and especially suited for predictions of the fire growth in the Room Corner Test, ISO 9705. The model includes the full mass and energy balance, species generation as well as soot and smoke production. It is a two-layer zone model. It uses analytical expressions for the different phenomena that need to be modelled for example the fire plume, flame height, ignition and flame spread. Sources for these expressions are published work for example by NIST. The fire growth model is largely based on work by Quintiere. BRANZFIRE is a general model and different room scenarios can be modelled. Input data for prediction of linings fire growth comes from the Cone Calorimeter.

Ignition and flame spread modelling in BRANZFIRE is based on similar physics as for the earlier discussed models. The peak heat flux from the ignition burner to the wall is for the Room Corner Test and the 100 kW source taken as 60 kW/m^2, see eq 3.3 in ref [64]. The peak heat flux to the ceiling above the burner is given as 120 kW/m^2.

This means very fast ignition of the tested material behind the ignition burner flame for most products. The governing equation for upward flame spread rate is given as

$$\frac{dy_p}{dt} = \frac{y_f - y_p}{t_{ign}} \qquad 35$$

where $y_f - y_p$ is the difference between the flame length in the upward direction and the pyrolysis front, i.e. similar to Karlsson. However, BRANZFIRE also includes burnout.

For the thermally thick material the ignition time is

$$t_{ign} = \frac{\pi}{4} k\rho c \left(\frac{T_{ign} - T_s}{\dot{q}''_{ff}} \right)^2 \qquad 36$$

Where $\dot{q}''_{ff}$ is called "heat flux ahead of the flame" and assumed to be 30 kW/m^2, cf. eq 19. BRANZFIRE gives an alternative way of calculating ignition time by taking the so-called Flux Time Product described by Silcock and Shields [65]. This procedure also assumes an inert solid heat heated to ignition temperature and is not discussed further in this work. The upward flame spread equations are used also for the flame spread in the ceiling and for the intersection between the walls and the ceiling. BRANZFIRE also has expressions for lateral and downward flame spread.

The interior surfaces of the room are heated by radiation and convection. BRANZFIRE models the radiation using a model described by Forney [66]. The ceiling, the upper wall, the lower wall and the floor transfer radiation independently between each other. Radiant heating from the flames are also considered. Radiation by soot particles and absorption by carbon dioxide and water vapour are modelled for both the upper and the lower layer. The upper wall includes the parts of the walls above the smoke layer interface and the lower wall includes the parts below the smoke layer interface. The gas layers and each of the wall, ceiling and floor surfaces are assumed to be at a uniform temperature. The radiation from the flames of the fire is assumed to be uniform in all directions and to originate from a single point source. The radiant heating is combined with the convective heating to form the boundary conditions at the surfaces for the calculations of the heat conduction. The convective heat transfer coefficient is found by assuming natural convection.

The convective heat transfer is then taken as $\dot{q}_c'' = h(T_g - T_s)$. The thermal inertia and the ignition temperature is taken from Cone Calorimeter data using Janssens method earlier described in section 3.1. The thermal inertia is needed for the calculation of heat transfer into the solid. The resulting calculated surface temperature then goes into equation 36 for calculation of ignition time and then flame spread.

The HRR from the burning room linings is based on the HRR as measured in the Cone Calorimeter. The model has different options but the preferred is to use cone data from multiple heat fluxes. The total predicted HRR from a Room Corner Test is given as (equation 3.13 from ref [64]).

$$\dot{Q}(t) = \dot{Q}_b + \sum_{i=1}^{N} \dot{Q}''^{N-i} \Delta A_i \qquad 37$$

where $t = N\Delta t$ and Δt is the time increment.

$\dot{Q}_b$ is the HRR from the ignition source and the summation formula gives the HRR from the product. The summation is similar as for Cone Tools, see eq 31. The data is taken from the Cone Calorimeter as measured at a heat flux matching the imposed heat flux to the wall. If the heat flux to the wall is outside what was measured in the cone then an interpolation procedure is used to calculate the needed HRR per unit area.

BRANZFIRE predictions have been verified for a number of scenarios. The products from the EUREFIC programme were used to predict the outcome in the Room Corner Test and they are reported in ref [67].

3.3.4 Others

There are more examples of analysis of correlations using simplifications that leads to an analytical formula as was done in section 3.2. Östman et al made a straightforward correlation to predict flashover time, [68], [69].

In [70] and [71] a simplified model by North et al, is applied to the same products discussed in this work. They use the correlation $\tau = 113 \frac{\rho}{\dot{q}_{fs}''^2}$ for the ignition time controlling the flame spread; $\dot{q}_{fs}''$ is the flame radiant heat flux. They then solve the flame spread equation section 3.1.2. with good results for both the Room Corner Test and the SBI test.

3.4 Prediction of experimental results

In this chapter, it will be shown how tests of wall linings in various configurations can be predicted using Cone Calorimeter data in the models outlined in chapter 3.2 and 3.3.

3.4.1 The Room Corner Test

Predictions of the HRR curves for the Room Corner Test according to Conflame, Cone Tools and the Karlsson model for a number of building products compared to experiments are shown in Figure 22.

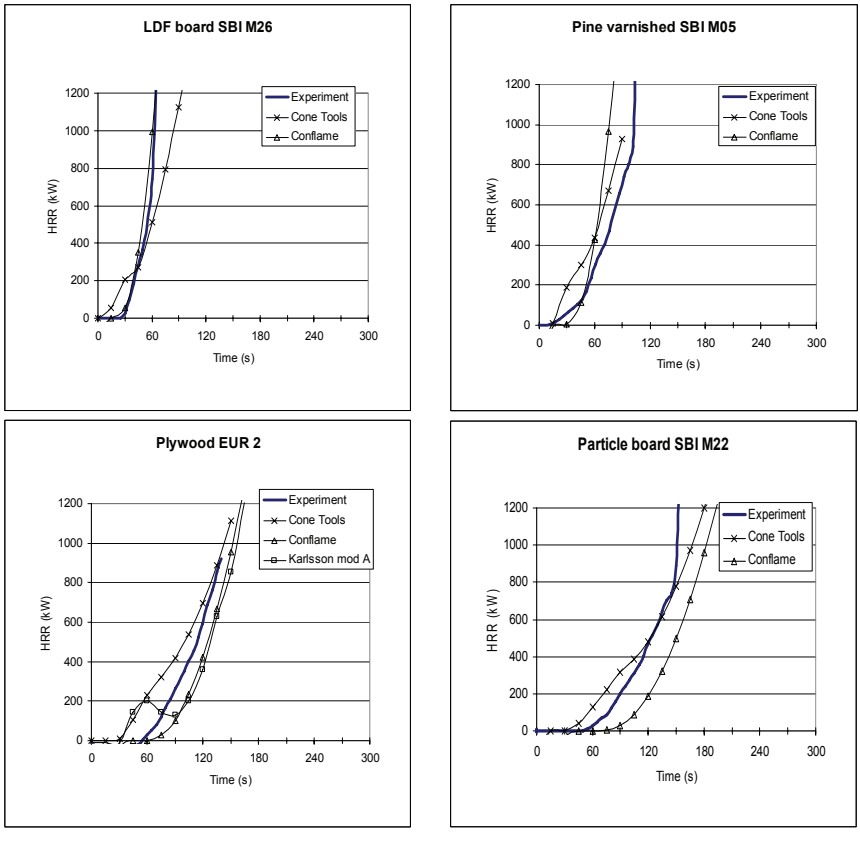

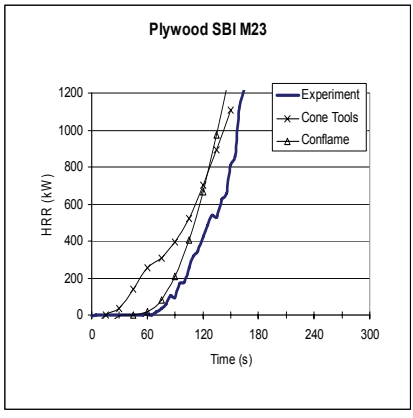
Plywood SBI M23
Experiment
Cone Tools
Conflame
HRR (kW)
Time (s)
0
200
400
600
800
1000
1200
0
60
120
180
240
300

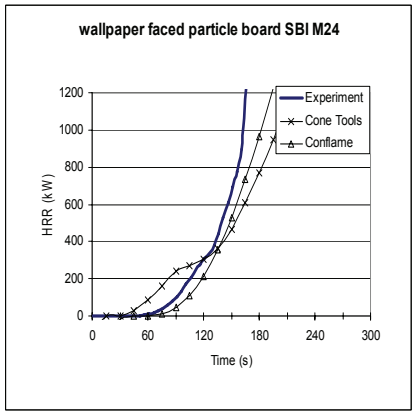
wallpaper faced particle board SBI M24
Experiment
Cone Tools
Conflame
HRR (kW)
Time (s)
0
200
400
600
800
1000
1200
0
60
120
180
240
300

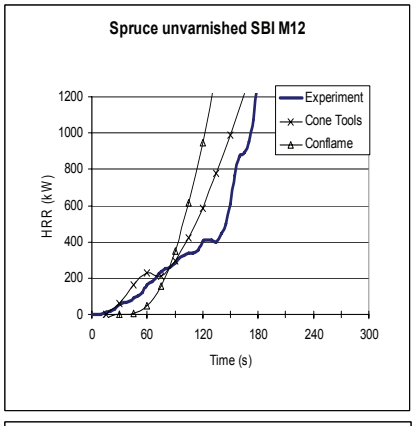
Spruce unvarnished SBI M12
Experiment
Cone Tools
Conflame
HRR (kW)
Time (s)
0
200
400
600
800
1000
1200
0
60
120
180
240
300

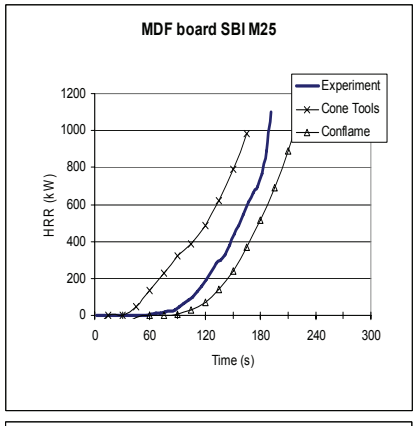
MDF board SBI M25
Experiment
Cone Tools
Conflame
HRR (kW)
Time (s)
0
200
400
600
800
1000
1200
0
60
120
180
240
300

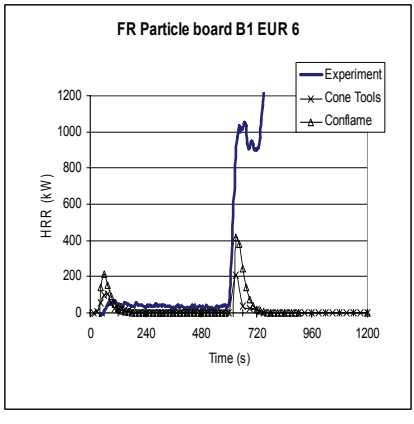
FR Particle board B1 EUR 6
Experiment
Cone Tools
Conflame
HRR (kW)
Time (s)
0
200
400
600
800
1000
1200
0
240
480
720
960
1200

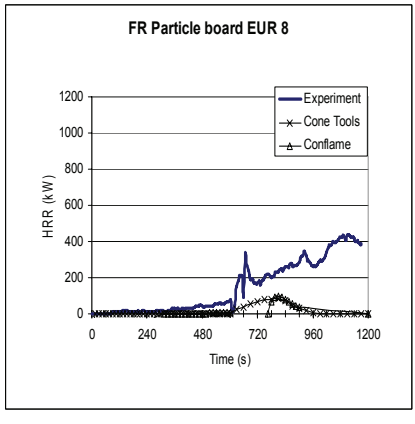
FR Particle board EUR 8
Experiment
Cone Tools
Conflame
HRR (kW)
Time (s)
0
200
400
600
800
1000
1200
0
240
480
720
960
1200

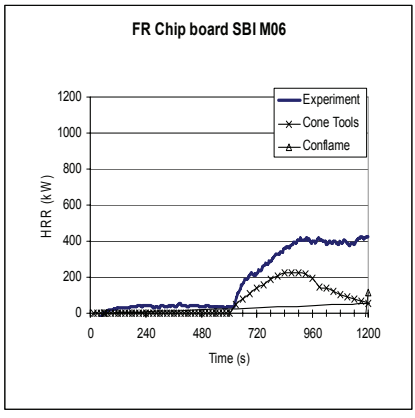
FR Chip board SBI M06
Experiment
Cone Tools
Conflame
HRR (kW)
Time (s)
0
200
400
600
800
1000
1200
0
240
480
720
960
1200

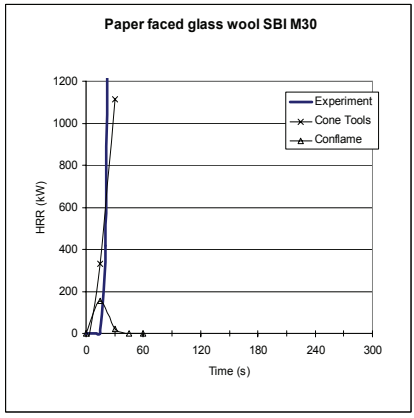
Paper faced glass wool SBI M30
Experiment
Cone Tools
Conflame
HRR (kW)
Time (s)
0
200
400
600
800
1000
1200
0
60
120
180
240
300

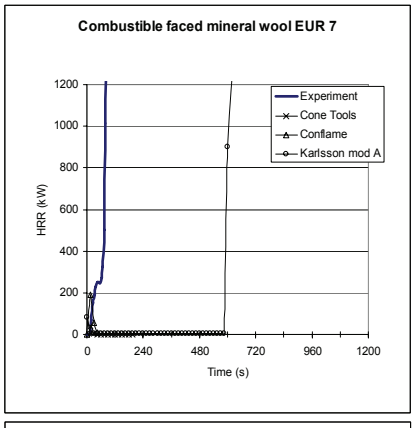
Combustible faced mineral wool EUR 7
Experiment
Cone Tools
Conflame
Karlsson mod A
HRR (kW)
Time (s)
0
200
400
600
800
1000
1200
0
240
480
720
960
1200

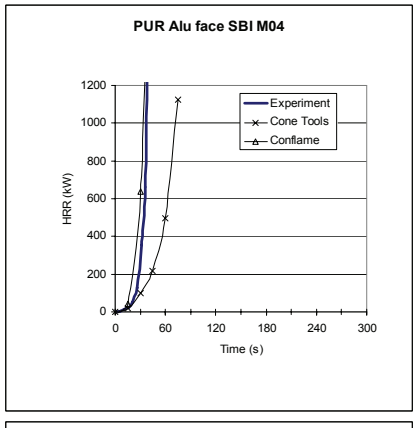
PUR Alu face SBI M04
Experiment
Cone Tools
Conflame
HRR (kW)
Time (s)
0
200
400
600
800
1000
1200
0
60
120
180
240
300

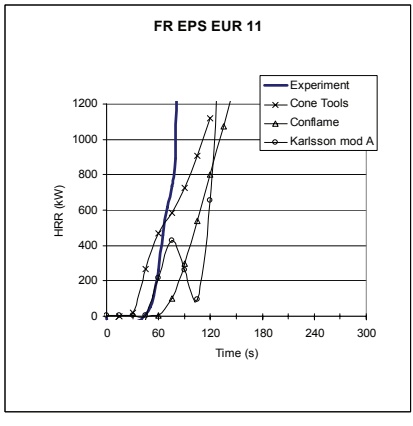
FR EPS EUR 11
Experiment
Cone Tools
Conflame
Karlsson mod A
HRR (kW)
Time (s)
0
200
400
600
800
1000
1200
0
60
120
180
240
300

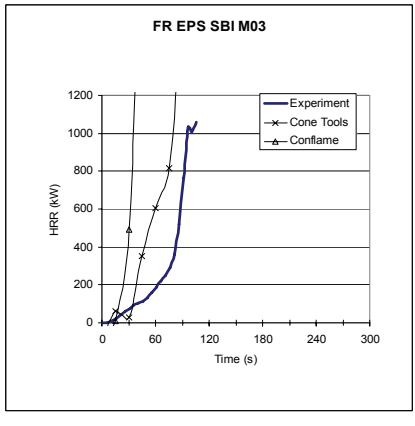
FR EPS SBI M03
Experiment
Cone Tools
Conflame
HRR (kW)
Time (s)
0
200
400
600
800
1000
1200
0
60
120
180
240
300

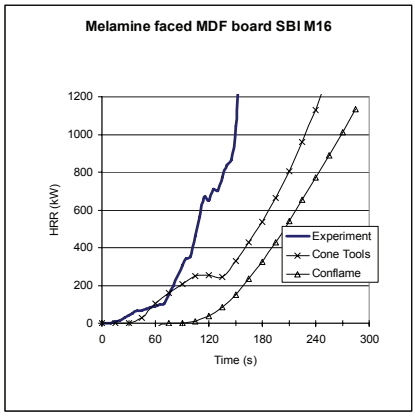
Melamine faced MDF board SBI M16
HRR (kW)
Time (s)
Experiment
Cone Tools
Conflame

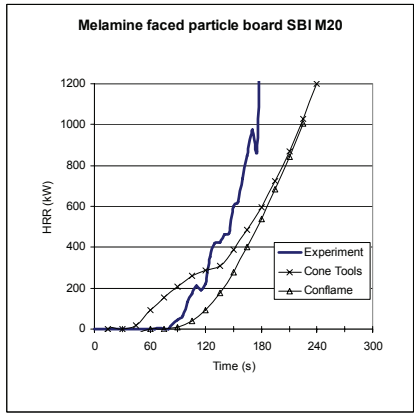
Melamine faced particle board SBI M20
HRR (kW)
Time (s)
Experiment
Cone Tools
Conflame

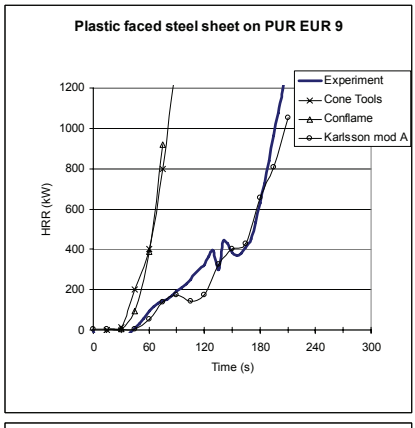
Plastic faced steel sheet on PUR EUR 9
HRR (kW)
Time (s)
Experiment
Cone Tools
Conflame
Karlsson mod A

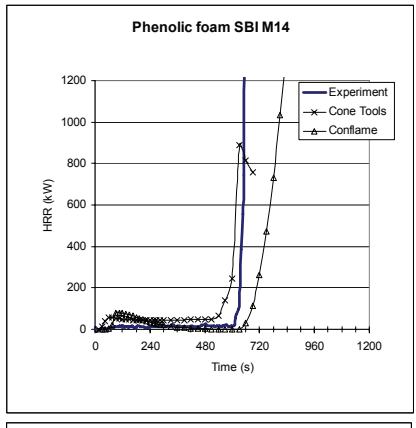
Phenolic foam SBI M14
HRR (kW)
Time (s)
Experiment
Cone Tools
Conflame

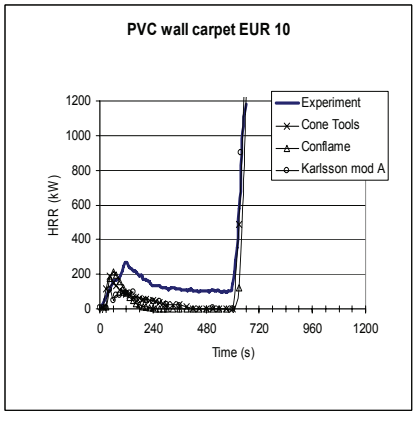
PVC wall carpet EUR 10
HRR (kW)
Time (s)
Experiment
Cone Tools
Conflame
Karlsson mod A

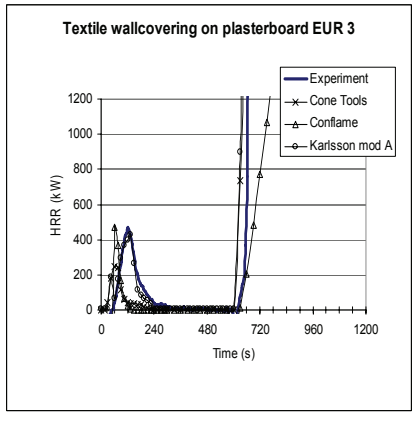
Textile wallcovering on plasterboard EUR 3
HRR (kW)
Time (s)
Experiment
Cone Tools
Conflame
Karlsson mod A

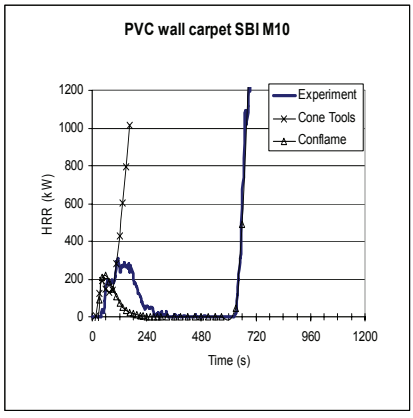
PVC wall carpet SBI M10
HRR (kW)
Time (s)
Experiment
Cone Tools
Conflame
0
200
400
600
800
1000
1200
0
240
480
720
960
1200

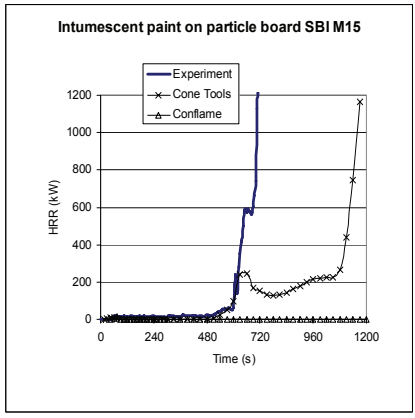
Intumescent paint on particle board SBI M15
HRR (kW)
Time (s)
Experiment
Cone Tools
Conflame
0
200
400
600
800
1000
1200
0
240
480
720
960
1200

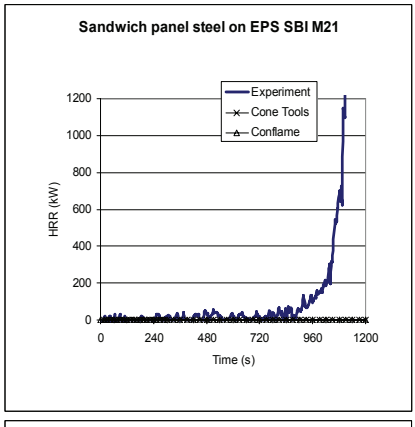
Sandwich panel steel on EPS SBI M21
HRR (kW)
Time (s)
Experiment
Cone Tools
Conflame
0
200
400
600
800
1000
1200
0
240
480
720
960
1200

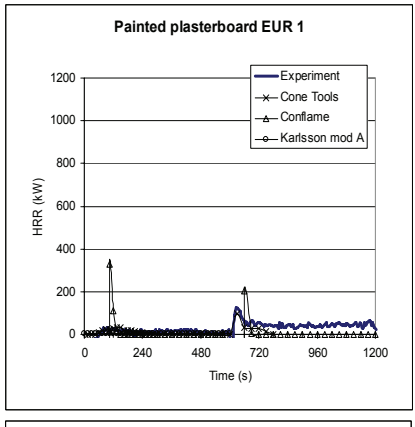
Painted plasterboard EUR 1
HRR (kW)
Time (s)
Experiment
Cone Tools
Conflame
Karlsson mod A
0
200
400
600
800
1000
1200
0
240
480
720
960
1200

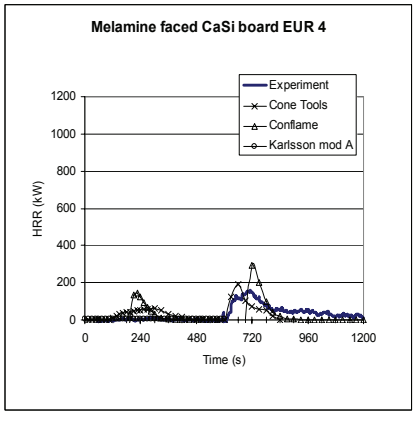
Melamine faced CaSi board EUR 4
HRR (kW)
Time (s)
Experiment
Cone Tools
Conflame
Karlsson mod A
0
200
400
600
800
1000
1200
0
240
480
720
960
1200

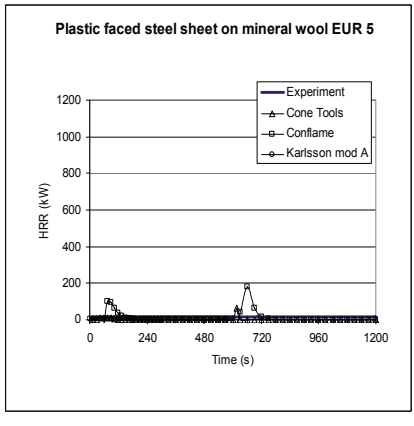
Plastic faced steel sheet on mineral wool EUR 5
HRR (kW)
Time (s)
Experiment
Cone Tools
Conflame
Karlsson mod A
0
200
400
600
800
1000
1200
0
240
480
720
960
1200

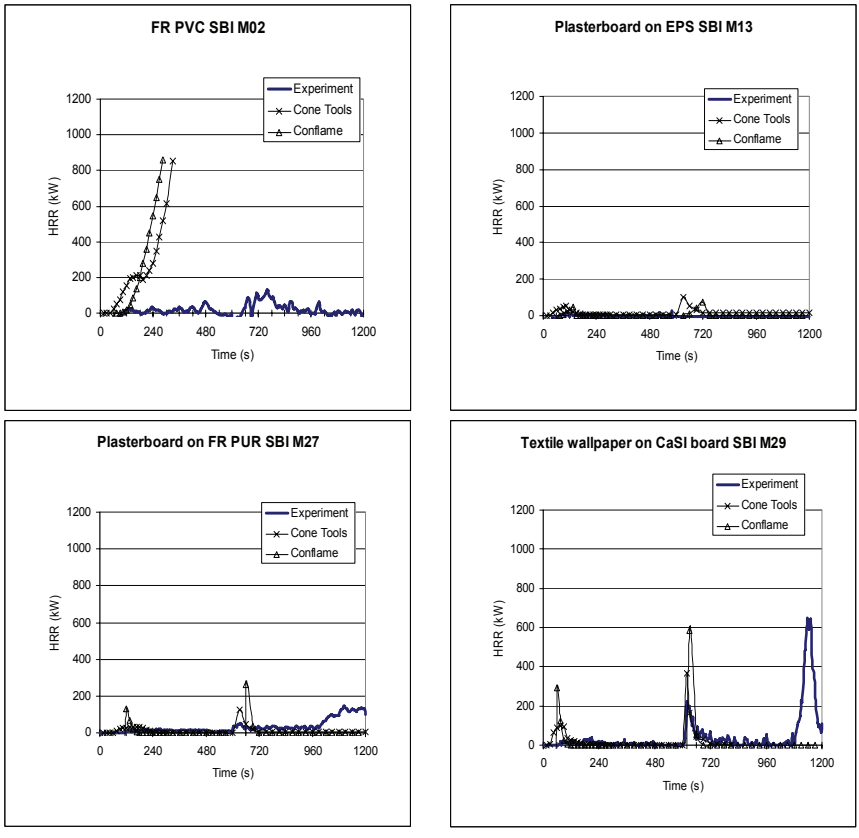

Figure 22. Comparison of experimental data from the Room/Corner Test with simulations made using Conflame, Cone Tools and Karlssons model. SBI XX refers to the SBI-project and the actual product number. EUR XX refers to the EUREFIC project and the actual product number.

The input HRR curve for the Cone Tools simulations where taken at 50 kW/m^2 incident heat flux in the Cone Calorimeter, i.e. similar to Conflame, eq 28- eq 29. (Cone Tools translates data from 50 kW/m^2 to the 25 kW/m^2 situation). Cone Tools 2.3.0, 2004 was used.

Karlssons predictions on the EUREFIC products are taken directly from his thesis [46]

The occurrence of flashover is predicted correctly in 28 and 26 out of 33 experiments for Cone Tools and Conflame respectively, i.e. 80-85 % of the cases. The selection of the studied products was made to represent typical use in buildings and at the same time to give a wide range of burning behaviour.

A building product selected randomly on the market therefore has a good chance of being correctly assessed by this type of analysis. However, when looking closer at the results it is clear that for certain products there are systematic errors in the predictions.

Untreated wood products are all predicted correctly. Differences in time predictions can be due to precisely what values of the scenario dependent parameters that are selected. Another factor is the ignition time of the product for a certain heat flux. Even small uncertainties due to measurement errors have a large influence.

FR particle board B1 EUR 6 is a borderline case. Cone Tools could predict flashover after 10 min depending on the input data [60].

Paper faced glass wool shows a very high narrow peak HRR in the Cone Calorimeter that gives an average HRR too small to reach the criterion of flame spread for Conflame. Cone Tools works better in this case by using temperature criteria. Combustible faced mineral wool EUR 7 is not working in either case. It is unclear why.

Sandwich panel steel on EPS SBI M21 is not igniting or giving HRR in the cone. This product is going to flashover in the Room Corner Test because the metal due to heating and subsequent bending cracks and exposes the EPS. In the large-scale test, EPS melts and pyrolysis gases can escape into the room and ignite. The small samples in the Cone Calorimeter cannot reproduce this behaviour (or in any other small-scale tests) and is therefore not suitable for this kind of product.

The FR PVC SBI M02 is predicted to give flashover. When the product was tested in the Room Corner Test there was no flashover. A possible explanation is that the chemistry is important and that air supply for combustion may differ between room scale and small scale, see section 3.5.

A few results on the EUREFIC products are also given in the supporting documentation for BRANZFIRE [67]. The result expressed as time to flashover is shown in Table 6.

Table 6. Results of predictions for the EUREFIC products using the BRANZFIRE code.

PRODUCT*	EXPRIMENTAL TIME TO FLASHOVER, MIN:SEC	PREDICTED TIME TO FLASHOVER (APPROXIMATELY) MIN:SEC. DATA AS GIVEN IN REF [67]
Painted plasterboard EUR 1	NO	NO
Plywood EUR 2	02:30	02:46
Textile wall covering on plasterboard EUR 3	10:60	10:46
Melamine faced CaSi board EUR 4	NO	NO
Plastic faced steel sheet on mineral wool EUR 5	NO	10:46
FR particle board B1 EUR 6	10:30	10:55
Plastic faced steel sheet on PUR EUR 9	03:15	01:26
PVC wall carpet on plasterboard EUR 10	10:55	10:28
FR EPS EUR 11	01:20	01:26

* Combustible faced mineral wool EUR 7 and FR particle board EUR 8 were omitted as the data was deemed uncertain, [67].

3.4.2 Small room experiments

A series of experiments [72] in a room of dimensions 1,2 m x 0,8 m x 0,8 m was done by the Lund University. The room size was 1/3 of the Room Corner Test. At one of the short sides there was an opening having a height of 0,67 m and a width of 0,56 m. The ignition source was a gas burner of similar type as used in the Room Corner Test but the size of the surface was only 70 mm x 70 mm. The output from the burner was 11 kW for 10 minutes and then increased to 33 kW for another 10 minutes. Flashover defined as flames coming out through the doorway corresponded to a HRR of 50-75 kW.

Conflame was applied to this situation for the first 10 minutes and the 11 kW ignition burner only.

The values used for equations 28 and 29 were: The factor C, see chapter 3.2, was scaled with room size, i.e. 1,2 m^2 x 1/3 = 0,4 m^2. The heat exposure from the flames on the fuel surface was taken to 25 kW/m^2 following the recommendation from Quintiere for small flames [48], [49]. Thus, the value of τ was taken from Cone Calorimeter data at 25 kW/m^2. The heat exposure from the ignition burner was taken to 25 kW/m^2 same as Karlsson [46]. Thus the value of t_{ign} was taken from Cone Calorimeter data also at 25 kW/m^2. Equations 28 and 29 become

$$\dot{Q}(t) = 0{,}4 \cdot 5{,}44 \cdot \dot{Q}''_p t_c \frac{1}{\tau^2}\left[e^{-\frac{(t-t_{ign})}{t_c}}\left(t - t_{ign} + 2t_c\right) + t - t_{ign} - 2t_c \right] \qquad 38$$

for $t \geq t_{ign}$, t is time elapsed after the start of the test.

The condition for no further flame spread was taken as $\dot{Q}''_{ave180s} \leq 75$ kW/m^2 as earlier discussed. The corresponding maximum area ignited was taken as the wall area behind the burner flame, 0,1 m^2. Thus, for no flame spread

$$\dot{Q}(t) = 0{,}1 \cdot 2{,}72 \cdot \dot{Q}''_p \frac{t - t_{ign}}{t_c} e^{-\frac{t-t_{ign}}{t_c}} \qquad 39$$

for $t \geq t_{ign}$, t is time elapsed after the start of the test.

The area covered by the products was 3,5 m^2 which was the maximum area that could burn. For HRR below 100 kW this area was never reached in the predictions.

The results for some products are shown below.

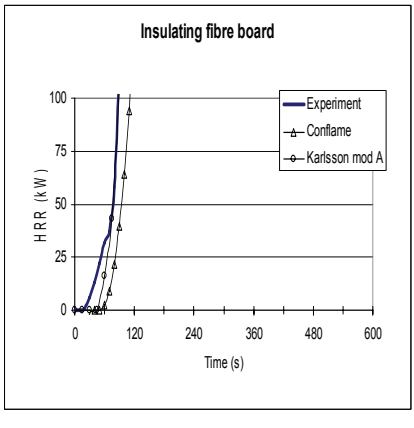

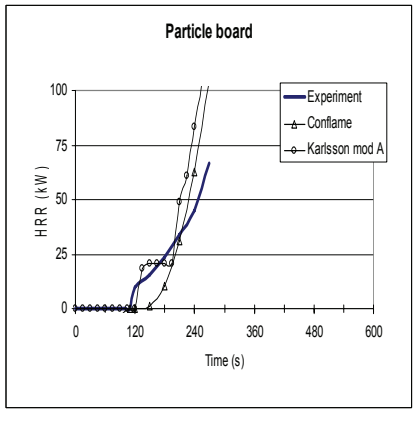

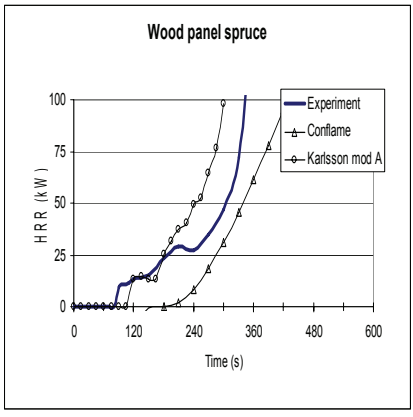
Wood panel spruce
HRR (kW)
Time (s)
Experiment
Conflame
Karlsson mod A

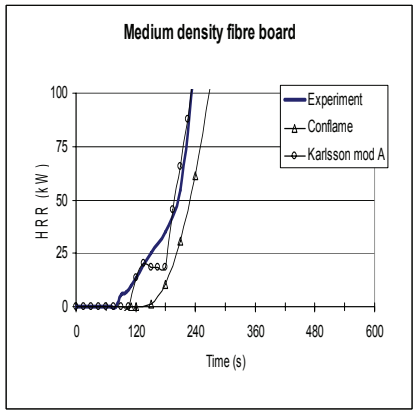
Medium density fibre board
HRR (kW)
Time (s)
Experiment
Conflame
Karlsson mod A

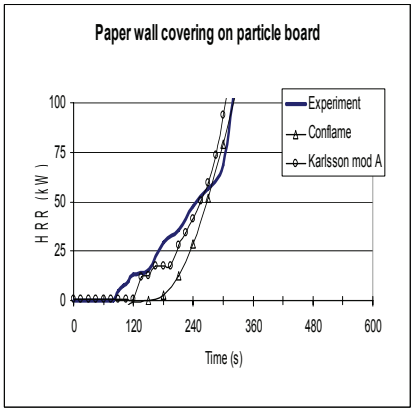
Paper wall covering on particle board
HRR (kW)
Time (s)
Experiment
Conflame
Karlsson mod A

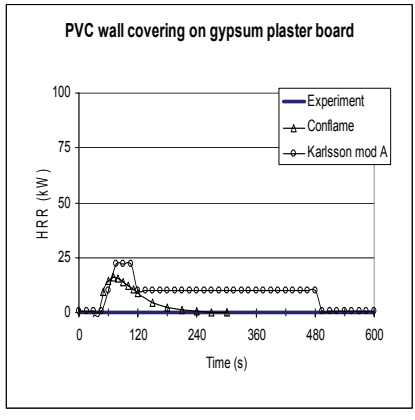
PVC wall covering on gypsum plaster board
HRR (kW)
Time (s)
Experiment
Conflame
Karlsson mod A

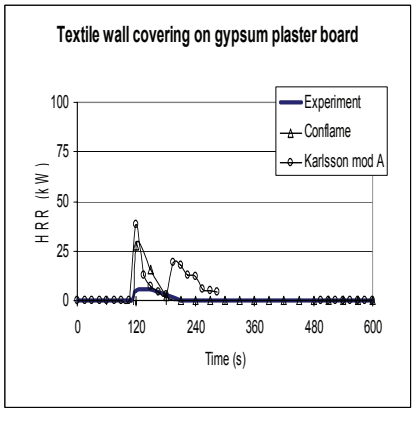
Textile wall covering on gypsum plaster board
HRR (kW)
Time (s)
Experiment
Conflame
Karlsson mod A

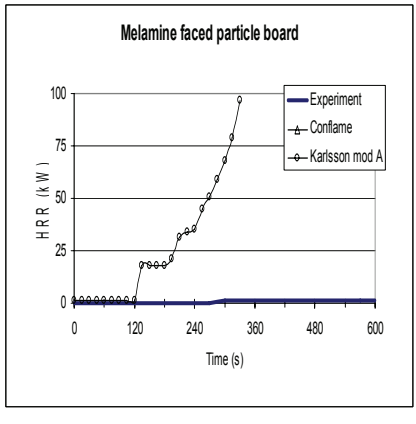
Melamine faced particle board
HRR (kW)
Time (s)
Experiment
Conflame
Karlsson mod A

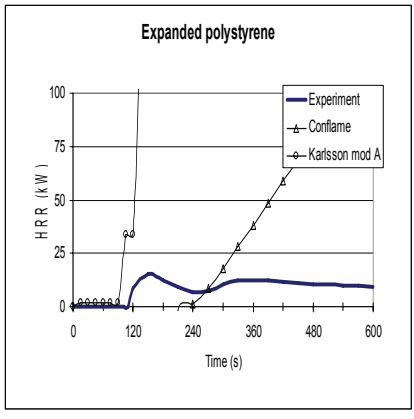

Figure 23. Experimental and predicted data for products tested in a room of 1/3 scale of the Room Corner Test.

Karlssons predictions are taken directly from his thesis [46].

The predictions are roughly of similar accuracy as for the Room Corner Test. The polystyrene when tested in the 1/3 scale exposed to the relative small heat fluxes will melt before igniting. The material will therefore escape from the heat attack, as the molten material will be on the floor. Contradictory to the case in the Cone Calorimeter where the horizontal sample holder will keep the material exposed to the heat flux. Therefore, the small room test shows a better result.

3.4.3 Large room experiment

Experiments were made in a room 4,0 m x 5,0 m and 2,4 m high. A door opening 0,8 m x 2,25 m was placed at the short wall, see Figure 24.

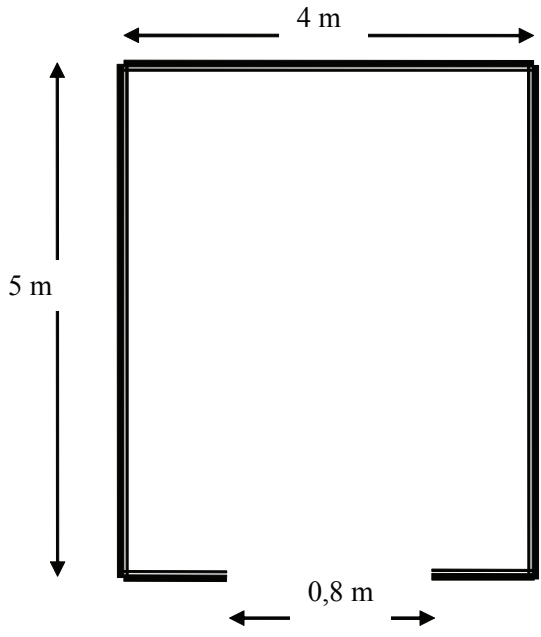

Figure 24. Room layout large-scale test

The room contained some furniture; two light chairs, a small table, a lamp standing on the floor, a TV and a bookcase. The linings were painted wood board with a PVC covering on the floor. The gas burner was the same as the burner used in the Room Corner Test but giving a constant heat output of 30 kW only and positioned in a corner away from the door opening. It was also away from the nearest furniture item. Thus, the ignition and early stages of the fire growth was attributed to the properties of the lining. The room has the same height and similar sized door opening as the Room Corner Test. Only the area is larger. Therefore the fire growth is assumed to be similar to the Room Corner Test. Conflame, eq 28 is taken using the same C factor, 1,2, and ignition time, τ, due to flame heat flux 35 kW/m^2. However, the ignition burner is only 30 kW form a burner designed for 100 kW/300 kW. Therefore the burner heat flux for calculating t_{ign} is arbitrarily taken as 25 kW/m^2. The result is shown in Figure 25.

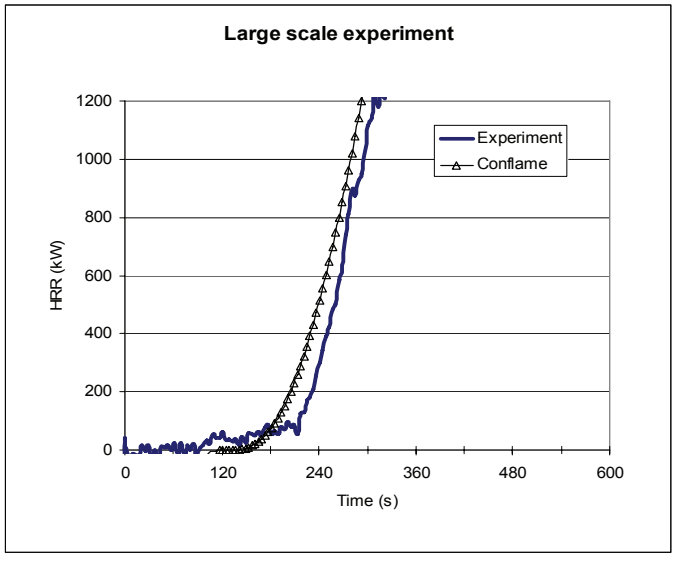

Figure 25. Measured and calculated data of HRR for large room test. The measured HRR curve is corrected for a 3,25 min time delay based on the reading from a thermocouple inside the burn room.

It is seen that the Conflame model works reasonable well also for this configuration. Flames emerged through the doorway at 5 min 20 sec corresponding to a HRR of about 1200 kW. The Cone Calorimeter input data is from MDF board SBI M25. The actual tested linings were particle board on the walls and a MDF type of board in the ceiling. The products were painted with ordinary water based paint. Input data is therefore not on the same products but was deemed realistic.

3.4.4 Very large room experiment

The EUREFIC project included tests in a very large room 9 m x 6,75 m and 4,9 m high, [29]. A 2 m x 2 m door opening was at the long side of the room. The products were mounted on the walls and the ceiling of the room. The burner heat output was 100 kW for 10 min, 300 kW for another 10 min and then 900 kW until flashover or test stop (about 30 min). A selection of the EUREFIC products was tested. BRANZFIRE documentation contains some predictions on these tests [67], see Table 7.

Table 7. Results of predictions for the EUREFIC products tested in a very large room using the BRANZFIRE code.

EUREFIC LARGE ROOM		
PRODUCT*	EXPERIMENT. THE HRR IS INCLUDING BURNER HEAT OUTPUT	PREDICTION (APPROXIMATELY). DATA AS GIVEN IN REF [67]
Plywood EUR 2	4000 kW at 17:30, flashover at 19:30 and 10 MW	4000 kW at 09:10
Textile wall covering on plasterboard EUR 3	3400 kW at 20:40	1200 kW at 20:40
FR particle board B1 EUR 6	1300 kW at 20:40	1100 kW at 20:40
PVC wall carpet on plasterboard EUR 10	1300 kW at 22:30	1200 kW at 21:15

* Combustible faced mineral wool EUR 7 and FR particle board EUR 8 were omitted as the data was deemed uncertain [67].

The large room size caused the fires to grow much slower and the larger ignition source of 900 kW was required for the fire to grow fast. Upward flame spread in the corner was another factor that influenced the result. With a ceiling of almost 5 m height, the upward flame spread becomes important for the overall fire development. The long times also caused burn through of wood products. In the experiment, the plywood burnt through and a pile of falling glowing pieces was formed at the floor in the corner. The glowing pile eventually started a fire along the lower parts of the walls, which lead to flashover in a shorter time compared to the usual flame spread along the ceiling and the upper walls. Fire models cannot predict this chain of events. BRANZFIRE predicts a much faster fire growth than actually happened for plywood. Using Conflame with the Room Corner Test parameters predicts an even faster growth. Kokkala et al [29] comments that the models for upward flame spread need improvements to cover the very large room case.

However, an important conclusion from the large room experiments was that fire growth in a small room, the Room Corner Test, seems to be more severe than the fire growth in a large room. The last three products, Table 7, all went to flashover shortly after the 300 kW heat exposure in the Room Corner Test experiments but did not go to flashover in this large room.

The concept to use Room Corner Test as reference scenario, which gives data on the "safe side", largely comes from the findings of these tests

3.4.5 The Single Burning Item, SBI

In the SBI test, the tested sample is placed in a corner configuration and ignited by a gas burner giving 30 kW of heat release rate [1]. There is no ceiling and once the sample has ignited the flames travel vertically to the top of the sample. Experience show that there is very little or very slow lateral flame spread except for products that are very flammable compared to wood. Another exception is the case when there is a burn through and the product starts to burn on two sides. This happens after a relatively long time and rarely influences the FIGRA value, see section 2.1. For the above reasons the flame spread rate during the early stages of a SBI test is approximated to be one-dimensional and constant. The growth of the burning area with time will then be the flame spread rate times the width of the advancing flame front. After test start the area growth with time in the SBI test then becomes

$$A(t) = C\frac{t - t_{ign}}{\tau} \qquad 40$$

for $t \geq t_{ign}$, t is time elapsed after the start of the test.

At a certain time when the flames has reached the top of the sample there is no lateral flame spread and the burning area is not growing any further. The SBI burner was developed to give a heat exposure of 30 kW/m^2 to the sample. However, detailed mapping of the heat exposure is still in progress. For the purpose of this work ignition time from cone experiments at 35 kW/m^2 is used. As the flames are small, τ is based on 25 kW/m^2 flame heat exposure as recommended by Quintiere [48], [49].

The maximum area that burns during the early stages of the SBI test is related to the area exposed by the flame. At the burner surface the base of the flame is 0,25 m for each wall. When approaching the top of the sample the influence of the burner flame is very small and the flame width at the top is then depending on the flames from the sample itself. This width is smaller then the burner width for many products. Thus the value 0,45 m^2 was assumed. To further simplify, the HRR per unit area is assumed constant and the 180 s average from the Cone Calorimeter is used instead of the curve. Equation 40 becomes

$$\dot{Q}_{SBI}(t) = C \cdot \dot{Q}''_{ave180s} \frac{t - t_{ign}}{\tau} \qquad 41$$

for $A(t)$ according to eq 40 $\leq$ 0,45 m^2 and C = 0,5 m^2

At the time when the burning area has reached the maximum value 0,45 m^2, i.e. for $t = \frac{0{,}45 \cdot \tau}{0{,}5} + t_{ign}$ then the HRR in the SBI test is maximum and eq 41 is replaced by $\dot{Q}_{SBI}(t)\,(\max) = \dot{Q}''_{ave180s}$ x 0,45 m^2

Figure 26 shows the result for two wood-based products.

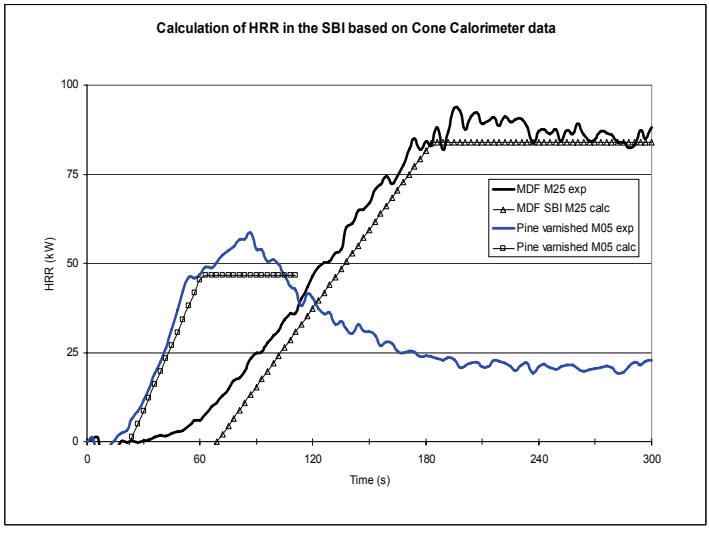

Figure 26. Comparison of measured and calculated HRR in the SBI test for two wood based products.

The correlation is quite good for these products. However, for low performance products of high flame spread the assumption of an area 0,45 m^2 does not hold. Larger areas burn in this case.

The FIGRA parameter can now be calculated as the slope of a straight line through origin and the predicted break point ($\dot{Q}_{SBI}(\max)$, t), cf. Figure 26. The results of the comparisons are shown in Figure 27.

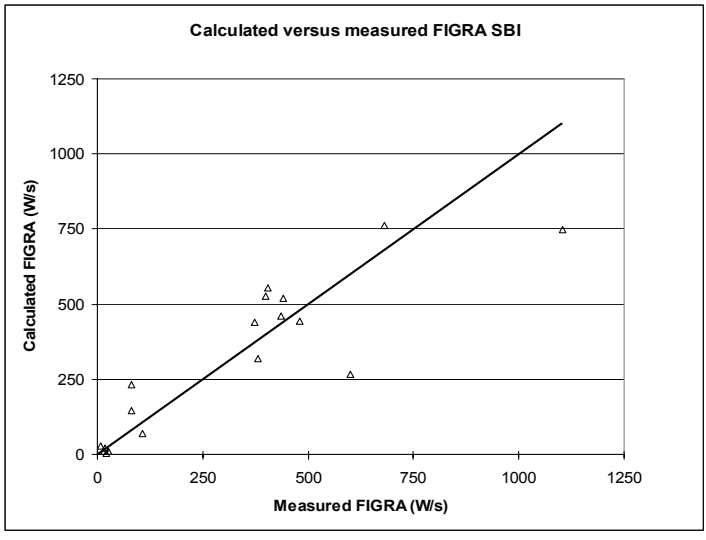

Figure 27. Comparison of calculated and measured FIGRA based on equation 41.

Although the approach is simple is gives a good agreement with test data. The outliers are LDF board and melamine faced MDF board. The LDF board is expected to show a higher measured value than calculated as it shows a large flame spread and the burning area becomes larger than assumed. The reason for the deviation for MDF board is not known. The scale in Figure 27 is limited to values interesting for product classification. The uncertainty of FIGRA values becomes large above these values. There are three products having FIGRA values of more than 1250 W/s. These are FR extruded polystyrene, PUR foam with aluminium foil and paper faced glass wool. The predicted FIGRA values are larger than 1250 W/s, which is consistent with experiment except for the paper, faced glass wool. The experimental value is about 3900 and the predicted value is 657. The difference is due the large flame spread for this product and the low value of $\dot{Q}''_{ave180s}$ as already discussed in the section 3.4.1, the Room Corner Test.

The above calculations suggest that FIGRA from the SBI test is proportional to $\dot{Q}''_{180s} / t_{ign}$ as measured in the Cone Calorimeter. In Figure 28 data from the Cone Calorimeter on $\dot{Q}''_{180s} / t_{ign}$ is compared with FIGRA from the SBI.

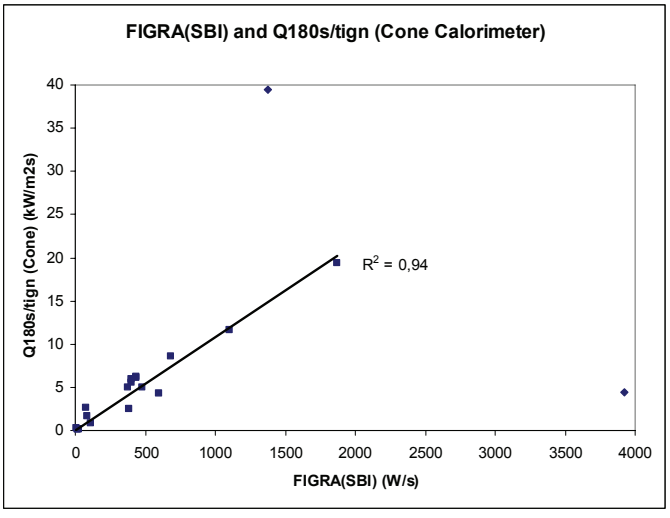

Figure 28. Comparison with 180 s average of HRR divided by ignition time in the Cone Calorimeter with FIGRA from the SBI for the same products. The correlation coefficient is given without the two outliers.

The correlation is quite good except for two outliers. The product having a very high FIGRA but a small value in the cone is paper faced glass wool SBI M30. Peak HRR is steep and narrow for this product. The 180 s average from the Cone Calorimeter is therefore very small and the resulting quotient is small. The average value is not a good way to represent the HRR from this product. FR extruded polystyrene SBI M03 is treated differently by the tests. The SBI has a vertical sample configuration and the product melts and moves away from the heat exposure. This is not happening in the cone as the melted material stays in place in the horizontal sample holder and is kept exposed to the heat.

Hakkarainen [73] applied a one-dimensional flame spread model of the type discussed in section 3.1.2 and tuned the parameters for the SBI. She also did a correlation basically scaling the products with functions using the group $\dot{Q}''^{n} / t_{ign}^{n}$. The results were good, more than 80% success in classification according to the European classification system for linings.

Steen Hansen [74] calculated FIGRA values based on Cone Calorimeter data. She used an exponential correlation function originating from Cone Tools for the area growth and used superposition to calculate the HRR curve for a SBI test. The area function was modified according to the product burning behaviour using statistical methods.

3.5 Discussion of thermal models

We can compare the predictions of time to flashover with the experiments. For a Room Corner Test experiment, we select 1000 kW to represent the HRR at flashover. As the ignition burner gives 100 kW for the first 10 minutes, the contribution from the product is 900 kW at flashover. The exact HRR at flashover in the Room Corner Test may differ somewhat. Other values have been proposed [75]. However, for the comparison it does not matter what exact level we chose. The corresponding HRR at flashover in the small-scale room test is taken as 50 kW [72] and in the large room experiment as 1200 kW. The predictions compared to experiment are shown in Figure 29 for products going to flashover when exposed to the lower heat output from the ignition source, (11 kW in small-scale room and 100 kW in the Room Corner Test).

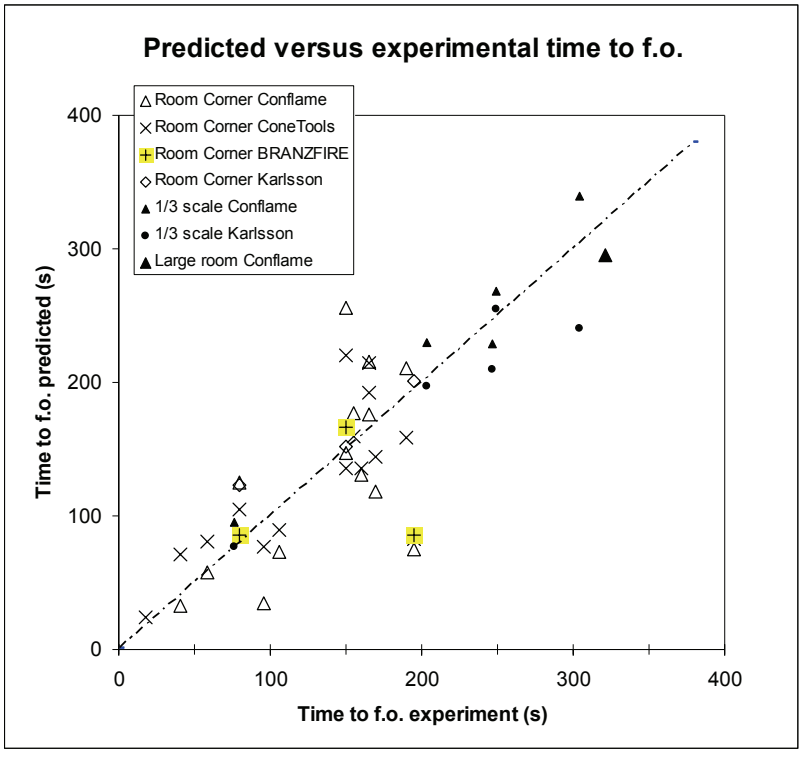

Figure 29. Predicted versus measured time to flashover for room fire experiments in different scales and with different models. The HRR at flashover varies from 50 kW to 1200 kW.

The correlation is good for the different models and scales. Most of the general scatter seems to be due to the how the model parameters are tuned combined with uncertainties in data. In one experiment the flashover occurred at about 200 s but the predictions by BRANZFIRE, Cone Tools and Conflame all show less than 100 s and almost identical values. The outlier is plastic faced steel sheet on PUR EUR 9, a sandwich panel. The small-scale test is not providing the required information for a correct prediction in this case, see below in this chapter. There are also some cases not seen in the plot where prediction of occurrence of flashover does not match the experiment. They are shown in the tables below.

Uncertainty in predictions should also be compared with uncertainty of experimental data. The accuracy at which HRR is measured in the Room Corner Test is about 10 % at the 150 kW level and about 7 % at the 1000 kW level [76]. For the Cone Calorimeter the uncertainty in the ignition time is the most important. ISO 5660 estimates that the repeatability $r = 2{,}3 + 0{,}255t_{ign}$ at 95 % confidence level. For wood, the ignition time is typically 50 s at 35 kW/m^2. Then r = 15 s. This variation would lead to big differences in predictions, see Figure 31.

Table 8 and Table 9 show products of high performance and products with an intermediate behaviour not shown in Figure 29.

Table 8. Data for products not giving flashover for the 100 kW ignition source in the Room/Corner Test.

PRODUCT TYPE	TIME TO FLASHOVER EXPERI-MENT (MIN:S)	TIME TO FLASH-OVER CONFLAME (MIN:S)	TIME TO FLASHOVER CONE TOOLS (MIN:S)	KARLS-SON	BRANZ-FIRE
FR part. board B1 EUR 6	*10:30*	*NO*	*NO*	-	*10:55*
Phenolic foam SBI M14	*10:40*	*12:59*	*10:02*	-	-
PVC wall carpet on plaster-board EUR 10	*10:55*	*10:49*	*10:37*	*10:35*	*10:28*
Text. wall covering on plaster-board EUR 3	*11:00*	*11:54*	*10:29*	*10:30*	*10:46*

PRODUCT TYPE	TIME TO FLASHOVER EXPERI-MENT (MIN:S)	TIME TO FLASH-OVER CONFLAME (MIN:S)	TIME TO FLASHOVER CONE TOOLS (MIN:S)	KARLS-SON	BRANZ-FIRE
PVC wall carpet on plaster-board SBI m10	*11:15*	*11:09*	*02:38*	-	-
Intumescent paint on part. board SBI M15	*11:40*	*NO*	*18:56*	-	-
Sandwich panel steel sheets on EPS SBI M21	*16:10*	*NO*	*NO*	-	-
Painted plaster-board EUR 1	*NO*	*NO*	*NO*	*NO*	*NO*
Melamine face CaSi board EUR 4	*NO*	*NO*	*NO*	*NO*	*NO*
Plastic face steel sheet on min. wool EUR 5	*NO*	*NO*	*NO*	*NO*	*10:46*
FR part. board EUR 8	*NO*	*NO*	*NO*	-	-
FR PVC SBI M02	*NO*	*04:52*	*05:36*	-	-
Plaster-board on EPS SBI M13	*NO*	*NO*	*NO*	-	-
Plaster-board on FR PUR SBI M27	*NO*	*NO*	*NO*	-	-
FR chip-board SBI M06	*NO*	*NO*	*NO*	-	-
Text. wall covering on CaSi board SBI M29	*NO*	*NO*	*NO*	-	-

Table 9. Data for products not giving flashover in the small-scale room test.

PRODUCT TYPE	TIME TO FLASHOVER EXPERIMENT (MIN:S)	TIME TO FLASHOVER CONFLAME (MIN:S)	TIME TO FLASHOVER KARLSSON (MIN:S)
Expanded polystyrene	*NO*	*06:38*	*02:02*
Melamine faced particle board	*NO*	*>10:00*	*04:30*
Textile wall covering on gypsum plasterboard	*NO*	*>10:00*	*NO*
PVC wall covering on gypsum plasterboard	*NO*	*>10:00*	*NO*

Experiment compared to prediction shows very good agreement for high fire performance products like plasterboard and thin linings on non-combustible calcium silicate boards. Melting materials and PVC products are not predicted so well.

Major features of the discussed models are summarised in Table 10.

Table 10. Comparison of the thermal models, (Room Corner Test case).

MODEL*	HRR INPUT DATA. FORM FOR $\dot{Q}''_{cone}(t)$	BURNING AREA AS A FUNCTION OF TIME. FORM FOR $A(t)$	IGNITION TIME USED TO CALCULATE BURNING AREA
Wickström/ Göransson (Cone Tools)	Actual HRR curve; $\dot{Q}''_{cone}(t)$ from one heat exposure	$A(t) = A_0\left[1 + a\frac{(t-t_x)^2}{t_{ign}}\right]$ A_0 = 2 m^2, a=0,025s^{-1} for 100 kW burner. For 300 kW burner A_0 = 5 m^2 and a=0,1 s^{-1}	t_{ign} from Cone Calorimeter at 25 kw/m^2 is used directly to calculate burning area with time
Karlsson	Actual HRR curves from tests or $\dot{Q}''_{cone}(t) = \dot{Q}''_p\ e^{-\lambda t}$ fitted to the actual cone curve	$\frac{dA}{dt} = \frac{K \cdot f(\dot{Q}''_{cone})}{\tau}$ integrated over time. The areas close to the burner are treated separately. K=0,01 m^2/kW	τ ***calculated for thermally thick solid exposed to 35 kW/m^2 **** heat flux from the advancing flame. $k\rho c$ and T_{ign} from cone data.
Wade** (BRANZ-FIRE)	Actual HRR curves $\dot{Q}''_{cone}(t)$ from tests of multiple heat exposures.	$\frac{dA}{dt} = \frac{K \cdot f(\dot{Q}''_{cone})}{\tau}$ integrated over time. The areas close to the burner are treated separately. K=0,0065 m^2/kW	τ ***calculated for thermally thick or thin solid exposed to 30 kW/m^2 heat flux from the advancing flame. $k\rho c$ and T_{ign} from cone data.
Sundström (Conflame)	$\dot{Q}''_{cone}(t) =$ $2{,}72\dot{Q}''_p \frac{t}{t_c} e^{-\frac{t}{t_c}}$ using test data of $\dot{Q}''_{ave180s}$ and $\dot{Q}''_p$	$A(t) = C\frac{(t-t_{ign})^2}{\tau^2}$ C = 1,2 m^2	τ and t_{ign} from Cone Calorimeter at 35 kw/m^2 ****is used directly to calculate burning area with time

* The models may also include in the total HRR , $\dot{Q}(t)$,the HRR from the burner, the HRR from the area behind the ignition source and the HRR of some area in the ceiling above the burner. Downward flame spread may also be included. However, these values are less interesting when comparing how the models deal with the HRR due to the flame spread which is leading to flashover.

** BRANZFIRE has several options and parameters can be changed, for example K. The default values are shown. Only the option of having data from several Cone Calorimeter tests (recommended) at different heat fluxes is shown.
*** The time to ignition used to calculate the flame spread also includes the effect of preheating of the surface in the room, i.e. eq 36. Cone Tools and Conflame use cone data directly when there is no preheating. This seems not to influence the results largely.
**** The heat flux at which the ignition parameters are measured is chosen to correspond with the scenario, e.g. 25 kW/m^2 is used when the scale is 1/3 of the Room Corner Test and the flames are small.

The models use the Cone Calorimeter data either numerically,

$\dot{Q}(t) = \sum_{i=1}^{N} \dot{Q}''_{cone}{}^{N-i} \Delta A_i$ (where $t = N\Delta t$), or analytically,

$\dot{Q}(t) = \int_0^t \dot{Q}''_{cone}(t-s) \frac{d}{ds}(A(s))ds$ for the total HRR in the room. The assumption is that the HRR curve in the Cone Calorimeter is the same as the HRR curve from an area element in the room fire.

There are differences in representing $\dot{Q}''_{cone}(t)$, the HRR input data from the Cone Calorimeter, see Figure 30.

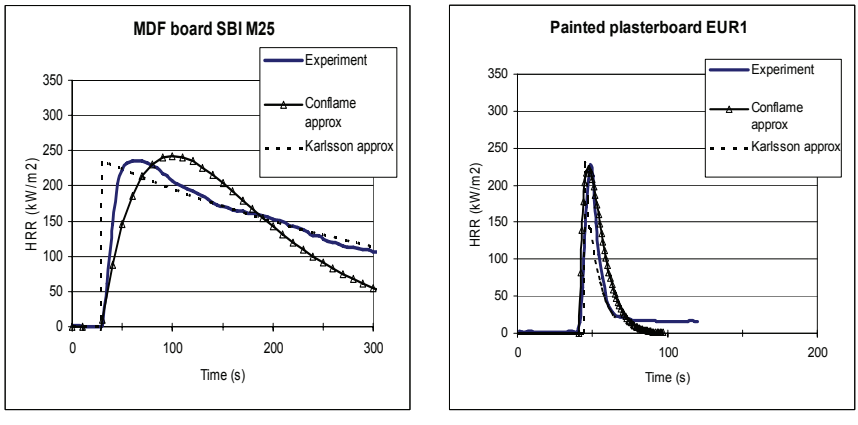

Figure 30. The three different ways the Cone Calorimeter HRR curve is used by the models for MDF board and painted plasterboard.

However, the differences in the representation of $\dot{Q}''_{cone}(t)$ are not directly seen in the predictions. When studying the data in Figure 29, Table 8 and Table 9 it appears that the selection of the expression for $\dot{Q}''_{cone}(t)$ is not critical.

Clearly, it is best to use the full curve from a Cone Calorimeter test, or even better curves from many tests at different heat exposures if available. However, the rather crude analytical expressions of the cone HRR curve works well with the advantage of allowing average values of scalar data to be used. The more important parameter for a good prediction is the ignition time, see Figure 31.

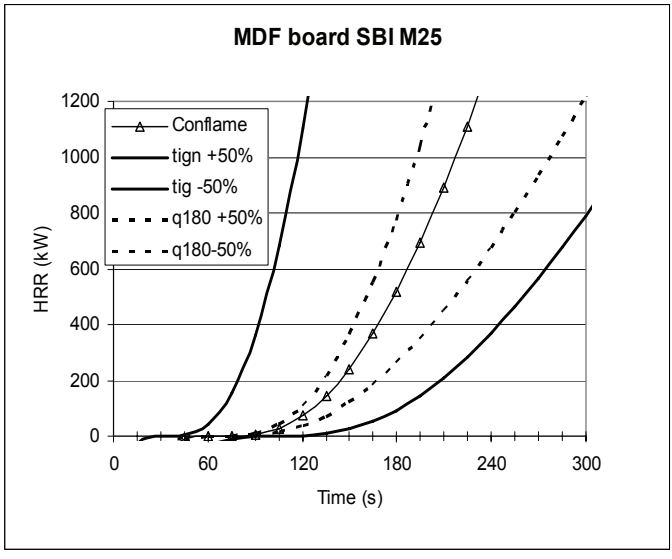

Figure 31. Sensitivity to a change of ± 50% in $\dot{Q}''_{ave180s}$ and t_{ign} (and τ) for MDF board, Conflame.

Changing the ignition time strongly changes the prediction. In addition, the range of ignition times is much larger than the variation of the HRR for the products. Ignition times at 35 kW/m^2 used in this work vary from 10s to 1000s while $\dot{Q}''_{ave180s}$ vary from 10 kW/m^2 to 200 kW/m^2.

The time to ignition due to the burner and the time to ignition associated with the flame spread are taken directly from the tests with the Cone Calorimeter (Conflame and Cone Tools) or it is calculated using $k\rho c$ and T_{ign} as input. If the data to calculate $k\rho c$ and T_{ign} comes from the Cone Calorimeter then there is principally little difference from using the cone ignition time directly. If it comes from another procedure then these thermal data may be different depending on what procedure is chosen. In either case, the assumption of which heat exposure that represents the predicted scenario is important for the result.

Simply because the selected heat exposure determines the ignition time which is sensitive to the result.

The discussed models all assume heat exposures in the range of 25-35 kW/m^2. BRANZFIRE and Karlsson models also calculates the surface temperature, T_s, in the mentioned equations thus including preheating which influences the time to ignition. Cone Tools and Conflame uses the ignition time directly from the cone where the initial surface temperature is ambient. Preheating may be important for the flame spread. However, for the data and scenarios studied in this work it does not seem to influence the results much. It seems that important factors for success in the predictions are: 1) Selection of flame heat exposure from the ignition source which determines the time to ignition of the product in the studied scenario and 2) Selection of flame heat exposure for the wind aided flame spread and the selection of the scenario dependent coefficient for the area growth (K, C or a) which determines the flame spread rate in the studied scenario.

However, there are certain products with a burning behaviour that makes them difficult to model and difficult to test. They often appear as outliers in the predictions regardless of model used. Below a few examples are given.

1. Products that have a protective layer on a combustible core material.
These kinds of products can show excellent fire properties that rely fully on the protective layer. If it fails, the product may burn as if there were no protection at all. Sandwich panels made of steel sheet with combustible insulation are typical examples.

The sandwich panels made of steel sheet with combustible foam insulation PUR EUR 9 and EPS SBI M21 went to flashover after 3 min 15 s and 16 min 10 s respectively. A possible process leading to flashover is the following. Heating by the ignition source is quite efficient because the product has good insulation properties. Thus, the foam will pyrolize due to the high temperature. Whether it results in a fire or not depends on the amount of pyrolysis gases, where they go and the efficiency of any flame-retardants added to the foam. If they escape to the zone where the flame from the ignition source is present then they may ignite. The additional heat result in more pyrolysis gases that will ignite and the fire will grow. On the other hand, if the pyrolysis gases escape from the hot zone then they will not ignite. The amount of gas will decrease as the supply of fuel is decreasing and there will be no fire growth. Cracks and openings appearing in the panel during the test and melting or not of the foam will influence where the pyrolysis gases go.

Neither of the discussed effects can be studied in the Cone Calorimeter test or any other small-scale test simply because the joints, the mechanical behaviour and the route for pyrolysis gases can not be tested or is just partially covered by the test. Theoretically, the SBI test should be the best due to its larger scale but also here there is very little if any correlation with the room fire [77, [78]. The fact that the steel sheet on PUR seems to be modelled correctly is just a coincidence. The small 10 cm x 10 cm cone sample has edges through which the pyrolysis gases escape and ignites early in the test. If these edges were covered with steel as in reality the resulting HRR in the cone test will be zero. In the room test, the poor performance relates to the structure. Better joints etc would have given a good large-scale result. The EPS sandwich panel gives flashover in the Room Corner Test but not in the predictions due to very late ignition of pyrolysis gases in the Cone Calorimeter.

Clearly modelling the fire behaviour of these types of products is a challenge. Governing phenomena for fire growth are mechanical distortion, transport of pyrolysis gases and melting. This rule out the models where it is assumed that the solid is inert until ignition. There are at least three problems in predicting the fire growth in a room for these types of products, 1) the small-scale test is not representing the processes controlling the real burning behaviour and 2) characteristic materials data is not available for the above-mentioned processes and 3) calculation models are not available for the processes.

2. Melting products

Melting products may or may not burn in a room configuration depending on how they are mounted. For example, a thermoplastic product mounted with screws and washers in the ceiling of the Room Corner Test can become soft around the washers due to the heating and fall to the floor early in the test. The result is no fire growth. However, the same product glued to the ceiling may cause a rapid flashover because the glue covers a large area and holds the product in place.

A gas burner giving a slowly growing HRR up to a constant value may not ignite a melting product because it is given time to melt and escape from the flame. However, a source that immediately reaches a high HRR may cause rapid fire growth because the product is heated fast and pyrolize before it melts. In extreme cases, one may find that a thicker product attached to a wall behaves better than a thinner product of the same material due the possibility for a thicker product to melt away further from the ignition source.

Melting products cannot escape when tested in the Cone Calorimeter. The sample holder is horizontal and the melted material stays exposed to the heat. Therefore, a cone test is sometimes more severe than a large-scale test.

When the product is easily ignited, for example not enough FR treated, the melting effects become unimportant. It will ignite when exposed to a flame. The polystyrene products tested here all came to flashover, the data from the Cone Calorimeter is consistent and the predictions agree with the occurrence of flashover, see Figure 22. However, for melting FR products the same three problems as for the protected products may occur.

3. Chemistry

The predictions tend to be incorrect for PVC products. The PVC wall carpets will be predicted to give an early flashover with very small changes in input data or model tuning. In the Room Corner Test, only the large ignition source leads to flashover. The FR PVC SBI M02 is in all cases predicted to give flashover but when the product was tested in the Room Corner Test there was no flashover. A PVC wall carpet tested in the SBI got a higher FIGRA value than was expected from the Room Corner Test, see Figure 5. For comparison, Cone Calorimeter test data on FR PVC and wallpaper on particle board is shown in Figure 32.

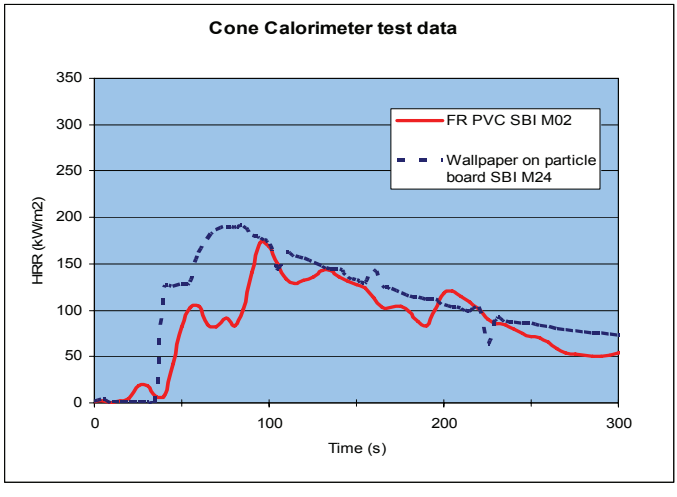

Figure 32. Test data from the Cone Calorimeter on FR PVC and wallpaper on particle board.

The FR PVC ignites at about the same time as the wallpaper on particle board and gives off nearly as much energy.

It is difficult to see how any prediction based on these results should differ much from each other. However, the wallpaper faced particle board went to flashover during a Room Corner Test experiment at about 2 min 45 s while the FR PVC showed very little burning. PVC is due to the chlorine content inherently flame retardant by chemically inhibiting the flame. A possible explanation is that this process is more efficient in the large-scale test than in the small-scale test. Modelling would require that the chemistry is included and that the small-scale test gives the required input data.

4 FIGRA used for prediction of the HRR history for a Room Corner Test experiment

FIGRA is a parameter that is a measure of hazard as it is correlated to the burning behaviour of products in reference scenarios, which in turn are assumed to reflect the real fire hazard, see section 2.1. Figure 17 shows that the relative precision of this hazard assessment for products under the CPD is quite good for a large variety of products. Fire hazard is estimated based on the occurrence of certain events in the reference scenario, e.g. flashover. However, only indirect is this a prediction of fire growth and in this section the possibility to use FIGRA for prediction of fire growth will be discussed.

Figure 33 below shows some experimental data from SBI tests.

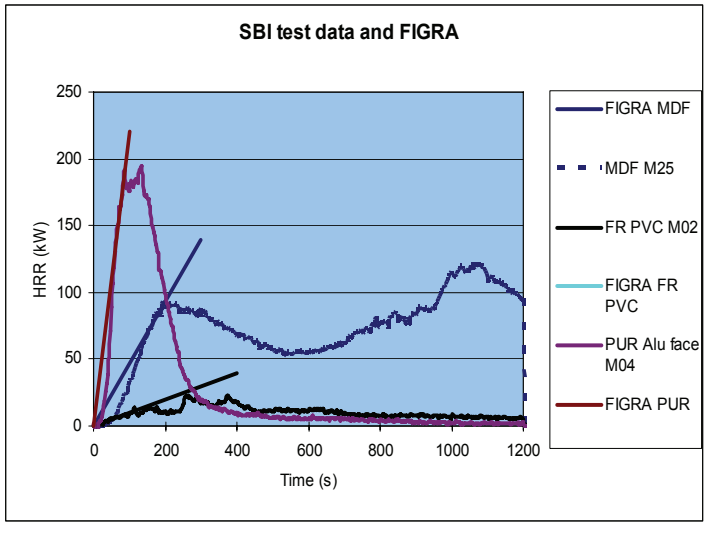

Figure 33. The HRR curves measured in the SBI and the corresponding FIGRA values for some products. The highest peak HRR refers to PUR and the lowest to FR PVC. The straight lines have the slope of FIGRA.

The straight lines have a tangential point with the HRR curves shortly before the point in time when the growth of the HRR in the SBI test becomes zero and subsequently declines.

As discussed earlier this point coincides with the flame spread reaching the top of the sample or stopping before for high performance products. The lateral flame spread that may follow tends to be slow or not happen at all depending on product. The increase in the HRR after about 10 minutes for the wooden product is a result of burn through and burning on the other side. In a Room Corner Test experiment, burn through will happen long after flashover and it is therefore not interesting in this work.

After ignition, the subsequent growth of the HRR is a function of both flame spread rate and HRR per unit area from the product. In the SBI, ignition time can be measured but the heat flux causing the ignition is from a flame giving only one exposure level that varies over the surface of the sample. The total HRR cannot easily be separated into HRR emanating from a given area element that is burning and the HRR due to the growth of the burning area through the flame spread. Consequently, it is very difficult to deduce material data for mathematical models e.g. thermal inertia, ignition temperature from an SBI test. Such calculations require input of heat flux versus ignition time and HRR per unit area for a known heat exposure. A SBI test gives a certain HRR curve, which is the result of the test scenario and the properties of the product. FIGRA is a straightforward way to represent an important property of that HRR curve. Short ignition time, fast flame spread and high HRR per unit area give a large FIGRA value and vice versa. If the test scenario changes then the HRR curve and FIGRA changes.

However, for a given scenario, the FIGRA parameter reflects product properties in that scenario as already shown in section 2.1. The scenario must be well defined and not be changed for different materials, like a standard test. Another condition is that the fire is fuel controlled, i.e. have a free supply of air.

4.1 FIGRA is a rate parameter

FIGRA is a combined rate parameter that shows the growth rate of a fire. Seen as a rate parameter it reflects the response rate of a certain material or product in a given fire scenario. FIGRA used for prediction of the fire growth should therefore be applied as a general function of the product FIGRA x t, i.e. $\dot{Q} = f(FIGRA \cdot t)$ where f is a function of some arbitrary form, polynomials, exponential functions etc. Thomas mentions three general growth laws for fire problems, linear, square and exponential [50].

For one-dimensional spread, we may assume a polynomial like $\dot{Q} \propto t$ or for horizontal spread on an area (without burnout) $\dot{Q} \propto t^2$ as already used in this work with the thermal theories assuming an inert solid. If the growth rate of HRR is assumed proportional to the HRR itself then $\dot{Q}$ will grow exponentially.

Data is available from the Room Corner Test. A given portion of the heat generated from the product in the room is used to heat the product that burns to produce more heat and so on. Thus for this case, the exponential growth relation is tried assuming that the growth rate of heat release rate is proportional to the heat release rate itself.

$$\frac{\partial \dot{Q}}{\partial t} = C_0 \dot{Q} \qquad 42$$

The solution to eq 42 is

$$\dot{Q} = be^{C_0 \cdot t} \qquad 43$$

The coefficient C_0 is the rate coefficient and *b* is a constant.
As earlier discussed, the fire growth depends on the specific scenario or test procedure as well as the product properties. Therefore, we separate C_0 into two coefficients; A scenario dependent coefficient, C, and a product dependant parameter, FIGRA, i.e. $C_0 = C \cdot FIGRA$ and

$$\dot{Q} = be^{C \cdot FIGRA \cdot t} \qquad 44$$

We take the constant *b* =1,0 kW because the most convenient solution is to do the correlation with one parameter only, C. At the time zero then $\dot{Q}$=1 kW ~ 0 kW.

This function will grow to infinity and would need a condition for the case when there is flame spread when the ignition burner in the Room Corner Test is raised to 300 kW after 600 s and a condition when there is no flame spread at all. These conditions have to be defined as a FIGRA minimum value as the correlation is based on this parameter only. The minimum FIGRA can be taken from experimental data or directly from the Euroclass limits.

However, if eq 44 works for the first 600 s then limiting conditions can be added without changing the substance. Therefore this study is limited to first 600 s of a Room Corner Test experiment.

From Figure 3 $FIGRA_{RC}$ is 7,5 kW/s when corresponding to flashover, 900 kW from the product, at 120 s in the Room Corner Test scenario. From Figure 5 it is seen that FIGRA(SBI) is about 620 W/s when $FIGRA_{RC}$ is 7,5 kW/s. Insertion of FIGRA(SBI) 620 W/s, t=120 s and $\dot{Q}$=900 kW into eq 44 then gives C = 0,091 kW^{-1}. Figure 34 shows experiment versus calculated data.

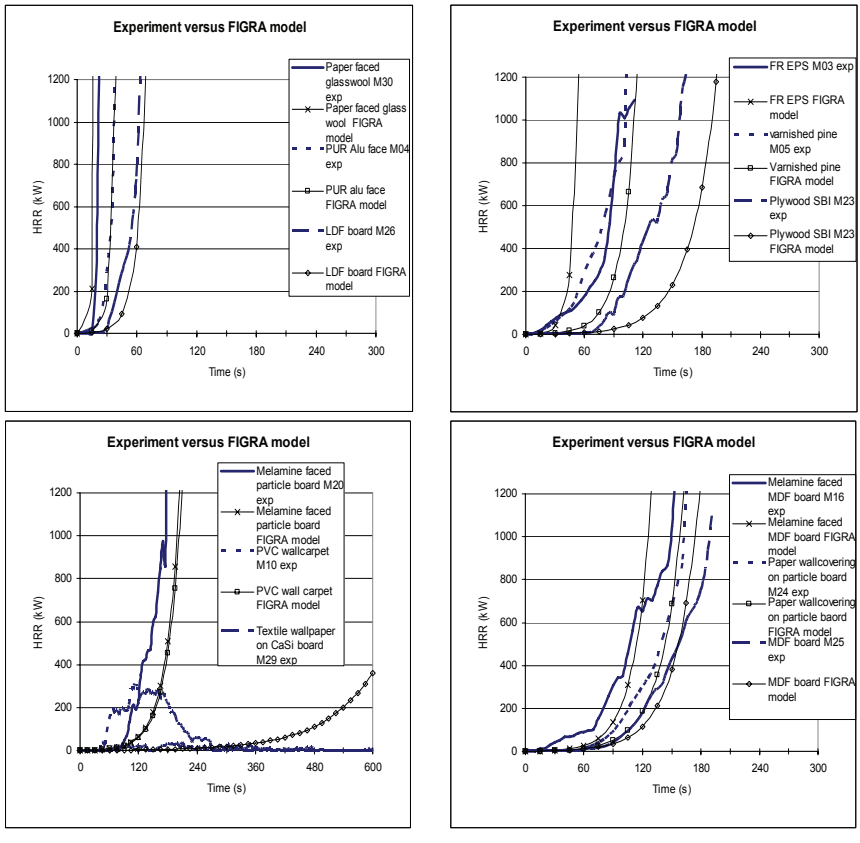

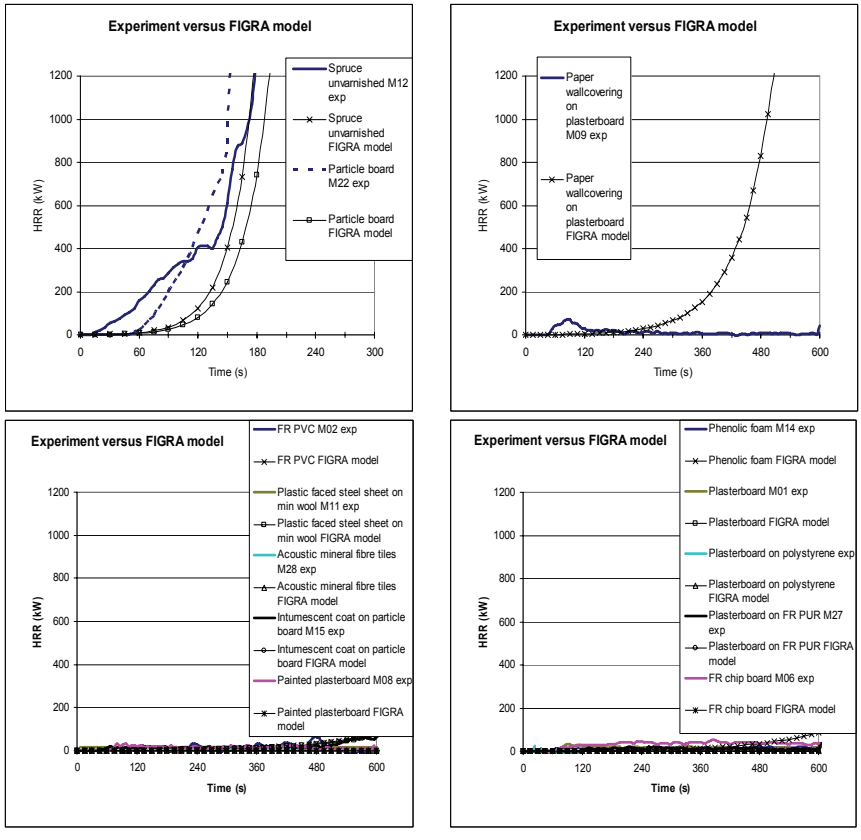

Figure 34. Comparison of experimental data from the Room Corner Test with predictions based on the FIGRA-model eq 44. Acoustic mineral fibre tiles M28 and unfaced rockwool M19 are not plotted as FIGRA ~ 0.

The agreement between the FIGRA-model and the experiments is surprisingly good considering the simplified approach. In Figure 35 the relation between predicted and measured time to flashover is shown.

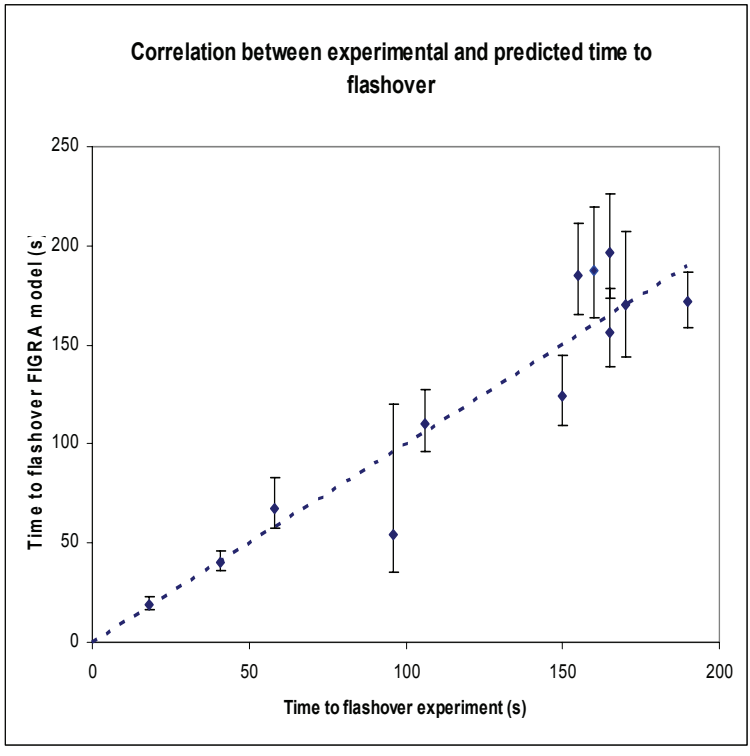

Figure 35. Correlation between experimental and predicted time to flashover (Room Corner Test data) for products going to flashover during the first 10 minutes of test. The dotted line shows the one-to-one relation.

The error bars given in the figure are taken from the round robin data of the SBI test [19]. The error bars were calculated using FIGRA(SBI) average for the midpoint. The upper and lower limits were then calculated using FIGRA(SBI) average plus respectively minus the standard deviation for reproducibility for that specific product. The relative spread in data for the individual products is therefore shown. Note that the error bars are not intended to cover all possible results with high probability. They will become larger depending on what confidence level that is chosen. In addition, the uncertainty of the large-scale data is not known. The present data comes from 10-15 laboratories and the first round robin while the SBI test procedure was still in development. The deviation from the one-to-one relation is more or less within data spread. The outlier having an experimental flashover time of about 100 s is expanded polystyrene, EPS. As earlier discussed, this material melts away from the ignition source and is often showing data spread.

Table 11 below shows the results for the other products.

Table 11. Predicted versus experiment for products not going to flashover during the first 600s in the Room Corner Test at an ignition source level of 100 kW.

PRODUCT	IS THERE FLASHOVER BEFORE 600 S ?	
	Experiment	Prediction FIGRA model
Plasterboard SBI M01	NO	NO
FR PVC SBI M02	NO	NO
PVC wall carpet SBI M10	NO	Yes at 200s
Phenolic foam SBI M14	NO	NO
FR Chip board SBI M06	NO	NO
Painted plasterboard SBI M08	NO	NO
Paper wall covering on plasterboard SBI M09	NO	Yes at 486s
Plastic-faced steel sheet on mineral wool SBI M11	NO	NO
Plasterboard on polystyrene SBI M13	NO	NO
Intumescent coat on particle board SBI M15	NO	NO
Unfaced rockwool SBI M19	NO	NO
Plasterboard on FR PUR SBI M27	NO	NO
Acoustic mineral fibre tiles SBI M28	NO	NO
Textile wallpaper on CaSi board SBI M29	NO	NO
Steel on EPS sandwich SBI M21	NO	NO

We see good agreement with two outliers out of 15, i.e. about 90% agreement. Again, the PVC wall carpet is over predicted as was the case for the earlier tried models based on the Cone Calorimeter. The paper wall covering on plasterboard is over predicted. However, this is a borderline case.

Figure 36 shows the correlation between experimental and predicted time to flashover in the Room Corner Test for Conflame, Cone Tools, the FIGRA model from the SBI, BRANZFIRE and Karlssons model.

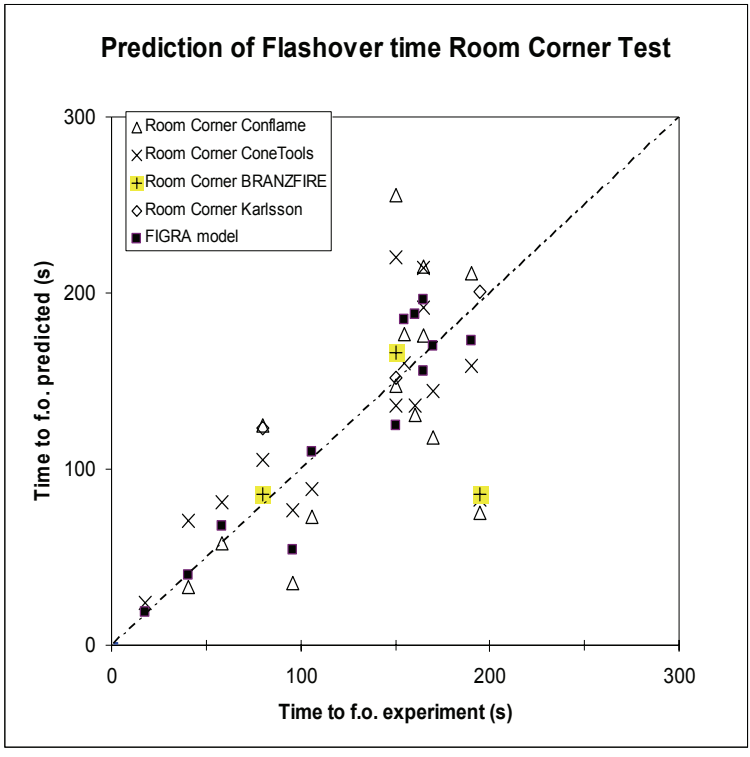

Figure 36. Correlation between predicted time to flashover and experimental value for Cone Tools, Conflame, BRANZFIRE and FIGRA model SBI test.

There are only minor differences in the success of the different predictions and the FIGRA model works as good as the thermal models or even slightly better in this case. The least square regression coefficient, R^2, for the FIGRA model is 0,88 which is quite good. Considering that the SBI data for FIGRA comes from 15 laboratories at a stage when the test was still under development it is surprisingly good. For certain products the larger size of the SBI test sample seems to be an advantage over the Cone Calorimeter. In addition, the similarity in the test configuration between the SBI and the Room Corner Test, a burner in a corner, may play a role.

The thermal models also tend to give similar predictions. If there is an overestimate of flashover time, they all tend to overestimate and vice versa. Probably this happens because the input test data is identical and because the physical treatment of this data is similar in the models.

For the products not shown in the diagram see, Table 8, Table 9 and Table 11.

4.2 Discussion of FIGRA and the use of the SBI test

In this work, FIGRA values obtained in SBI tests are shown to correlate with four different reference scenarios and two standard tests, i.e. six different experimental situations. The product categories are interior linings, cables and pipe insulation, i.e. three different product categories of varying geometrical shape. The materials involved are wood, paper, PVC, melamine, PUR, PIR, PE, EPS, XPS, vinyl rubber, wool, cotton, calcium silicate, plaster, stone wool, glass wool, varnish, paint and so on. About 100 large-scale experiments and more than 1000 small-scale tests are used for the calculations. Data comes from 17 European laboratories. Thus, the usefulness and versatility of the FIGRA parameter is well based on experimental evidence considering the large and diversified database on which the conclusions in this work are drawn.

FIGRA values determined in different standardised small-scale tests correlate. The correlation coefficient, R^2, using least square regression, is 0,94 both when FIGRA for the SBI test is compared with FIGRA for the ISO 21367 test and when compared with $\dot{Q}''_{180s} / t_{ign}$ for the Cone Calorimeter, see Figure 15 and Figure 28.

FIGRA is rank ordering products in a consistent way and shows a strong correlation (R^2 is about 0,9 see Table 5) with large scale reference scenarios for hazard assessment. The FIGRA parameter is in other words a measure of a products fire hazard, see section 2.6.

FIGRA used for prediction HRR versus time and the time to flashover for linings in the Room Corner Test works well, see Figure 36 and Table 11. The correlation coefficient R^2 is 0,88 for the time to flashover predictions.

FIGRA is one single parameter, which characterises a products tendency to contribute to the growth of the HRR. The definition of FIGRA contains threshold values. These are important as they filter out early ignitions followed by a small peak of the HRR which otherwise might cause a large, unrealistic FIGRA value. The threshold values must be chosen in relation to the scenario. A large-scale test requires a larger threshold value than a small-scale test. In the SBI 0,4 MJ is used as threshold for some of the classes. This is for example 40 kW for 10 s, which is substantial in a test where a typical peak HRR from a product is about, or less than 100 kW.

FIGRA is an integral parameter as there are a number of basic product properties that results in a FIGRA value. FIGRA combines HRR and time (ignition) in one value, HRR/time. Cone Tools and Conflame use two parameters, ignition time and HRR separately to characterise a product, (but use it in the combination HRR/time). The time to ignition can be separated into the product parameters thermal inertia, $k\rho c$, and ignition temperature, T_{ign}. Other models use thermal inertia, ignition temperature and HRR i.e. a handful of parameters to characterise a product. These also still include integral parameters, although they are "more" basic. Thermal inertia determined from experimental data and the thermal theory only results in an effective value including also e.g. the influence from melting and pyrolysis. The ignition temperature is depending on the rate of pyrolysis and the mixing with air and it also becomes an effective value. The Fire Dynamics Simulator or FDS, discussed below is an advanced so-called CFD code. It uses 18 parameters to describe product properties, which perhaps is the required number of basic product properties for general fire modelling.

An integral parameter will suffer from the fact that there are different combinations of basic properties that will result in the same value of the integral parameter. Therefore, two products with the same value of the integral parameter may not show consistent behaviour when exposed to different fire situations. One or the other of the basic parameters may be more important when changing scenario. For the same reason the value of the integral parameter will depend on the specific test that is used to measure it. The FIGRA parameter is at the top of the "hierarchy" of integral parameters and is therefore not a basic product property. Due to its definition, HRR/time, the value of FIGRA is different for different scenarios. However, for a given scenario FIGRA provides effective product properties useful for classification and correlation between scenarios, which is used to estimate fire hazard of the product. As an example, it is useful for prediction of fire growth of linings in the Room Corner Test.

5 The Fire Dynamics Simulator, FDS, used for prediction of the HRR history for a Room Corner Test experiment

NIST Fire Dynamics Simulator or FDS is a Computational Fluid Dynamics, CFD, model of fire driven fluid-flow [79], [80]. Being a CFD-model, it is a general and versatile tool applicable to a very broad field of fire situations. The model solves the Navier-Stokes equations appropriate for the thermally driven flows, smoke and heat transport in fires. The equations are solved for a number of cells in a rectilinear grid. The size of a cell should be small enough depending on the specific problem. A direct numerical simulation is practically not possible as the computer power required is far above what is available.

Therefore, for room fire problems FDS simulates turbulence by LES, Large Eddy Simulation. This means that turbulent eddies that are smaller than is resolved by the grid are "modelled" by a sub-grid model, the Smagorinsky form of LES. Modelling radiation, combustion and convection contain other simplifications. For these and other reasons, the grid size is very important for the solution. In general the smaller the size of the grid the better accuracy. In addition, the non-linear nature of the used equations makes the calculations sensitive to the grid size.

FDS version 4 includes a model for flame spread and fire growth that was tried on test data for MDF SBI M25, LDF SBI M26 and Spruce unvarnished timber SBI M12 already analysed in this work. The input data is shown in Table 12.

Table 12. Input data used in FDS calculations

Simulation no	Thick-ness* (mm)	Density* (kg/m^3)	T** ignition (C)	Heat of** Vaporization (kJ/kg)	Thermal** conductivity, (W/mK)	Specific heat capacity (kJ/kgK)
MDF 1	12	700	320	400	0,15	1,5
MDF 2	12	700	320	400	0,15	1,5
MDF 3	12	700	320	400	0,15	1,5
MDF 4	12	700	320	400	0,15	1,5
MDF 5	12	700	320	400	0,15	1,5
LDF 1	12	250	320	400	0,10***	1,207***

Simulation no	Thick-ness* (mm)	Density* (kg/m^3)	T** ignition (C)	Heat of** Vaporization (kJ/kg)	Thermal** conductivity, (W/mK)	Specific heat capacity (kJ/kgK)
LDF 2	12	250	320	400	0,10***	1,207***
Spruce 1	10	450	320	400	0,20	1,3
Spruce 2	10	450	320	400	0,20	1,3

Cont.

Simulation no	Char** density (kg/m^3)	Thermal** conduc-tivity of char, (W/mK)	Specific** heat capacity of char (kJ/kgK)	Critical** mass flux (kg/m^2s)	A-factor (m/s)	Activa-tion energy, E_A (kJ/mol)	Grid size (cm)
MDF 1	80	0,2	2,5	0,012	0,015	33	20
MDF 2	80	0,2	2,5	0,012	0,0025	24	10
MDF 3	80	0,2	2,5	0,012	0,0371	37	5
MDF 4	80	0,2	2,5	0,012	3,0E-04	13	5
LDF 1	30	0,2	2,5	0,012	0,67	46	20
LDF 2	30	0,2	2,5	0,012	0,003	20	20
Spruce 1	150	0,12	1,5	0,012	0,0651	36	20
Spruce 2	150	0,12	1,5	0,012	0,015	29	20

* Measured
** Hietaniemi et al [81]. They used a grid size of 20 cm.
*** Göransson [82]

The chemical reactions were in all cases the same as all the products are cellulose. The reaction parameters were taken from the library that comes with FDS, see Table 13. The moisture fraction was in all cases assumed to be 0,1.

Table 13. Reaction parameters used for the wood products in the FDS calculations

SOOT_YIELD	= 0,01
NU_O2	= 3,7
NU_CO2	= 3,4
NU_H2O	= 3,1
MW_FUEL	= 87,0
EPUMO2	= 11000

Other parameters were taken as default, e.g. parameters for radiation calculations.

The data in Table 12 is mainly from Hietaniemi et al [81] who used it for MDF and Spruce. They have developed the sub-model for pyrolysis in FDS . It was used to model the Cone Calorimeter, the Room Corner Test also with only partial linings, the SBI, cavity fires, furniture and pool fires with very good results using large grid sizes (20 cm in the Room Corner Test) [81]. Data on LDF board was available in [82].

There are 18 input parameters required for a FDS simulation (E_A is calculated from the A-factor and the critical mass flux) which are specific for the fuel. Some of them are easy to obtain or measure, others are difficult. Other parameters like the thermal conductivity are temperature dependent. The uncertainties of the input data are rarely known and are likely to be large in some cases. Göransson [82] measured ignition temperature on wood products using thermocouples and a thermographic phosphorescence technique at different radiant heat exposures of a sample. For LDF and MDF he got ignition temperatures ranging from about 250 to 400 deg C depending on measurement technique and heat exposure. A value of 320 deg C is reasonably in the middle of this span.

This study was limited to running simulations changing parameters believed to have a large influence of the result. The A-factor and the corresponding activation energy were found to be very important for the results.

The pyrolysis model for charring materials in FDS 4 uses the assumption that the pyrolysis rate follows an Arrhenius relation for a first order chemical reaction

$$\dot{m}'' = A(\rho_s - \rho_{char}) \cdot e^{-E_A/RT} \qquad 45$$

where ρ_s is the density of the virgin material, ρ_{char} is the density of the char and R is the universal gas constant.

The constant A and the activation energy, E_A, in this relation are rarely known for real products. An alternative approach in FDS is to prescribe the "critical mass flux" and the ignition temperature. The code will then select values of A and E_A so that the fuel starts to burn at the "critical mass flux" when the surface is at the ignition temperature. Tewarson reports a value of the critical mass loss rate of 5 g/m^{2}s for flame spread to occur, [57]. FDS uses a default value of 20 g/m^{2}s for the critical mass loss rate at which the fuel burns when it has reached ignition temperature. In this case, 12 g/m^{2}s from Hietaniemi et al [81] is used. However, a simulation where this parameter was changed to 5 g/m^{2}s did not make any difference.

In Figure 37 simulations of Room Corner Test experiments with the input data from Table 12 and Table 13 are shown together with the corresponding test results for the wood products

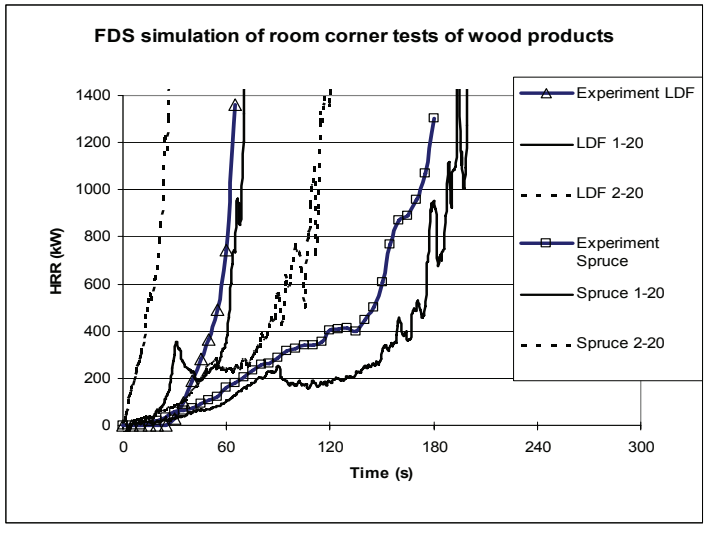

Figure 37. FDS simulation of wood products. Grid size 20 cm.

The results are quite good for optimum values of A and E_A. For the simulation with LDF 2-20 and Spruce 2-20, the activation energy was reduced.

When less energy is required for pyrolysis the HRR grows faster. The effect is large, at about the same as when the time to ignition was changed in the thermal models, see Figure 31.

The MDF simulations where done changing the grid size. The 20 cm size grid is rather course. The ignition burner is covered by one cell and therefore the modelling of the flame is crude. For coarse grids, FDS uses a correlation for the flame height and another correlation to distribute the heat release over the flame surface, see [79] paragraph 3.2.2. Therefore, simulations were made reducing the grid size to 10 cm and to 5 cm. The results for MDF are shown in Figure 38.

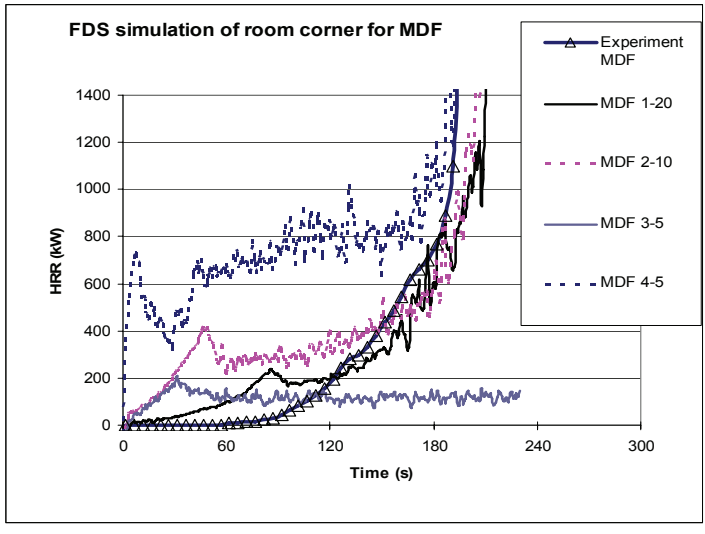

Figure 38. Simulation with FDS for MDF using different grid sizes.

When the grid size was changed to 5 cm and the activation energy was kept as about the same as for the 20 cm grid, then the result was no fire growth, the predicted HRR never exceeded 200 kW, MDF 3-5. Therefore, when the grid size was changed the activation energy was also changed. For the 10 cm grid, MDF 2-10, it had to be changed from 33 kJ/mol to 24 kJ/mol and for the 5 cm grid it had to be changed to 13 kJ/mol, MDF 4-5. The result is about the same prediction of time to flashover but prior to that the predicted HRR differs much. With the lower activation energies, FDS predicts considerable pyrolysis at lower temperatures that gives a high HRR. The reasons for these results are not known. A possibility is that the grid should be smaller. A grid of 1 cm or smaller should be used for resolving the process in the flame spread better.

However, when going from 5 cm grid size (in this case about 24 h simulation time on a fast computer) to 1 cm the simulation time increases by a factor of 625, which was beyond the scope of this work. However, FDS technical reference guide points out the difficulties of modelling flame spread and heat release with a CFD code. The guide mentions three major uncertainties when modelling heat release: "(1) properties of real materials and real fuels are often unknown or difficult to obtain, (2) the physical processes of combustion, radiation and solid phase heat transfer are more complicated than their mathematical representations in FDS, (3) the results of calculations are sensitive to both the numerical and physical parameters."

6 Discussion and summary

The European harmonised system for testing and classification the reaction to fire of construction products was developed to reduce trade barriers while at the same time allowing the European regulators to maintain their traditional safety requirements. Trade and safety are the basic ideas behind the system. It must therefore be based on science as well as on tradition and it must fit the needs of the market and the regulators in many countries. Important properties of the European testing and classification system is therefore that it is

a) Understandable and usable for fire experts, regulators, industry and the public
b) Reflecting fire hazard of construction products in practise
c) Allowing the national regulatory systems to be maintained only with minor changes
d) Not distorting the markets for the industry
e) Validated, reliable, credible and acceptable throughout more than 30 countries

All these requirements are impossible to fulfil without compromises. On the other hand violating substantially any of the points above will not be acceptable. A proposal for a so-called “long term solution” based on mathematical fire modelling is no longer considered. A combination of national systems from the largest European countries was rejected. Reasons were problems with some of the points above.

The European system has a parameter for classification, FIGRA, which is clear and simple to use and the relation to product hazard can be quantified as described in this work. National regulations at present in about 30 countries have adopted the system and adapted their national regulations accordingly. The market distortions are confined to only a few product groups. The reliability and credibility is constantly under surveillance as the system is running under legal obligations on a large market. All challenges have (so far) been met with success.

A key to success to estimate the products fire hazard are the reference scenarios. With a reference scenario available, it is possible to demonstrate the hazard of a product, see section 2.6.

In this work so-called thermal models were compared with data on a large number of common building products, linings, in four room configurations ranging from about 1 m^2, to a small bed room (3,6 m x 2,4 m), to a large living room and to a very large room (9 m x 7 m and 5 m high). In all cases, the linings were mounted on both the walls and the ceiling. In addition, the SBI test was studied.

A straightforward analytical formulation was developed based on the assumption of constant flame spread rate, Conflame. Conflame uses scalar data from a Cone Calorimeter test, the peak HRR per unit area and the average HRR per unit area during 180 s at 50 kW/m^2 radiant heat exposure. From these data, an analytical expression of the cone HRR curve as a function of time is calculated. To simulate the time to ignition a heat flux representing the ignition source in the experiment is needed, for example 35 kW/m^2 for a Room Corner Test experiment for the 100 kW ignition source. To simulate the flame spread a heat flux representing the heat exposure of the flames in the experiment is needed, for example 25 kW/m^2 in the 1 m^2 small room. The analytical HRR curve and the ignition times associated with the ignition source and the flame spread respectively are then used for prediction of the HRR curve of a Room Corner Test, other smaller and larger room fires or the SBI test, see section 3.2. Conflame is only requiring scalar input values from the Cone Calorimeter for these calculations. Another feature is that it uses average values.

Conflame, Cone Tools, Karlssons model and BRANZFIRE were studied in relation to experimental data. Conflame and Cone Tools are basically scaling the flame spread rate, or growth rate of the burning area with the inverse of the ignition time for a certain heat flux measured in the Cone Calorimeter. A scenario dependent coefficient is matching the calculated area growth with experiments. Karlssons model and BRANZFIRE use small-scale data (mostly cone data) to calculate the thermal inertia and the ignition temperature. They use the flame spread theory developed by Quintiere. A scenario dependent coefficient, the flame area coefficient, K, is used to match data with experiment. BRANZFIRE is a complete multi compartment two-zone model that solves the full heat and mass balance of the room. It is applicable to many scenarios. The heat exposure assumed for the flame spread process is 25 – 35 kW/m^2 for all the models discussed here. Comparison of experiments with predictions showed good agreement for all the models cf. Figure 29 and Table 8.

Computational Fluid Dynamics, CFD, models are different from the thermal models as they solve the basic heat and mass balance equations for a large number of small control volumes. Therefore, they are general and useful for arbitrary scenarios and problems. The Fire Dynamics Simulator (FDS) was used

to simulate some Room Corner Test experiments on wood. The built in flame spread model was tried. The simulations were quite sensitive to the chosen grid size and to changes of the activation energy required for pyrolysis. It is clear that good input data is needed for a successful simulation. The FDS technical reference guide also points out that more research and development are needed for the modelling of HRR.

The thermal models are in principle using the products HRR per unit area, $\dot{Q}''$, divided by the time to ignition, ($\dot{Q}'' / t_{ign}$) or ($\dot{Q}'' / \tau$), as a basis for predictions of the HRR in the room scale and in the SBI. $\dot{Q}''$ is a function of time and position and the total HRR in the room scale is obtained by superposition using numerical expressions or the Duhamel integral, see section 3. HRR per unit area and time to ignition at a certain heat exposure reflect properties of the product. This fact is used in the definition of the FIGRA parameter.

FIGRA, FIre Growth RAte, is calculated as the maximum value of the function (HRR/elapsed test time), i.e. $\dot{Q} / t$. The time in this case is including the time to ignition due to exposure of the ignition source and the ignition time related to the flame spread. A large HRR in a short time results in a large FIGRA value and vice versa. Seen as a rate parameter it reflects the response rate of a certain material or product in a given fire scenario. FIGRA is a so-called integral parameter, not an intrinsic material property and the value changes when the test scenario changes. For details, see section 4.2.

For defined situations, the FIGRA parameter is consistently rank ordering products for their tendency to fire growth in several scenarios. Plotting the FIGRA values for about 100 products tested in all classification tests required for reaction to fire in the European system versus data from all the involved reference scenarios results in a global least square correlation of 0,89. This can be seen as a measure of how well the European system can reflect fire hazard of building products. For details, see section 2.6.

The FIGRA parameter also correlates between standard tests. FIGRA calculated for the SBI test correlates well with FIGRA calculated for a small-scale test for plastics, ISO 21367 and with $\dot{Q}''_{180s} / t_{ign}$ calculated for the Cone Calorimeter, see Figure 15 and Figure 28.

The function $\dot{Q} = 1{,}0 \cdot e^{0{,}091 \cdot FIGRA \cdot t}$ (HRR in kW and time t in s) predicts the HRR history of a Room Corner Test experiment quite well.

In Figure 36 data on prediction of flashover time in the Room Corner Test from the thermal models based on the Cone Calorimeter as well as the FIGRA correlation based on SBI data is plotted together, see also Table 11. The results are quite good, and the straightforward FIGRA correlation for the available data in this case works as good as the models based on cone data. The correlation coefficient for prediction of flashover time is 0,88. The products not going to flashover during the first 10 minutes of testing in the Room Corner Test is predicted correctly as "no flashover" in about 90% of the cases.

Common for most comparisons with the FIGRA parameter is that correlation coefficients are typically 0,9. This holds for many different products in different scenarios, data from different laboratories and for the straightforward model of the HRR history in the Room Corner Test.

This work demonstrates the versatility of the FIGRA parameter in a legal environment, the European system, and for product hazard assessment, through reference scenarios. It further demonstrates how FIGRA is related to product parameters used in so-called thermal models. The European countries took a large step forward from old testing and classification systems by the introduction of the reaction to fire requirements under the CPD. It is hoped that this system will be further improved and developed. For example the link between the thermal models and the European system should be explored further. A major step forward in fire growth modelling would be the further development of the CFD codes so that they can predict flame spread and HRR for general cases. This requires input data that are basic product properties not influenced by the test procedure. A new generation of tests have to be developed for that purpose. According to my opinion the best way forward is to develop the models in co-operation with test developers. The reason is simple: It is a very large and expensive project to develop completely new test procedures and it needs agreement between laboratories, regulators and industry to do so. It is a commitment of many years that will only happen if one can foresee an implementation and a real improvement over the systems used today.

7 Annex A – Input data

Input data used for calculations are shown in Table 14 and Table 15 below. Many calculations and diagrams in the thesis are based on other data not given here due to space limitations. It is available in the sources referred to, for example the SP database or the various reports.

There are three series of data. The s-products, Table 15, were tested in large and small scale [17], [72], [83]. The EUREFIC data and the SBI data are available in [38], [39] and [19]. The three series of products, s, EUREFIC and SBI, have very similar specifications. For that reason, the needed HRR data for the small room predictions with Conflame was taken from the EUREFIC and the SBI series of products having similar specifications although not being from the same batch. As earlier discussed, the result is not as sensitive for variations in HRR data as for the ignition time. Products not used in simulations are indicated in the tables. Either data was not available or a product with a similar specification was already used. The FIGRA values are according to classification scheme as given in EN 13501-1.

Table 14. Data from the Cone Calorimeter and the SBI tests used for calculations of HRR in the Room Corner Test, the large-scale test and the SBI test.

PRODUCT*	ID	$\dot{Q}''_{ave180s}$ (kW/m^2) *	$\frac{\dot{Q}''_{ave180s}}{t_{ign}}$ (kW/m^{2}s) *	$\dot{Q}''_p$ (kW/m^2) *	t_c (s) *	t_{ign} at 35 kW/m^2 (s)	t_{ign} at 55 kW/m^2 (s)	FIGRA (W/s)
Painted plasterboard	EUR 01	21	0,48	218	6	100	39	-
Plywood	EUR 02	173	6,72	276	46	51	-	-
Textile wall covering on plasterboard	EUR 03	59	2,66	322	12	51	17	-
Melamine faced CaSI board	EUR 04	40	0,36	96	28	193	92	-
Plastic faced steel sheet on	EUR 05	19	0,56	70	18	62	29	-

PRODUCT*	ID	$\dot{Q}''_{ave180s}$ (kW/m^2) *	$\frac{\dot{Q}''_{ave180s}}{t_{ign}}$ (kW/m^{2}s) *	$\dot{Q}''_p$ (kW/m^2) *	t_c (s) *	t_{ign} at 35 kW/m^2 (s)	t_{ign} at 55 kW/m^2 (s)	FIGRA (W/s)
mineral wool								
FR particle board B1	EUR 06	38	1,95	141	18	39	17	-
Faced rockwool	EUR 07	13	2,89	129	7	7	-	-
FR particle board	EUR 08	31	0,16	31	43	375	165	-
Plastic faced steel sheet on PUR	EUR 09	141	8,29	253	39	24	-	-
PVC wall carpet on plasterboard	EUR 10	65	4,45	138	32	29	11	-
FR EPS	EUR 11	117	4,25	636	12	53	-	-
Plasterboard	SBI M01					0	0	21
FR PVC	SBI M02	115	2,62	173	51	84	37	81
FR EPS	SBI M03	197	39,37	291	52	10	-	1375
Aluminium faced rigid PUR; 40 kW/m2	SBI M04	81	19,36	79	60 **	5	-	1869
Pine varnished timber	SBI M05	104	8,63	218	32	23	-	681
FR Chip board	SBI M06	54	0,11	67	87	928	408	25
Painted plasterboard	SBI M08	-	-	-	-	-	-	16
Wallpaper on plasterboard	SBI M09	-	-	-	-	0	0	154
PVC wall carpet on plasterboard	SBI M10	65	4,97	145	30	25	11	374

PRODUCT*	ID	$\dot{Q}''_{ave180s}$ (kW/m^2) *	$\frac{\dot{Q}''_{ave180s}}{t_{ign}}$ (kW/m^{2}s) *	$\dot{Q}''_p$ (kW/m^2) *	t_c (s) *	t_{ign} at 35 kW/m^2 (s)	t_{ign} at 55 kW/m^2 (s)	FIGRA (W/s)
Plastic face steel sheet on mineral wool	SBI M11	-	-	-	-	0	0	78
Spruce unvarnished timber	SBI M12	105	6,17	167	46	34	-	440
Plasterboard on EPS; 40 kW/m^2	SBI M13	12	0,22	89	9	72	32	9
Phenolic foam	SBI M14	31	1,63	39	79	36	16	82
Intumescent paint on particle board	SBI M15	2	0,10	22	6	38	17	16
Melamine faced MDF board	SBI M16	133	3,01	272	33	84	-	601
Unfaced rock wool	SBI M19	-	-	-	-	-	-	1
Melamine faced particle board	SBI M20	133	3,59	243	38	71	-	381
Sandwich panel steel on EPS; 40 kW/m^2	SBI M21	1	0,01	0	0	97	48	21
particle board	SBI M22	187	6,24	239	75	57	-	404
Plywood birch	SBI M23	131	5,95	218	43	42	-	399
Wall paper faced particle board	SBI M24	141	5,02	190	63	54	-	479
MDF board	SBI M25	187	6,14	238	77	69	-	436
LDF board	SBI M26	87	11,64	140	46	14	-	1103

PRODUCT*	ID	$\dot{Q}''_{ave180s}$ (kW/m^2) *	$\frac{\dot{Q}''_{ave180s}}{t_{ign}}$ (kW/m^{2}s) *	$\dot{Q}''_p$ (kW/m^2) *	t_c (s) *	t_{ign} at 35 kW/m^2 (s)	t_{ign} at 55 kW/m^2 (s)	FIGRA (W/s)
Plasterboard on FR PUR; 40 kW/m^2	SBI M27	13	0,14	87	9	111	49	17
Acoustic mineral fibre tiles	SBI M28	-	-	-	-	-	-	0
Textile wallpaper on CaSi board	SBI M29	22	0,78	192	7	54	24	108
Paper faced glass wool; kW/m^2	SBI M30	12	4,44	153	5	3	-	3923

*Normally data at 50 kW/m^2 Cone Calorimeter heat exposure. When only HRR data at 40 kW/m^2 was available $\dot{Q}''_{ave180s}$ at 40 kW/m^2 was used directly. This concerned only products that either burned very rapidly or not at all and the influence on the modelling results was deemed to be small.

** Nearest value to fulfil for $\dot{Q}''_{ave180s}$

Table 15. Data from the Cone Calorimeter used for calculations of HRR in the small room test (1/3 scale of the Room Corner Test).

PRODUCT	ID	Source for $\dot{Q}''_{ave180s}$, $\dot{Q}''_p$ and t_c	t_{ign} at 25 kW/m^2 (s)
Insulating fibre board	s1	SBI M26	43
Medium density fibre board	s2	SBI M25	123
Particle board	s3	SBI M22	123
Gypsum plasterboard	s4	-	NI
PVC wall covering on gypsum plasterboard	s5	EUR 10	41

PRODUCT	ID	Source for $\dot{Q}''_{ave180s}$, $\dot{Q}''_p$ and t_c	t_{ign} at 25 kW/m^2 (s)
Paper wall covering on gypsum plasterboard	s6	-	106
Textile wall covering on gypsum plasterboard	s7	EUR 3	115
Textile wall covering on mineral wool	s8	-	30
Melamine faced particle board	s9	-	NI
Expanded polystyrene, EPS	s10	EUR 11	223
Rigid polyurethane foam	s11	-	4
Wood panel, spruce	s12	SBI M12	169
Paper wall covering on particle board	s13	SBI M24	139

NI = No ignition

When there is no ignition the Conflame formulation predicts no fire growth. For products s6, s8 and s11 data was not available.

8 References

1. EN 13823, “Reaction to fire tests for building products-Building products excluding floorings exposed to the thermal attack by a single burning item.”, Brussels, Belgium.

2. “Mid term report of WP3a: Use of the SBI Room/Corner Test parameters.”, internal work package report of the SBI project, Not published, 1998, Brussels, Belgium

3. ”Summary of principles leading to the SBI classification system”, prepared by Official Laboratories Group, European Commission, Directorate General III Industry, Industrial affairs II: Capital goods industry, Construction, RG N138, Not published, 1998, Brussels, Belgium

4. FIPEC Final Report to the European Commission, SMT Programme SMT4-CT96-2059, 410pp, ISBN 0 9532312 5 9, London 2000.

5. EUREFIC Seminar proceedings, Interscience Communications Ltd, London, ISBN 0 9516320 19.

6 ”The SBI Project”. Project leader TNO Fire laboratory, Holland. Reported to the European Commission during 1998. Various parts are published separately, e.g. the SBI round robin and the Euroclass system. References are given in this work when a certain topic in this large project is discussed.

7. Williamson, R. B., Fischer, F., ”Fire growth experiments – toward a standard room fire test”, WSS-79-48, 1979, Department of Civil Engineering and Lawrence Berkley Laboratory, University of California, Berkley, USA.

8. ”Proposed Standard Method for Room Fire Test of Wall and Ceiling Materials and assemblies”, Annual book of ASTM standards, part 18, 1982, Philadelphia, USA.

9. 2000 HSC Code, International Code of Safety for High-Speed Craft, 2000, resolution MSC.97(73) adopted on 5 December 2000, IMO, International Maritime Organisation London, England 2001

10. FTP Code, International Code for Application of Fire Test Procedures, Including fire test procedures referred to and relevant to the FTP Code, Resolution MSC.61(67), IMO, International Maritime Organisation London, England 1998.

11. The Construction Products Directive, Council Directive 89/106/EEC, 21 December 1988, Brussels, Belgium, 1988

12. ”European Business Facts and Figures, Data 1995-2005”, European Commission, Eurostat, ISSN 1681-2050.

13. Sundström, Björn, Van Hees, Patrick och THURESON, Per. ”Results and Analysis from Fire Tests of Building Products in ISO 9705, the Room/Corner Test”, The SBI Research Programme, 1998, 33 s, SP rapport 1998, nr 11. ISBN 91-7848-716-1.

14. COMMISSION DECISION of 8 February 2000 implementing Council Directive 89/106/EEC as regards the classification of the reaction to fire, performance of construction products. (2000/147/EC)

15. EN 13501-1, “Fire classification of construction products and building elements-Part 1: Classification using test data from reaction to fire tests” , CEN, Brussels, 2002

16. Sundström, B., “European Classification of Building Products”, Proceedings of the 8th International Fire Science & Engineering Conference (Interflam ‘99), Edinburgh, Scotland, 1999.

17. Sundström, B., “Full Scale Fire Testing of Surface Materials. Measurements of Heat Release and Productions of Smoke and Gas Species”, SP-Rapp 1986:45, Swedish National Testing and Research Institute, 1986.

18. EN 14390, “Fire Test-Large-scale room reference test for surface products”, CEN, Brussels, 2007

19. “SBI (Single Burning Item) Second Round Robin”, EGOLF (European Group of Official Laboratories for Fire testing), ENTR/2002/CP11, report to the European Commission 2005-01-31

20. Axelsson, J., Sundström, B., Rohr, U., "Development of a common European system for fire testing and classification of pipe insulation", Ninth International Interflam Conference Edinburgh September 2001, Volume 1, p485-494, Interscience communications Ltd, ISBN 0 9532312 8 3.

21. Sundström, B., and Axelsson, J., "Development of a common European system for fire testing of pipe insulation based on EN 13823 (SBI) and ISO 9705 (Room/Corner Test)", SP-report 2002:21. ISBN 91-7848-871-0

22. COMMISSION DECISION of 26 August 2003 amending Decision 2000/147/EC implementing Council Directive 89/106/EEC as regards the classification of the reaction-to-fire performance of construction products (2003/632/EC)

23. ISO/DIS 20632 "Reaction-to-fire tests - small room corner test for pipe insulation products or systems".

24. Sundström, B., Axelsson, J., and Van Hees, P., "A proposal for fire testing and classification of cables for use in Europe." Report to the European commission and the fire regulators group. SP, 2003-06-19

25. Sundström, B., Axelsson, J., and Van Hees, P., "A new European system for fire testing and classification of cables". Tenth International Interflam Conference Edinburgh July 2004, Volume 1, p5-15, Interscience communications Ltd, ISBN 0 9541216-3-5.

26. COMMISSION DECISION of 27 October 2006 amending Decision 2000/147/EC implementing Council Directive 89/106/EEC as regards the classification of the reaction-to-fire performance of construction products (2006/751/EC)

27. ISO 21367-2007, "Plastics -- Reaction to fire -- Test method for flame spread and combustion product release from vertically oriented specimens" ISO, Geneva 2007, Switzerland.

28. Blanc, C., "A new (MEDIUM) scale test to predict the fire behaviour of materials for the Building in relation with intermediate scale test", Fire and Materials Conference, San Francisco, 2005.

29. Kokkala, M., Göransson, U., Söderbom, J., "EUREFIC-Large scale fire experiments in a room with combustible linings. Some results from the project 3 of the EUREFIC fire research programme". SP-report 1990:41, ISBN 91-7848-247-X, Borås, Sweden.

30. ISO 13943, "Fire Safety Vocabulary", Geneva.

31. Babrauskas, V., "Ignition handbook", ISBN 0-9728111-3-3, Fire Science Publishers, 2003 Vytenis Babrauskas.

32. Lawson, D.I., Simms, D.L., "The Ignition of Wood by Radiation", British Journal of Applied Physics 3, pp 288-292 (1952)

33. Holman, J.P., "Heat Transfer", Mc Graw Hill inc, ISBN 0-07-029598-0

34. Tewarson, A., "Generation of Heat and Chemical Compounds in Fires", SFPE handbook of Fire Protection Engineering, 3rd edition, ISBN 087765-451-4, pp 3-82--3-89.

35. Janssens, M., "Fundamental Thermophysical Characteristics of Wood and their Role in Enclosure Fire Growth", PhD Dissertation, University of Gent, Belgium, 1991.

36. Janssens, M., "Piloted Ignition of Wood: A Review", Fire and Materials 15 1991, pp 151-167, John Wiley & Sons Ltd.

37. Janssens, M., Dillon, S.E., Allwein, S., "Characterizing the Thermal Environment of the Cone Calorimeter for Analyzing Ignition Data of Materials", Interflam 2001 proceedings, pp125-135, Interscience Communications ltd, London 2001.

38. Thureson, P., "EUREFIC - Cone Calorimeter Test Results. Project 4 of the EUEFIC fire research programme", SP-report 1991:24, Swedish National Testing and Research Institute, Borås, Sweden, 1991.

39. SP-Fire Technology data base at www.sp.se/fire/fdb

40. ASTM E 2058, "Standard Methods of Test for Measurement of Synthetic Polymer Material Flammability Using a Fire Propagation Apparatus (FPA)"

41. Quintiere, J.G., Harkleroad, M.F., "New Concepts for Measuring Flame Spread Properties", NBSIR 84-2943, National Bureau of Standards, 1984

42. ASTM E 1321-97A (reapproved 2002), "Standard Test Method for Determining Material Ignition and Flame Spread Properties"

43. Barauskas, V., Wetterlund, I:, "Comparative data from LIFT and Cone Calorimeter Tests on 6 Products, Including Flame Flux Measurements", SP-report 1999:14, Swedish National Testing and Research Institute, Borås 1999

44. Combustion Fundamentals of Fire, Edited by Geoffrey Cox, Academic press ltd 1995, ISBN 0-12-194230, chapter 2 "The solid phase", Fernadez-Pello

45. Saito, K., Quintiere, J.G., Williams, F.A., "Upward Turbulent Flame Spread" Proc. First International Symposium on Fire Safety Science, Hemisphere Publishing Corporation, N.Y. 1984

46. Karlsson, B., "Modelling Fire growth on Combustible Lining Materials in Enclosures", PhD Thesis, TVBB 1009, Lund University Department of Fire Safety Engineering, 1992.

47. Wade, C., "A Room Fire Model Incorporating Fire Growth on Combustible Lining Materials", Master's thesis, Worcester Polytechnic Institute, Worcester, MA, April 1996.

48. Quintiere, J.G., Harkleroad, M.F., Hasemi, Y., "Wall Flames and Implications for Upward Flame Spread", Final report, National Bureau if Standards, Gaithersburg, USA, Building Research Institute, Tsukuba, Japan, Journal of Combustions Science and Technology, Vol 48, No. 3 & 4, pp 191-222, 1986.

49. Quintiere, J.G., "Surface Flame Spread", SFPE Handbook of Fire Protection Engineering, 3rd edition, ISBN 087765-451-4, pp. 2-246 to 2-257

50. Combustion Fundamentals of Fire, Edited by Geoffrey Cox, Academic press ltd 1995, ISBN 0-12-194230, chapter 5 "The Growth of Fire-Ignition to Full Involvement", P.H. Thomas

51. Wickström, U., Göransson, U., "Prediction of Heat Release Rates of Surface Materials in Large-Scale Fire Tests Based in Cone Calorimeter Results", J. Testing and Evaluation, 15, pp 364-370, 1987.

52. Wickström, U., Göransson, U., "Full-Scale/Bench-Scale Correlations of Wall and Ceiling Linings", Heat Release in Fires edited by V. Babrauskas and S.J. Grayson pp 461-477, Elsevier Science Publishers ISBN 1-85166-794-6, 1992.

53. ISO 9705 part 2, "Reaction-to-fire tests — Full-scale room tests for surface products —Part 2: Technical background and guidance", Geneva.

54. Lattimer, B.Y., Hunt, S.P., Sorathia, H., Blum, M., Gracik, T., McFarland, M., Lee, A., Long, G., "Development of a Model for Predicting Fire Growth in a Combustible Corner", NSWCCD-TR-64-99/07, U.S. Navy 1999, West Bethesda, MD, USA

55. Söderbom, J., EUREFIC-Large Scale Tests According to ISO DIS 9705, SP-report 1991:27, Swedish National Testing and Research Institute, Borås, Sweden, 1991.

56. Kokkala, M. A., Thomas, P.H., Karlsson, B., "Rate of Heat Realease and Ignitability Indices for Surface Linings", Fire and Materials 17, pp 209-216 1993

57. Tewarson, A., "Generation of Heat and Chemical Compounds in Fires", SFPE handbook of Fire Protection Engineering, 3rd edition, ISBN 087765-451-4, pp 3-146—3-147.

58. Quintiere, J.G., "A theoretical basis for flammability properties", Fire and Materials Vol 30, 2006, pp 175-214, Wiley

59. CBUF - Fire Safety of Upholstered Furniture - the final report on the CBUF research programme, edited by Björn Sundström, European Commission Measurements and Testing Report EUR 16477 EN, pp 168-170.

60. Van Hees, P., Hertzberg, T., Hansen, A. S., "Development of a Screening Method for the SBI and Room Corner using the Cone Calorimeter, Nordtest project 1479-00, SP-report 2002:11, Borås , Sweden

61. Wade, C., Barnett, J., "A room-corner model including fire growth on linings and enclosure smoke-filling". Journal of Fire Protection Engineering, 8(4):27-36, 1997.

62. Wade, C., LeBlanc, D., Ierardi, J., Barnett, J., "A room-corner fire growth and zone model for lining materials". Second International Conference of Fire Research and Engineering, 1997.

63. Wade, C., "A new engineering tool for evaluating the fire hazard in rooms". Proceedings of the Building Control Commission International Convention, April 1999.

64. Wade, C., BRANZFIRE, Technical Reference Guide, Study Report No. 92 (revised 2004)

65. Silcock, G., Shields, T., "A protocol for analysis of time-to-ignition data from bench scale tests". Fire Safety Journal, 24:75 p95, 1995.

66. Forney, G., "Computing radiative heat transfer occurring in a zone model". Fire Science & Technology, 14:31p47, 1994.

67. Wade, C., BRANZFIRE 2004, Compilation of Verification Data, November 2004

68. Östman, B., Nussbaum, R.M., "Flame Spread Predictions in the Room Corner Test based on the Cone Calorimeter, pp 211-219, Proceedings of the 5th International Fire Science & Engineering Conference (Interflam '90), England, 1990.

69. Östman, B., Tsantaridis, L., "Correlation between Cone Calorimeter Data and Time to Flashover in the Room Corner Test", Fire and Materials Vol. 18, pp 205-209, 1994.

70. North, G.A., ”An Analytical Model for Vertical Flame Spread on Solids: An Initial Investigation”, Fire Engineering research report 99/12 March 1999, School of Engineering, University of Canterbury, Private bag 4800, Christchurch, New Zealand

71. North, G., Karlsson, B., Gojkovic, D., Van Hees, P., “Simple Analytical and Numerical Techniques for Modelling Flame Spread on Solids”, Department of Fire Safety Engineering Lund University, Report 7014, Lund 2001, Sweden

72. Andersson, B., ”Model Scale Compartment Fire Tests with Wall Lining Materials”, LUTVDG/(TVBB-3041) ISSN 0282-3756, Lund University Department of Fire Safety Engineering, 1988.

73. Hakkarainen, T., “Correlation studies of SBI and Cone Calorimeter test results”, Proceedings of the 9th International Fire Science & Engineering Conference (Interflam 2001), Edinburgh, Scotland, 2001.

74. Steen Hansen, A., “Prediction of Heat Release in the Single Burning Item Test”, Fire and Materials 26 2002, pp 87-97, John Wiley & Sons Ltd.

75. Babrauskas, V., Peacock, R.D., Reneke P.A., ”Defining flashover for fire hazard calculations: Part II”, Fire Safety Journal 38 (2003), pp 613-622

76. Axelsson, J., Andersson, P., Lönnermark, A., VAn Hees, P., Wetterlund, I., ”Uncertainty of HRR and SPR measurements in SBI and Room/Corner Test”, Proceedings of the 9th International Fire Science & Engineering Conference (Interflam 2001), Edinburgh, Scotland, 2001.

77. Van Hees, P., Johansson, P., “The need for full-scale testing of sandwich panels, comparison of full-scale tests and intermediate-scale tests”, Proceedings of the 9th International Fire Science & Engineering Conference (Interflam 2001), Edinburgh, Scotland, 2001.

78. Van Hees, P., ”Fire behaviour of sandwich panels”, Chapter 6, pp 149-163, Flammability testing of materials used in construction, transport and mining, Handbook edited by Vivek B. Apte, Woodhead Publishing, ISBN-13: 978-1-85573-935-2, Cambridge, England, 2006.

79. McGrattan, K., ”Fire Dynamics Simulator (Version 4) Technical Reference Guide”, Fire Research Division, Building and Fire Research Laboratory in co-operation with VTT Building and transport, Finland, NIST Special Publication 1018, March 2006.

80. McGrattan, K., Forney, G., ”Fire Dynamics Simulator (Version 4) Users Guide”, Fire Research Division, Building and Fire Research Laboratory in co-operation with VTT Building and transport, Finland, NIST Special Publication 1018, March 2006.

81. Hietaniemi, J., Hostikka, S., Vaari, J., ”FDS simulation of fire spread-comparison of model results with experimental data”, VTT Building and transport, ISBN 951-38-6556-8, Helsinki, Finland, 2004.

82. Göransson, U., ”Determination of Material Properties for Fire Modelling” Doctoral Thesis, ISBN 91-628-6640-0, Lund Institute of Technology, Department of Fire Safety Engineering, Lund, Sweden, 2005.

83. Östman, B.A-L., Tsantaridis, L.D., ” Ignitability in the Cone Calorimeter and the ISO Ignitability Test”, Proceedings of the 5th International Fire Science & Engineering Conference (Interflam 1990), Canterbury, England, 1990.